

Calcium Absorption Across Epithelia

JOOST G. J. HOENDEROP, BERND NILIUS, AND RENÉ J. M. BINDELS

Department of Physiology, Nijmegen Center for Molecular Life Sciences, University Medical Center Nijmegen, Nijmegen, The Netherlands; and Department of Physiology, Campus Gasthuisberg, KU Leuven, Belgium

I. Introduction	374
II. Paracellular Transport	374
A. Tight junction	374
B. Regulation	375
III. Transcellular Transport	376
A. Calcium entry	376
B. Cytosolic diffusion	378
C. Extrusion mechanisms	379
IV. Epithelial Calcium Channels	380
A. Molecular diversity	380
B. Ion selectivity/gating mechanisms	382
C. Modulation of channel activity	388
D. CRAC and TRPV6	391
E. Molecular structure of TRPV5 and TRPV6	392
V. Sites of Epithelial Calcium Transport	393
A. Kidney	393
B. Gastrointestinal tract	395
C. Others	396
VI. Regulation of Epithelial Calcium Transport	398
A. Regulation by 1,25-(OH) ₂ D ₃	398
B. Regulation by PTH	400
C. Regulation by calcitonin	401
D. Regulation by stanniocalcin	401
E. Regulation by estrogens	402
F. Regulation by thyroid hormone	402
G. Regulation by dietary Ca ²⁺	403
H. Regulation by the Ca ²⁺ -sensing receptor	403
I. Regulation by associated proteins	404
J. Diuretics	406
K. Immunosuppressants	407
VII. Characterization of Epithelial Calcium Channel Knockout Mice	408
A. TRPV5 knockout mice	408
B. TRPV6 knockout mice	410
VIII. Outlook	410

Hoenderop, Joost G. J., Bernd Nilius, and René J. M. Bindels. Calcium Absorption Across Epithelia. *Physiol Rev* 85: 373–422, 2005; doi:10.1152/physrev.00003.2004.—Ca²⁺ is an essential ion in all organisms, where it plays a crucial role in processes ranging from the formation and maintenance of the skeleton to the temporal and spatial regulation of neuronal function. The Ca²⁺ balance is maintained by the concerted action of three organ systems, including the gastrointestinal tract, bone, and kidney. An adult ingests on average 1 g Ca²⁺ daily from which 0.35 g is absorbed in the small intestine by a mechanism that is controlled primarily by the calcitropic hormones. To maintain the Ca²⁺ balance, the kidney must excrete the same amount of Ca²⁺ that the small intestine absorbs. This is accomplished by a combination of filtration of Ca²⁺ across the glomeruli and subsequent reabsorption of the filtered Ca²⁺ along the renal tubules. Bone turnover is a continuous process involving both resorption of existing bone and deposition of new bone. The above-mentioned Ca²⁺ fluxes are stimulated by the synergistic actions of active vitamin D (1,25-dihydroxyvitamin D₃) and parathyroid hormone. Until recently, the mechanism by which Ca²⁺ enter the absorptive epithelia was unknown. A major breakthrough in completing the molecular details of these

pathways was the identification of the epithelial Ca^{2+} channel family consisting of two members: TRPV5 and TRPV6. Functional analysis indicated that these Ca^{2+} channels constitute the rate-limiting step in Ca^{2+} -transporting epithelia. They form the prime target for hormonal control of the active Ca^{2+} flux from the intestinal lumen or urine space to the blood compartment. This review describes the characteristics of epithelial Ca^{2+} transport in general and highlights in particular the distinctive features and the physiological relevance of the new epithelial Ca^{2+} channels accumulating in a comprehensive model for epithelial Ca^{2+} absorption.

I. INTRODUCTION

The maintenance of the extracellular Ca^{2+} concentration is of utmost importance for many vital functions of the body. In face of large variations in Ca^{2+} in- and output, the organism is equipped with a set of regulatory systems to keep the plasma Ca^{2+} levels around a value of 2.5 mM. To this end, the Ca^{2+} fluxes between the extracellular compartment and several organ systems are tightly controlled.

Ca^{2+} absorption occurs in epithelia, including kidney, intestine, placenta, mammary glands, and gills. In mammals, the small intestine and kidney constitute the influx pathways into the extracellular Ca^{2+} pool, while fish have an additional specialized organ for Ca^{2+} uptake, the gills (426). In addition, during reproductive events, Ca^{2+} transport in the placenta and mammary glands can seriously influence the Ca^{2+} balance (29, 345). For instance, during lactation, plasma Ca^{2+} levels can significantly drop due to Ca^{2+} excretion into the milk. Furthermore, during pregnancy Ca^{2+} transport from the mother to the fetus takes place across the placenta and challenges the plasma Ca^{2+} concentration. The Ca^{2+} demand is great in children during skeletal growth and decreases gradually with advancing age. Finally, factors as pH, extracellular Ca^{2+} concentration, and various hormones have been shown to influence the Ca^{2+} movement across epithelia (37, 129, 175).

In general, Ca^{2+} transport is mediated by a complex array of transport processes that are regulated by hormonal, developmental, and physiological factors. The distinct processes by which Ca^{2+} can be absorbed across epithelial tissues include paracellular and transcellular pathways. The paracellular pathway allows the direct exchange of Ca^{2+} between two compartments, while the transcellular route involves transport across at least two plasma membrane barriers (Fig. 1). The vitamin D metabolite 1,25-dihydroxyvitamin D_3 [$1,25\text{-(OH)}_2\text{D}_3$] and parathyroid hormone (PTH), among others, are prominent hormones controlling the Ca^{2+} balance.

Numerous methods have been utilized to study the process of Ca^{2+} absorption. Traditionally, metabolic balance, micropuncture, and radioactive tracer techniques were employed to estimate epithelial Ca^{2+} fluxes in humans and animal models. More recently, freshly isolated epithelia and established cell models were used to measure Ca^{2+} transport by radioisotopes of Ca^{2+} and fluores-

cent indicators. Finally, molecular biological tools were applied to identify and characterize the individual transport proteins and to develop new animal and cell models to further delineate the process of Ca^{2+} transport. As a consequence, current research is beginning to define the molecular mechanisms, the regulation, and coordination of the epithelial Ca^{2+} transport mechanisms (35, 125). Here, we review our present understanding of these processes in detail and discuss potential implications for further research.

II. PARACELLULAR TRANSPORT

A fundamental function of epithelia is to separate different compartments within the organism and to regulate the exchange of substances between them (151, 425). Epithelia consist of a continuous layer of individual cells, and the intercellular spaces between the epithelial cells are very narrow, but nonetheless allow the diffusion of small molecules and ions (152). This route is called the paracellular pathway, which must be regulated for the epithelium to remain selectively permeable (Fig. 1). Depending on the functional requirements of an epithelium, there may be small or large amounts of solutes flowing passively through this path. The tight junction constitutes the barrier to the passage of ions and molecules through the paracellular pathway (5). In general, the importance of this route has not been as thoroughly investigated as the role of the transepithelial pathway. However, recent studies identifying the molecular components of the paracellular transport route as causally related to particular inherited diseases, including familial hypomagnesemia (353), hypertension (429), and autosomal recessive deafness (428), confirm the importance of paracellular transport.

A. Tight Junction

The tight junction is a specialized membrane domain at the most apical region of polarized epithelial cells that not only creates a primary barrier to prevent paracellular transport of solutes, but also restricts the lateral diffusion of membrane lipids and proteins to maintain the cellular polarity. Tight junctions are intercellular structures in which the plasma membranes of adjacent epithelial cells come into very close contact. These structures consist as

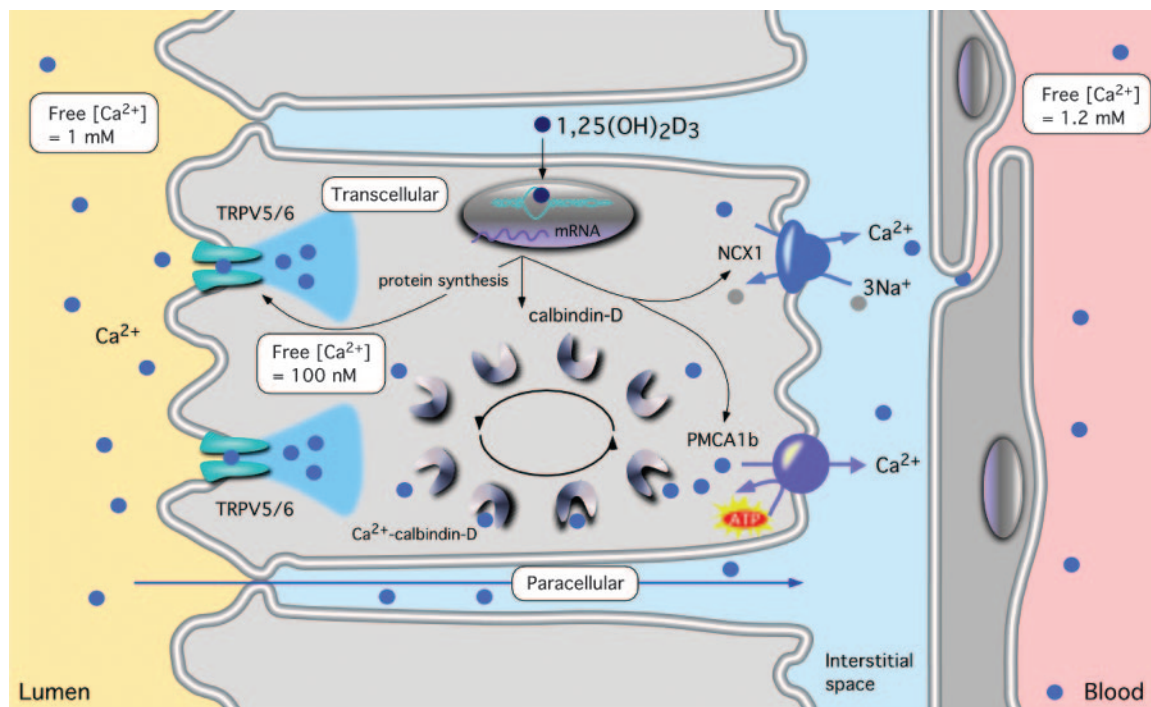


FIG. 1. Mechanism of epithelial Ca^{2+} transport. Epithelia can absorb Ca^{2+} by paracellular and transcellular transport. Passive and paracellular Ca^{2+} transport takes place across the tight junctions and is driven by the electrochemical gradient for Ca^{2+} (blue arrow). The active form of vitamin D, 1,25-dihydroxyvitamin D_3 [$1,25\text{-(OH)}_2\text{D}_3$], stimulates the individual steps of transcellular Ca^{2+} transport by increasing the expression levels of the luminal Ca^{2+} channels, calbindins, and the extrusion systems. Active and transcellular Ca^{2+} transport is carried out as a three-step process. Following entry of Ca^{2+} through the (hetero)tetrameric epithelial Ca^{2+} channels, TRPV5 and TRPV6, Ca^{2+} bound to calbindin diffuses to the basolateral membrane. At the basolateral membrane, Ca^{2+} is extruded via a ATP-dependent Ca^{2+} -ATPase (PMCA1b) and a $\text{Na}^+/\text{Ca}^{2+}$ exchanger (NCX1). In this way, there is net Ca^{2+} absorption from the luminal space to the extracellular compartment.

linear arrays of integral membrane proteins, which include occludin, claudins, and several immunoglobulin superfamily members, such as the junctional adhesion molecule (98, 152, 248). The claudin family consists of at least 20 related integral membrane proteins with four transmembrane (TM) domains and functions as major structural components of the tight junctional complex, while occludin is an accessory protein involved in the tight junction formation of which three isoforms have been described (262, 378, 384).

It has been hypothesized that tight junctions behave similar to conventional ion channels, while others have suggested a function as water-filled channels with no ion selectivity (5, 384, 434). Recently, it was shown by applying new technology that the tight junction complex manifests biophysical properties of ion channels including ion and size selectivity, concentration-dependent ion permeability, competition between permeable molecules, anomalous mole-fraction behavior, and sensitivity to pH (378). This latter study suggests that discrete ion channels are being inserted in the tight junction to facilitate paracellular ion transport. This is further supported by the disease mutations documented in claudins (434). Mutations in claudin-16, which are associated with a renal Mg^{2+} wasting syndrome, implicate this particular claudin in paracel-

lular resorption of Mg^{2+} and Ca^{2+} , but not monovalent ions (353). Mutations in claudin-14 cause nonsyndromic recessive deafness, and this tight junction protein is essential to maintain the electrochemical gradient between the endolymph and its surrounding tissues (428).

B. Regulation

Movement of ions through the tight junctions is a passive process, which largely depends on the concentration gradient of the permeable ions and the electrical gradient across the epithelium. Hormones and factors affecting the electrochemical gradient across the epithelium, therefore, indirectly influence the passive fluxes through the tight junctions. The tight junction permeability itself is dynamically regulated under various physiological conditions (152, 299). Tight junctions undergo modulation by growth factors, cytokines, bacterial toxins, hormones, and other factors (30, 134, 153, 419). Some studies suggest that phosphorylation of tight junction proteins plays a role in tight junction assembly and function. Modulation of protein kinase C (PKC) disrupts the cell-cell junctions of epithelial cells, whose action is supposedly mediated by mitogen-activated protein kinase (419).

Recently, the serine-threonine kinase WNK4 has been identified as part of the junctional complex, and mutations in this protein cause pseudoaldosteronism type II, a Mendelian trait featuring hypertension (429). Furthermore, a serine-threonine-dependent phosphorylation of tight junction proteins has been shown to enhance the paracellular permeability in rabbit nasal epithelium (294). These studies underline the essential role of serine-threonine kinase in the regulation of the paracellular route, but the precise mechanism remains to be established.

III. TRANSCELLULAR TRANSPORT

Transcellular Ca^{2+} transport is a multistep process, comprised of the transfer of luminal Ca^{2+} into the enterocyte or renal epithelial cell, the translocation of Ca^{2+} from point of entry to the basolateral membrane, and finally active extrusion from the cell into the circulatory system (Fig. 1).

A. Calcium Entry

Ca^{2+} is postulated to enter the epithelial cell via Ca^{2+} -selective channels at the luminal membrane under the influence of a steep, inwardly directed electrochemical gradient. The molecular nature of the apical entry mechanism has remained obscure for a long time. In the past, the mechanism responsible for the luminal entry of Ca^{2+} has been extensively characterized in renal and intestinal cells, but these studies have not led to the definite identification of this Ca^{2+} transporter. A variety of studies implicated Ca^{2+} channels in mediating Ca^{2+} entry in absorptive epithelia (206, 228, 443). From these studies it is likely that several distinct Ca^{2+} channels, which resemble the classified voltage-dependent Ca^{2+} channels in part, are present in cells of the distal part of the nephron (443). Previous studies indicated the presence of the pore-forming subunit α_{1A} or $\alpha 1$ of a Ca^{2+} channel expressed in the Ca^{2+} -transporting renal cells. In general, voltage-sensitive Ca^{2+} channels are heteromeric, multisubunit proteins, as has been well demonstrated for the skeletal muscle (69) and brain (431) channels, and their properties are not only determined by the $\alpha 1$ -subunit itself, but also depend on the presence of regulatory subunits. Of these, the β_3 -subunit might be an interesting subunit, which can influence such fundamental channel properties as current amplitude (355), kinetics (226, 355, 400), voltage dependence (355), and regulation by cyclic nucleotide-dependent protein kinases (216). Stimulation of the Ca^{2+} influx channel in the renal distal tubule by the calcitropic hormone PTH is thought to be mediated by both protein kinase A (PKA) and PKC (124, 170). Comparable studies in rat duodenum pointed to acute effects of $1,25\text{-(OH)}_2\text{D}_3$ on Ca^{2+} influx in isolated enterocytes (112–

114, 144, 152). This calcitropic hormone significantly increased $^{45}\text{Ca}^{2+}$ uptake within 1–10 min in a dose-dependent manner (249). The effects of $1,25\text{-(OH)}_2\text{D}_3$ were mimicked by the Ca^{2+} channel agonist BAY K 8644 and completely abolished by nifedipine and verapamil. Incubation of duodenal cells with $1,25\text{-(OH)}_2\text{D}_3$ rapidly (1–5 min) increased cAMP levels. Forskolin caused a rapid increase in Ca^{2+} uptake by enterocytes that was similar to the action of the hormone. Moreover, pretreatment of cells with the specific cAMP inhibitor $R_p\text{-cAMPS}$ suppressed the changes in $^{45}\text{Ca}^{2+}$ influx induced by $1,25\text{-(OH)}_2\text{D}_3$. These results suggested the involvement of a Ca^{2+} channel activation through the cAMP/PKA-pathway by $1,25\text{-(OH)}_2\text{D}_3$ in mammalian intestinal cells (249). However, the physiological significance of these postulated Ca^{2+} channels with respect to Ca^{2+} influx during Ca^{2+} (re)absorption remains unclear, since most of the studies were performed in single cell systems rather than in polarized epithelia derived from kidney or duodenum epithelia. With the use of these nonpolarized cell preparations, it was not feasible to discriminate between apical versus lateral Ca^{2+} influx. Until now, two polarized confluent epithelial cell systems representing active duodenal and renal Ca^{2+} (re)absorption have been studied. First, Caco-2 cells were employed, which represent an intestinal cell line derived from a human colorectal carcinoma that spontaneously differentiates under standard culture conditions in a tissue that exhibits functional duodenal transport processes (144). These cells become polarized columnar epithelial cells, form tight junctions and domes, and express several markers that are unique to differentiated small intestinal epithelium (e.g., high sucrase-isomaltase mRNA and protein levels) (72). Caco-2 cells exhibit saturable apical-to-basolateral Ca^{2+} transport kinetics, net transport is positive in the apical-to-basolateral direction, and the rate of transport can be increased by pretreatment with $1,25\text{-(OH)}_2\text{D}_3$ (114, 143). Vitamin D-induced upregulation of Ca^{2+} transport requires transcriptional events (114) and is modulated by changes in the vitamin D receptor (VDR) content of the cell (342). Second, the use of primary cultures and immortalized cell lines originating from the renal distal tubular cells greatly facilitated our understanding of Ca^{2+} influx in these cells and how PTH and $1,25\text{-(OH)}_2\text{D}_3$ regulate transepithelial Ca^{2+} transport. Two groups, Bindels and co-workers (36–39, 170, 172, 177, 320, 389–391) and Gesek and Friedman and co-workers (12, 120, 124, 126–128, 139, 138, 246, 427), have used immunodissected cell lines from rabbit and mouse kidney, respectively, to investigate PTH-stimulated Ca^{2+} transport. These studies verified that PTH increases transepithelial Ca^{2+} transport and suggested that both PKA and PKC participate in this process (124, 170). In addition, Bindels and co-workers demonstrated that the primary cultures of rabbit connecting tubule (CNT) and cortical collecting duct (CCD) cells exhibit many charac-

teristics of the original epithelium, including 1,25-(OH)₂D₃- and vasopressin-stimulated Ca²⁺ reabsorption (36–39, 50, 170, 172, 177, 218). The stimulatory effect of cAMP/PKA on apical Ca²⁺ influx is in agreement with a report of Tan and Lau (377), describing a 25-pS, cAMP-sensitive apical Ca²⁺ channel in rabbit kidney CNT cells, that is inhibited by dihydropyridine agonists and depolarization. However, luminal administration of a variety of Ca²⁺ channel antagonists, including dihydropyridines, failed to affect Ca²⁺ absorption in primary cultures of these CNT tubules, suggesting that Tan and Lau (377) did not study the apical entry Ca²⁺ mechanism.

Previous studies indicated that over a wide range of transepithelial Ca²⁺ transport rates, the Ca²⁺ influx at the apical membrane is correlated in a 1:1 fashion with the apical to basolateral ⁴⁵Ca²⁺ flux (320). The mechanism underlying this tight coupling could in principle be located at three distinct Ca²⁺ transport positions, namely, influx, cytosolic diffusion, or efflux (175, 320). Ca²⁺ influx across the apical or luminal membrane could be the rate-limiting step for transcellular Ca²⁺ transport. This would imply that the availability of cytosolic Ca²⁺ for the basolateral Ca²⁺ efflux pumps controls the rate of Ca²⁺ efflux. This is in line with the finding that apical H⁺ directly inhibits the Ca²⁺ influx pathway and consequently decreases the intracellular Ca²⁺ concentration, which in turn limits the Ca²⁺ extrusion (37). In addition, extracellular H⁺ are known to inhibit voltage-gated Ca²⁺ channels in excitable tissues by changing their conformations and modifying their gating properties.

To unravel the molecular identity of the apical Ca²⁺ influx protein in Ca²⁺-transporting epithelia, several different experimental strategies have been employed. The classic approach of purification of the Ca²⁺ transporter followed by amino acid sequencing of the isolated peptide has been hindered by the lack of a rich source of channel protein. In another strategy, a calbindin-D_{28K} affinity column has been applied to purify associated proteins potentially involved in transepithelial Ca²⁺ (re)absorption (191). Previous studies indicated that the intracellular Ca²⁺ concentration is a critical determinant for Ca²⁺ influx. In theory, the Ca²⁺ buffer calbindin, which reaches submillimolar concentrations in these epithelial cells, might interact with this putative influx channel to buffer and bind Ca²⁺ in a rapid way to facilitate an efficient Ca²⁺ transport. This attempt, however, did not unveil the molecular identity of the Ca²⁺ influx mechanism. Alternatively, investigators have focused on homology-based cloning strategies using sequences of previously described voltage-gated Ca²⁺ channels (21, 22, 397, 443), but also this approach did not result in the identification of the apical Ca²⁺ entry transporter.

Subsequently, functional expression cloning using a rabbit primary CNT/CCD cDNA library in *Xenopus laevis* oocytes was applied by Hoenderop et al. (178). This tech-

nique has previously been successful for the cloning of several epithelial transporters (66). The rationale to use the functional expression cloning approach was threefold: 1) mRNA isolated from primary cultures of rabbit CNT tubules, when injected in oocytes, induced a ⁴⁵Ca²⁺ uptake two to three times above background; 2) transcellular Ca²⁺ transport in primary cultures of rabbit CNT tubules was not affected by voltage-gated Ca²⁺ channel blockers, which allowed us to distinguish between voltage-gated Ca²⁺ channels and the Ca²⁺ transporter involved in transepithelial Ca²⁺ transport; and 3) the absence of a substantial endogenous Ca²⁺ influx in *Xenopus laevis* oocytes. Based on these characteristics, an expression cloning strategy was established to identify the apical Ca²⁺ entry channel. First, a cDNA library from poly(A)⁺ RNA isolated from primary cultures of rabbit kidney CNT and CCD was generated and subsequently screened for Ca²⁺ uptake activity in *Xenopus laevis* oocytes in the presence of a cocktail of known voltage-gated Ca²⁺ channel antagonists, including nifedipine, verapamil, and Ba²⁺. After an extensive screening procedure, a single transcript was isolated encoding for a novel epithelial Ca²⁺ channel, named ECaC1 and recently renamed as the transient receptor potential channel TRPV5 (178, 257).

To study the functional characteristics of this new Ca²⁺ channel, TRPV5 was initially heterogeneously expressed in *Xenopus laevis* oocytes and later in human embryonic kidney (HEK293) cells. Functional data on TRPV5 include ⁴⁵Ca²⁺ uptake, electrophysiology using voltage-clamp and patch-clamp experiments, and fluorimetric measurements (see sect. iv). In short, the channel was inhibited in order of potency by La³⁺ > Cd²⁺ > Mn²⁺. Permeability to Na⁺ was negligible in the situation where Ca²⁺ and Na⁺ were both present, whereas Ba²⁺ and Sr²⁺ did not affect the Ca²⁺ influx. These experiments unequivocally demonstrated that TRPV5 exhibits the defining properties of Ca²⁺ influx in Ca²⁺-transporting epithelia. Subsequently, Hediger and co-workers (257, 304) applied the functional expression cloning technique and identified the Ca²⁺ transporter 1 (CaT1 or recently renamed as TRPV6) from rat intestine, which shares 80% amino acid identity with TRPV5 (note: TRPV5 is also known in the literature as ECaC, ECaC1, and CaT2, whereas TRPV6 has been named previously CaT1, ECaC2, and CaT-like). Electrophysiological studies demonstrated that the characteristics of TRPV6 are comparable to those measured for TRPV5, but its expression pattern is more ubiquitous (see sect. iv). The functional properties of TRPV5 and TRPV6 are in line with those of epithelial Ca²⁺ (re)absorption, providing the first evidence that these transporters are the anticipated Ca²⁺ influx proteins initiating the process of transcellular Ca²⁺ transport, which is described in detail in section iv (Fig. 1) (175, 302).

B. Cytosolic Diffusion

Epithelial cells involved in transcellular Ca^{2+} transport are continuously challenged by substantial Ca^{2+} traffic through the cytosol, while simultaneously maintaining low levels of cytosolic Ca^{2+} . To date, two models have been proposed to explain transport of Ca^{2+} across these cells. First, the facilitated diffusion model in which the basal rate of Ca^{2+} uptake and Ca^{2+} extrusion from the absorptive epithelial cell is proposed to be sufficient to accommodate the elevated rate of transport observed after vitamin D stimulation. In contrast, mathematical modeling predicts that intracellular diffusion is the rate-limiting step (58, 357). There are two major subclasses of vitamin D-dependent Ca^{2+} -binding proteins, calbindin- $\text{D}_{9\text{K}}$ and calbindin- $\text{D}_{28\text{K}}$. These cytosolic proteins have been proposed as shuttles that can bind Ca^{2+} and facilitate the Ca^{2+} diffusion between the apical and basolateral surfaces of the cell. Calbindin- $\text{D}_{28\text{K}}$ is highly conserved during evolution and present in kidney, small intestine (only birds), pancreas, placenta, bone, and brain, and calbindin- $\text{D}_{9\text{K}}$ is present in highest concentrations in small intestine as well as in kidney (only mouse). The expression level of these calbindins in kidney and intestine is closely correlated with the efficiency of Ca^{2+} (re)absorption and, therefore, these proteins play a central role in the facilitated diffusion model. Second, a vesicular model was proposed in which the absorptive cells use lysosomes to sequester Ca^{2+} and facilitate its movement to the basolateral membrane (230). Formation of Ca^{2+} -enriched vesicles is initiated by influx of Ca^{2+} through Ca^{2+} channels in the apical or luminal membrane. The rapid increase in Ca^{2+} concentrations in close vicinity to the apical membrane disrupts the actin filaments near the Ca^{2+} channels and initiates the formation of endocytic vesicles. Ca^{2+} bind to calmodulin (CaM) associated with myosin I or alternatively CaM-associated with the Ca^{2+} channels, which leads to inactivation of the channels. Inactivation of the Ca^{2+} channels causes a decrease in the free Ca^{2+} levels close to the apical membrane, and the actin filament network can be restored. The formed Ca^{2+} -containing vesicles are transported by microtubules and fuse with lysosomes (230). While calbindins have been found to associate with lysosomes, the role of these Ca^{2+} -binding proteins in this latter model is less clear. Experimental evidence suggests, however, an important role in epithelial Ca^{2+} transport, which is best described by the first model in which calbindin- $\text{D}_{9\text{K}}$ and calbindin- $\text{D}_{28\text{K}}$ facilitate the cytosolic diffusion of Ca^{2+} from the apical influx to the basolateral efflux sites and acts as cytosolic Ca^{2+} buffer to maintain low intracellular Ca^{2+} levels during changes in transcellular Ca^{2+} transport (35, 107, 108). Interestingly, calbindin- $\text{D}_{9\text{K}}$ may directly enhance plasma membrane Ca^{2+} -ATPase (PMCA) activity (417). Due to the relatively slow binding kinetics of these Ca^{2+} -binding

proteins, Ca^{2+} signaling can occur independently of transcellular Ca^{2+} movement mediated by calbindin- $\text{D}_{9\text{K}}$ and calbindin- $\text{D}_{28\text{K}}$ (218). Depending on the vitamin D state, the cytosolic calbindin-D concentration can reach values in the submillimolar range, which is indeed sufficient to fulfill the above-mentioned functions (see sect. VI A) (38, 106).

Previously, a homozygous mutant of calbindin- $\text{D}_{28\text{K}}$ gene-knockout mice was generated by gene targeting which developed normally (3, 23, 361, 362). These animals exhibited a two times higher urinary Ca^{2+} excretion compared with wild-type littermates, but no significant differences in serum Ca^{2+} , PTH, or in serum and urinary Mg^{2+} and phosphate were observed (361). This suggests that the hypercalciuria induced by calbindin- $\text{D}_{28\text{K}}$ deficiency is compensated by, for instance, increased intestinal absorption of Ca^{2+} . Renal calbindin- $\text{D}_{9\text{K}}$ expression was not affected in these knockout mice. The cytosolic Ca^{2+} transport function of calbindin- $\text{D}_{9\text{K}}$ remains to be confirmed, since calbindin- $\text{D}_{9\text{K}}$ knockout mice have not been generated until now.

The calbindins, like CaM, belong to a group of intracellular proteins that bind Ca^{2+} with high affinity and undergo structural changes upon binding (33). Each calbindin is encoded by a separate gene, and there is no direct association between the two genes. In fact, nature has produced a wide variety of EF-hand Ca^{2+} -binding proteins (i.e., calbindin- $\text{D}_{9\text{K}}$, calbindin- $\text{D}_{28\text{K}}$, CaM, parvalbumin, S100, troponin C) that display minor overall sequence homology (307). An important functional feature of CaM and troponin is their ability to interact with and regulate the function of voltage-gated Ca^{2+} channels in a Ca^{2+} -dependent fashion. The ubiquitously expressed CaM directly interacts with an IQ motif present in the carboxy termini of these channels where it functions as a Ca^{2+} sensor (358). This IQ motif is, however, not present in TRPV5 and TRPV6. At present, it is unknown whether calbindin- $\text{D}_{9\text{K}}$ or calbindin- $\text{D}_{28\text{K}}$ could fulfill a similar Ca^{2+} sensor function for which a specific interaction with TRPV5 and/or TRPV6 would be required. Freud and Christakos (118) reported an interaction of calbindin- $\text{D}_{28\text{K}}$ with microsomal membranes in kidney (118), whereas Shimura and Wasserman (351) showed that calbindin- $\text{D}_{28\text{K}}$ is associated with purified chicken intestinal brush-border membranes. Together with the striking colocalization of calbindin- $\text{D}_{9\text{K}}$ and/or calbindin- $\text{D}_{28\text{K}}$ in all TRPV5/6-expressing tissues, this suggests a functional interaction between these two proteins. Future experiments are needed to delineate whether the function of calbindin is restricted to its buffer capacity maintaining low Ca^{2+} concentrations in close vicinity of the channel mouth or whether a physical interaction between calbindin and TRPV5/6 is needed to exert a direct regulatory function.

C. Extrusion Mechanisms

The efflux of Ca^{2+} occurs against a considerable electrochemical gradient, and two Ca^{2+} transporters have been located in the basolateral membrane of absorptive cells to extrude Ca^{2+} , i.e., a $\text{Na}^+/\text{Ca}^{2+}$ exchange mechanism (NCX) and a Ca^{2+} -ATPase (PMCA).

1. The $\text{Na}^+/\text{Ca}^{2+}$ exchanger

To date, three genes for NCX, designated *NCX1*, *NCX2*, and *NCX3*, have been identified in mammals. Similarities between these proteins include a homology of ~70% sequence identity, the presence of an amino-terminal signal sequence, two sets of multiple transmembrane α -helices near the ends of the protein, and a large intracellular loop (46, 340). Splicing of RNA transcripts is a general characteristic of the NCX genes in mammals to generate diversity. Reilly and Shugrue (325) published the sequence of the rabbit kidney NCX1, and in kidney the expression of this transporter is restricted to the distal part of the nephron where it is predominantly localized along the basolateral membrane (40, 171, 240). NCX1 is widely distributed in many different mammalian tissues, whereas NCX2 and NCX3 are only expressed in brain and skeletal muscle (236, 275). Unfortunately, specific inhibitors of NCX1 are not available to substantiate the relative importance of this exchanger for overall Ca^{2+} reabsorption. Bindels and co-workers (39, 391) demonstrated that NCX1 is the primary extrusion mechanism, whereas only a minor amount of Ca^{2+} in the distal tubular cells is extruded by the plasma Ca^{2+} pump. NCX1 is also expressed in the basolateral membrane of the enterocytes (164, 210, 387). In fish enterocytes, NCX appears to be the main mechanism by which transcellular Ca^{2+} fluxes are extruded from the cells at the basolateral surface, whereas in mammals PMCA is the predominant extrusion mechanism (115, 164, 337, 387). Together these functional studies suggest that in kidney, basolateral Ca^{2+} extrusion is mainly carried out via NCX1, whereas $\text{Na}^+/\text{Ca}^{2+}$ exchange seems of minor importance in the small intestine. Recently, it was demonstrated that targeted deletion of *NCX1* results in *NCX1*-null embryos that do not have a spontaneously beating heart and die in utero (219, 327). Therefore, this animal model is, unfortunately, not suitable to verify the importance of NCX1 in renal epithelial Ca^{2+} transport.

In addition, several K^+ -dependent $\text{Na}^+/\text{Ca}^{2+}$ exchangers (NCKX) have been described (46, 308). Northern blot analysis demonstrated that some isoforms [i.e., NCKX4 (235) and NCKX6 (65)] of this family are expressed in epithelia including small intestine and kidney. Ubiquitous expression of these exchangers in various tissues suggests a key role in regulating intracellular Ca^{2+} homeostasis in mammalian cells. It remains to be estab-

lished whether these transporters play a role in epithelial Ca^{2+} transport.

2. Regulation of NCX

Kimura et al. (212) were the first to directly measure a NCX current. Their experiments were carried out in guinea pig cardiac myocytes and provided evidence that the NCX exchanger actually generates a measurable membrane current in which the exchanger can translocate a net positive charge across the plasma membrane (100). The stoichiometry of NCX has been investigated by several groups, and calculations varied from 3 $\text{Na}^+ : 1 \text{Ca}^{2+}$ (15) to 4 $\text{Na}^+ : 1 \text{Ca}^{2+}$ (266, 267), indicating that this transporter is electrogenic. Comprehensive functional studies in oocytes and mammalian cell systems indicated that NCX is regulated by several factors including the membrane potential, PKC activation, protons, nucleotides, and calciotropic hormones (46).

Interestingly, it has been shown that NCX1 is regulated by PTH. Functional data demonstrated that PTH markedly stimulates Ca^{2+} reabsorption in the distal part of the nephron primarily by augmenting NCX1 activity via a cAMP-mediated mechanism.

However, the exact mechanism by which PTH activates the exchanger remains controversial. Initial experiments suggested that the kidney isoform of NCX1 is poorly activated by PKA (161). In another study, it was found that PTH does not affect the intracellular Ca^{2+} concentration (312), indicating that the activation of NCX1 cannot be explained by increased substrate availability. Moreover, it was postulated that PTH increases Cl^- conductance in DCT cells leading to decreased intracellular Cl^- activity and membrane hyperpolarization (137). Hyperpolarization of the basolateral membrane will increase the $\text{Na}^+/\text{Ca}^{2+}$ exchange rate. Therefore, coactivation of apical Ca^{2+} entry through TRPV5 occurs under conditions that are favorable for basolateral Ca^{2+} extrusion (see also sect. iv). Other studies on isolated basolateral membrane vesicles implied that the PTH-induced rise in the intracellular Ca^{2+} concentration is not required for the stimulatory effect of PTH (195). Whether PTH stimulation affects expression of the NCX1 mRNA or the protein itself is not known. In addition to PTH, the calciotropic hormone $1,25\text{-(OH)}_2\text{D}_3$ also regulates the renal expression of NCX1. Studies in vitamin D-deficient knockout models showed an impressive downregulation of NCX1 mRNA that could be normalized by $1,25\text{-(OH)}_2\text{D}_3$ supplementation (sect. vi) (169). In these animal models there was no significant downregulation of PMCA in line with a primary role of NCX in Ca^{2+} extrusion. These findings point to a supportive role of the exchanger in vitamin D-stimulated Ca^{2+} reabsorption.

3. PMCA

PMCA is a high-affinity Ca^{2+} efflux pump present in virtually all eukaryotic cells, wherein they are responsible for the maintenance and resetting of the resting intracellular Ca^{2+} levels (45). Four genes encode separate isoforms designated *PMCA1–4*. In addition, alternative splicing of the transcripts yields a large variety of splice variants differing mainly in their carboxy-terminal amino acid sequence (365, 369). PMCA is a universal system for the extrusion of Ca^{2+} in cells. In kidney, PMCA is, in contrast to NCX, present in all nephron segments with highest expression in the basolateral membrane of cells lining the distal part of the nephron. Compared with other nephron segments, the distal convoluted tubule (DCT) possesses the highest Ca^{2+} -ATPase activity (95) and exhibits the strongest immunocytochemical reactivity for PMCA protein expression (48, 49, 245). Studies at the transcript level using RT-PCR and advanced tissue microdissection techniques indicated that all four PMCA isoforms are distinctively expressed in the kidney, and variable abundance of the individual isoforms along the different regions of the nephron has been documented (369). Other studies using RT-PCR on whole kidney RNA as well as studies at the protein level have been controversial but suggested that PMCA1 and PMCA4 are the major isoforms expressed in the kidney, while PMCA2 and PMCA3 may be minor components (246). Based on the fact that PMCA1 and PMCA4 are widespread, while PMCA2 and PMCA3 are more tissue specific, it has been suggested that PMCA1 and PMCA4 are housekeeping isoforms involved in the maintenance of cellular Ca^{2+} homeostasis (365). At variance with this conclusion is the observation that PMCA1b transcripts were definitely observed in rabbit CNT and CCD, whereas expression of the PMCA2 isoform was not (171, 213). In addition, Kip and Strehler (213, 214) demonstrated in Madin-Darby canine kidney (MDCK) cells that PMCA4b plays a significant role in basolateral Ca^{2+} extrusion. Furthermore, PMCA1b is the predominant isoform and abundantly expressed in the small intestine, where NCX1 is expressed at a low level. These data suggest indirectly that PMCA1b is the principal Ca^{2+} extrusion mechanism in intestinal Ca^{2+} absorption.

4. Regulation of PMCA

In general, there is only limited data available regarding the regulation of PMCA by hormones or signaling mechanisms. Several studies indicated that PMCA is positively regulated by $1,25\text{-(OH)}_2\text{D}_3$ in the intestine to increase Ca^{2+} absorption. Cai et al. (64) addressed the effect of vitamin D on the synthesis of the chicken intestinal PMCA mRNA. Northern blot analysis indicated that repletion of vitamin D-deficient chickens with vitamin D increases PMCA mRNAs in the duodenum, jejunum, ileum, and colon. After injection of $1,25\text{-(OH)}_2\text{D}_3$ intrave-

nously in these deficient chickens, duodenal PMCA mRNA tended to increase by 2 h, reached a maximum at ~16 h, and returned to baseline levels at 48 h (64). These results were confirmed by Johnson and Kumar (199), who demonstrated that $1,25\text{-(OH)}_2\text{D}_3$ causes an increase in abundance of the PMCA and stimulates Ca^{2+} -pumping activity. Kip and Strehler (214) showed that $1,25\text{-(OH)}_2\text{D}_3$ upregulates the expression of the PMCA (mainly PMCA4b) in MDCK cell lysates in a time- and dose-dependent manner. Interestingly, $1,25\text{-(OH)}_2\text{D}_3$ caused a decrease of the PMCA in the apical plasma membrane fraction and a concomitant increase of the number of pumps in the basolateral membrane. Functional transport assays demonstrated that transcellular $^{45}\text{Ca}^{2+}$ flux from the apical-to-basolateral compartment was significantly enhanced by $1,25\text{-(OH)}_2\text{D}_3$. These findings confirm that $1,25\text{-(OH)}_2\text{D}_3$ is a positive regulator of the PMCA in MDCK cells.

Prince and colleagues (90) demonstrated a stimulatory effect of estrogen and dihydrotestosterone on PMCA activity measured in isolated vesicles from Madin-Darby bovine kidney cells (MDBK) with a magnitude comparable to that of $1,25\text{-(OH)}_2\text{D}_3$. Unlike $1,25\text{-(OH)}_2\text{D}_3$, which stimulates PMCA protein expression in MDBK cells, neither estrogen nor dihydrotestosterone increased PMCA protein expression (90). This suggests that these latter hormones regulate Ca^{2+} transport by increasing PMCA activity, rather than by increasing PMCA protein abundance. Furthermore, PMCA activation is dependent on CaM, and inhibition of CaM is in turn known to prevent PMCA stimulation. In MDCK cells, trifluoperazine and calmidazolium, two inhibitors of CaM, decreased the Ca^{2+} transport by 45 and 33%, respectively (213). Kip et al. (213) used a variety of agents known to inhibit the PMCA in these cells to determine the contribution of the Ca^{2+} pump to transcellular Ca^{2+} flux. Interestingly, ~30% of this flux was due to PMCA and the remaining flux depended on a $\text{Na}^+/\text{Ca}^{2+}$ exchange process. These results are in line with the dominant role of NCX1 in transcellular Ca^{2+} flux studies in cultured rabbit kidney cells isolated from CNT and CCD (39).

IV. EPITHELIAL CALCIUM CHANNELS

A. Molecular Diversity

TRP channel proteins constitute a large and diverse family of proteins that are expressed in many tissues and cell types (74, 256). The large functional diversity of TRPs is reflected in their diverse permeability to ions, activation mechanisms, and involvement in biological processes ranging from pain perception to male aggression. Mammalian homologs of the *Drosophila* TRP gene encode a family of at least 20 ion channel proteins (Fig. 2). They are

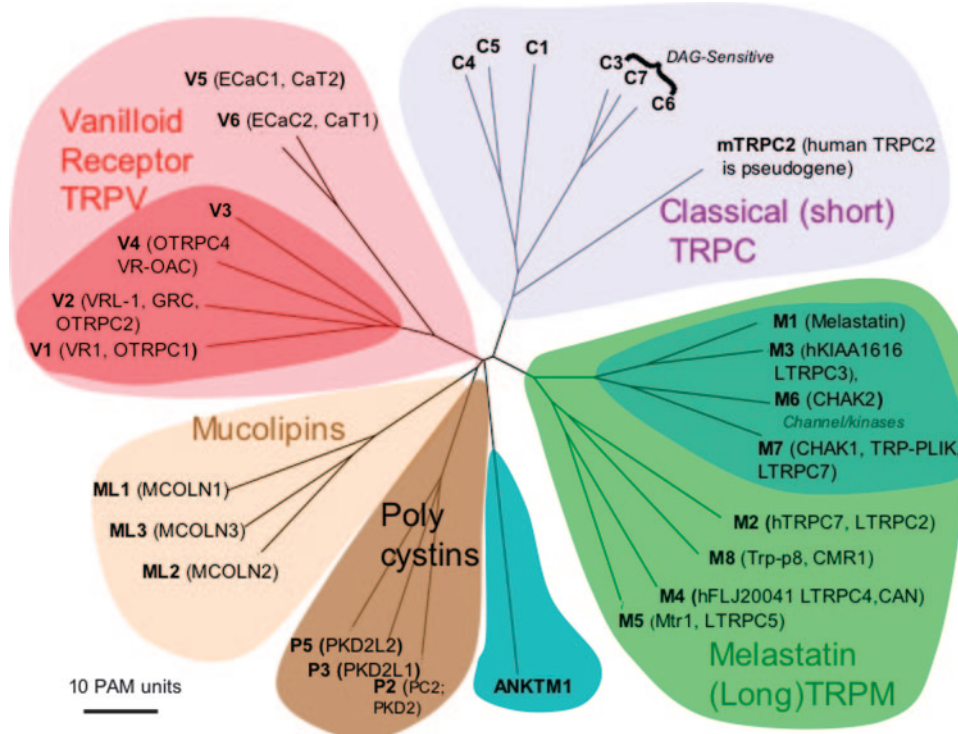


FIG. 2. Mammalian TRP family tree. The evolutionary distance between the TRP channels is shown by the total branch lengths in point accepted mutations (PAM) units, which is the mean number of substitutions per 100 residues. The tree was calculated using the neighbor-joining method for human, rat, and mouse sequences. [From Clapham (74).]

widely distributed in mammalian tissues, but most of their specific physiological functions are largely unknown. The molecular structure that is conserved among all members of the TRP family is a channel subunit, containing six TM spanning domains and a pore region loop, that most prob-

ably assemble into tetramers to form unique ion channels allowing the influx of cations into cells (Fig. 3A) (182). The TRP channels can be divided by sequence homology into at least six subfamilies, designated TRPC (canonical or classical), TRPV (vanilloid), TRPM (melastatin), TRPP

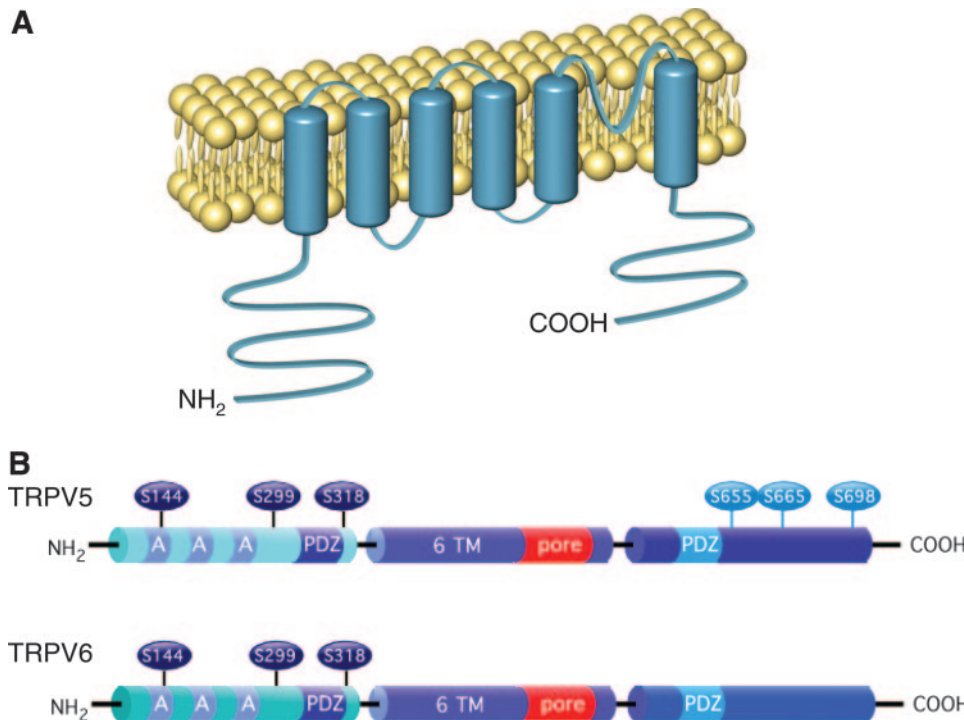


FIG. 3. Structural organization of TRPV5 and TRPV6. A: the epithelial Ca^{2+} channels are 730 amino acids long with a predicted molecular mass of 83 kDa. TRPV5 and TRPV6 contain a core domain consisting of 6 transmembrane (TM) segments. In addition, a large cytosolic amino and carboxy terminus are present containing ankyrin repeats. Between TM5 and TM6 there is a short hydrophobic stretch predicted to be the pore-forming region of these channels. Inner and outer side of the membrane is indicated. B: potential regulatory sites in the amino and carboxy tail of TRPV5 and TRPV6 including ankyrin repeats and PDZ motifs and conserved PKC phosphorylation sites.

(polycystins, PKD-type), TRPA (for ankyrin), TRPML (for mucolipin), and the more distant subfamily TRPN (N for “nomp” no mechano-receptor potential). ANKTM1, a new member of the TRP ion channel family recently implicated in the detection of noxious cold, is sufficiently different from members of the other TRP subfamilies to warrant assigning this protein to a new subfamily, referred to as TRPA (201, 368). While there is only one mammalian TRPA member, there are four in flies and two in worms (74, 77). To maintain consistency with the rest of the TRP nomenclature, it is recommended to refer to ANKTM1 as TRPA1 in future studies as suggested and approved by the HUGO nomenclature committee. Polycystic kidney disease is an autosomal-dominantly inherited disease causing progressive development of cysts in the kidney and liver (268, 269). Nearly all cases result from mutations in either *PKD1* or *PKD2* genes, both of which encode proteins of the TRP family. *PKD1* and *PKD2* are usually lumped together in the TRPP branch, but the two groups have a markedly different molecular architecture and represent distinct phylogenetic branches of the superfamily. *PKD1* is a very large protein of 12 TM segments, whereas *PKD2* has the predicted topology of the TRP channel consisting of 6 TM spanning domains and clearly conduct ions (156). Importantly, TRPP channels are mainly expressed in ciliated epithelial cells (270).

Sequence alignments revealed that TRPC, TRPM, and TRPV, but not the TRPP channels, contain a characteristic six-amino acid motif located in the carboxy terminus (41). An intriguing subfamily within the TRP superfamily is the TRPV subfamily consisting of six members. This group of channels includes TRPV1–4, which respond to heat, osmolarity, odorants, and mechanical stimuli, whereas epithelial Ca^{2+} channels TRPV5–6 have been implicated in maintaining the body Ca^{2+} balance by facilitating Ca^{2+} (re)absorption in kidney and small intestine (175, 180, 302).

The epithelial Ca^{2+} channel family is restricted to two members, and genomic cloning demonstrated that these Ca^{2+} channels are transcribed from distinct genes rather than being splice variants (181, 301). *TRPV5* and *TRPV6* are juxtaposed on the human chromosome 7q35 with a distance of only 22 kb, which suggests an evolutionary gene duplication event. The same situation was observed in the mouse genome in which *TRPV5* and *TRPV6* are localized on chromosome 6 in a region that is syntenic to human chromosome 7q33–35 (180, 301). There is one other example found as a direct repeat of two homologs TRP channels. Comparable to the TRPV5/6 couple, *TRPV3* is located juxtaposed the *TRPV1* gene at a distance of 7.5 kb (41). To date, TRPV5 and TRPV6 have been cloned from many species including rabbit, rat, mouse, and human (181). The identified sequences exhibit an overall homology of ~75%. Strikingly, several domains in TRPV5/6 are completely conserved within these species including the core structure of the protein consisting

of 6 TM segments and the pore region, ankyrin repeats, PDZ motifs, and putative PKC phosphorylation sites, of which three are conserved among all identified TRPV5/6 channels (Fig. 3A). Detailed sequence analysis of TRPV5 and TRPV6 revealed the identification of several putative phosphorylation sites including PKC, PKA, and cGMP-dependent kinase (89). For instance, in rabbit TRPV5, two combined putative phosphorylation sites for PKA and cGMP-dependent kinase (S669 and T709) were originally identified (178). However, these predicted phosphorylation sites are not conserved in other species or in TRPV6. This is in contrast to the putative PKC phosphorylation sites of which three are conserved within the complete TRPV5/6 subfamily (Fig. 3A) (181). However, the physiological relevance of the conserved PKC sites is not clear, since mutations of these putative regions did not affect channel activity in HEK293 cells (Hoenderop and Bindels, unpublished data). To date, no information is available about the phosphorylation of TRPV5 and TRPV6. In addition, TRPV5 and TRPV6 contain PDZ motifs and ankyrin repeat domains in the amino-terminal region, which are also present in a diverse range of receptors and ion channels including the TRP superfamily. PDZ motifs are recognized by PDZ domains that are modular protein interaction domains playing a role in protein targeting and protein complex assembly (292). There is evidence that they can regulate the functions of their ligands in addition to serving as scaffolds. Although binding to carboxy-terminal motifs appears to be the typical mode of interaction, PDZ domains could also interact with internal motifs that are present in TRPV5/6. In general, ankyrins link transporters and cell adhesion molecules to the spectrin-based cytoskeletal elements in specialized membrane domains (197). Neural-specific isoforms of ankyrin have been demonstrated to participate in the maintenance and targeting of ion channels to subcellular regions in cells (217). So far, no PDZ domain- or ankyrin domain-interacting proteins have been identified.

B. Ion Selectivity/Gating Mechanisms

1. Basic biophysical properties

The conspicuous biophysical hallmarks of TRPV5, which are also representative for TRPV6, are shown in Figure 4 (181, 444). In HEK293 cells heterogeneously expressing TRPV5, currents through TRPV5 can be activated under conditions of high intracellular buffering of Ca^{2+} by hyperpolarizing voltage steps. In the absence of divalent cations, large inward currents are observed, which show a typical time-dependent increase (“gating”) and are constant over more than 1 min (Fig. 4A). Outward currents are extremely small, indicating that the channel is nearly completely inwardly rectifying. In the presence of Mg^{2+} , but the absence of Ca^{2+} , the initial currents are

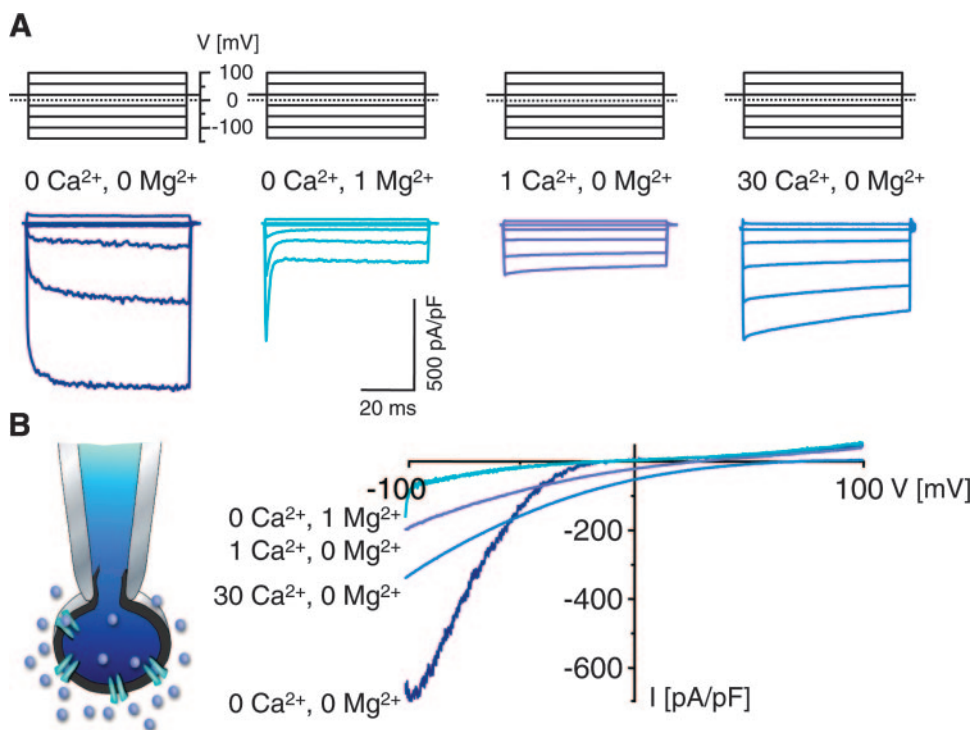


FIG. 4. Hallmarks of currents through TRPV5. *A*: currents are activated in HEK293 cells transfected with TRPV5. Holding potential is +20 mV; test steps were applied from +140 to -100 mV in 40-mV increments. Extracellular ionic conditions are changed from *left to right*: nominally Ca²⁺- and Mg²⁺-free extracellular solution, nominally Ca²⁺-free solution with 1 mM free Mg²⁺, 1 mM Ca²⁺ but nominally free Mg²⁺, 30 mM Ca²⁺ in a nominally Mg²⁺-free solution. Note the increase in current due to elevation of the extracellular Ca²⁺ concentration and the fast inhibition (block) in the presence of Mg²⁺. Same calibration was used for all current protocols. *B*: current-voltage (*I-V*) relationships from the same cell as shown in *A*. Ionic conditions are indicated at the *left* of each *I-V* curve. Note the rightward shift of the reversal potential for increased extracellular [Ca²⁺]. The fast current decay in 1 mM Mg²⁺ reflects the fast inactivation seen in the step protocol. [Modified from Vennekens (403).]

large and rapidly inactivate due to block by extracellular Mg²⁺, which is driven into the open pore by the hyperpolarizing voltage. In the presence of Ca²⁺, but in a nominally Mg²⁺-free solution, currents through TRPV5 increase again when the extracellular Ca²⁺ concentration is elevated. If the extracellular Ca²⁺ concentration is changed from 0 to 30 mM, then 1) increasing extracellular Ca²⁺ up to 100 μ M reduces the current amplitudes through TRPV5/6, and 2) an increase from an extracellular Ca²⁺ concentration of 100 μ M up to 30 mM or higher enhances the current again. This finding is reminiscent of the anomalous mole fraction behavior described previously for L-type voltage-gated Ca²⁺ channels (4, 85, 163). In analogy to L-type Ca²⁺ channels, permeation through TRPV5/6 can be described by "repulsion" pore models considering a pore consisting of two high-affinity binding sites, whereby the double occupation of the two binding sites by either Na⁺ or Ca²⁺ provides the "drive" for Ca²⁺ conduction due to mutual repulsion of the two cations (403, 406) or by a three binding-site model in which two low-affinity sites flank a high-affinity binding site for Ca²⁺ (181, 403, 406). The current through TRPV5/6 is carried exclusively by Ca²⁺ at extracellular Ca²⁺ concentrations exceeding 10 μ M.

Figure 5 shows single-channel data for Na⁺ currents through TRPV5 in inside-out patches. Current-voltage relationships show inward rectification also at the level of single channels. Conductance between -200 and -100 mV is \sim 75 pS, whereas between -100 and +20 mV values were obtained of \sim 35 pS (Fig. 5A). So far, no reliable single-channel measurements have been performed in the

presence of extracellular Ca²⁺. Ensembled currents show a similar time course as macroscopic currents including a gating phase at the beginning of the hyperpolarizing voltage step (Fig. 5B). The range of single-channel conductances for monovalent cations are all in a similar range between 40 and 70 pS and are obviously, although not compared in detail under identical condition, similar for TRPV5 and TRPV6 (285, 402, 444). These values are important in regard to the controversy of whether TRPV6 might form the CRAC pore (see below). Another typical feature of currents through TRPV5/6 is the inactivation at negative potentials (Fig. 6). This inactivation is nearly complete if Ca²⁺ is the charge carrier and is delayed when Ba²⁺ substitutes Ca²⁺ (Fig. 6A). Currents of monovalent cations through TRPV5/6 do not inactivate. This feature is typical for a Ca²⁺-dependent component of inactivation. Repetitive stimulation of TRPV5/6 currents by short hyperpolarizing pulses consequently result in a decay of the current (Fig. 6B). The respective current-voltage relationships are shown in Figure 6, *C* and *D*. The slow recovery from inactivation in divalent cation-free solution after the Ca²⁺-dependent decay is a further typical hallmark of TRPV5/6 channels. The time to 50% recovery from inactivation, dependent on the size of the Ca²⁺ inward currents, is in the range of 1–2 min for TRPV5 and between 40 and 60 s for TRPV6.

Although all the above-described structural aspects and basic electrophysiological properties of TRPV5 and TRPV6 are rather similar, some differences remain which concern permeability of divalent cations, kinetics of Ca²⁺-

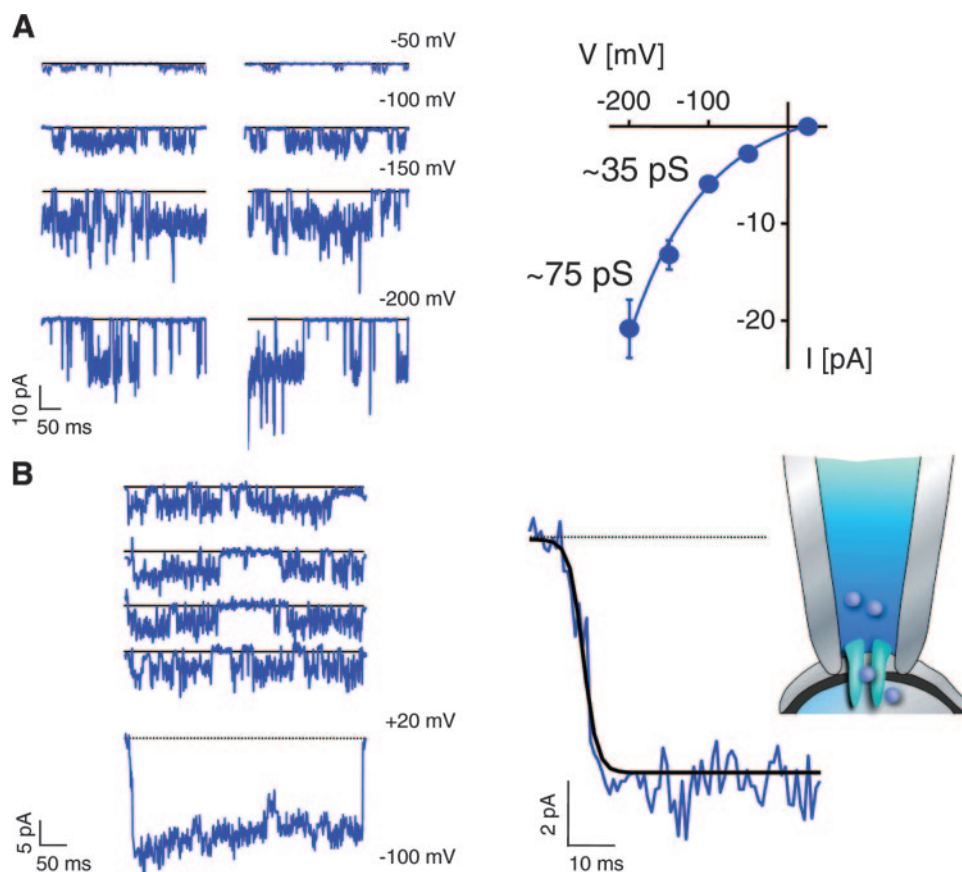


FIG. 5. Single-channel currents through TRPV5 channels. *A*: Na^+ currents through TRPV5 channels in cell-attached patches. Cells were zeroed in an isotonic extracellular K^+ solution. Pipette solution contains 140 mM Na^+ in the absence of Ca^{2+} and Mg^{2+} , 5 mM EDTA. Two consecutive sweeps are shown for potentials. From amplitude histograms, single-channel current-voltage relationships were constructed (*I-V*). Conductance was measured from the *I-V* slope between -200 and -100 mV and -100 and $+20$ mV. Estimation of the single-channel conductance is 75 and 35 pS, respectively. Note that also at the single-channel level inward rectification occurs. *B*: ensemble-averaged current from 82 sweeps for a voltage step from $+20$ mV to -100 mV. Note the similarities between ensemble-averaged current and whole cell currents. Increasing the time resolutions (*right*) unmasks a slow gating behavior at the single-channel level as shown in the whole cell experiment step. (From B. Nilius, unpublished data.)

dependent inactivation, and recovery from inactivation (Fig. 7). Interestingly, these typical differences could be explained by sequence differences between TRPV5 and TRPV6. Ba^{2+} permeates TRPV5 better than TRPV6, e.g., the current ratio $I_{\text{Ba}}/I_{\text{Ca}}$ is ~ 0.9 for TRPV5, but only 0.4 for TRPV6. TRPV6 clearly shows a fast component of inactivation, which is less obvious for TRPV5, e.g., time to 10% inactivation at hyperpolarizing steps to -100 mV is ~ 125 ms for TRPV5 but only ~ 40 ms for TRPV6. More dramatic are the kinetic differences when Ba^{2+} is the charge carrier. Fast inactivation is about twofold prolonged when Ca^{2+} is substituted by Ba^{2+} for TRPV5, but ~ 20 times for TRPV6 (Fig. 8) (281). Interestingly, the structural determinants of these differences seem not to be located in either the amino or carboxy terminus, but in the TM2-TM3 linker. Swapping of the TM2-TM3 linker of TRPV6 to TRPV5 confers the kinetic and permeation phenotype of TRPV6 to TRPV5, whereas swapping of the amino or carboxy termini is ineffective (Fig. 7, *A* and *B*) (281). Interestingly, this first intracellular loop is entirely encoded by one exon and could, therefore, provide an example of how a single exon may alter function (302). Furthermore, functional differences concern the recovery from Ca^{2+} -dependent inactivation, which is about three times slower for TRPV5 compared with TRPV6 (181). Changes in the inactivation phase of TRPV6 have been

reported by mutations of the histidine residue H587 in the carboxy terminus close to TM6 of TRPV6, which is not present in TRPV5 (375). This residue might be involved in the fast inactivation of TRPV6 (302, 375). Also, some striking pharmacological differences are present, e.g., ruthenium red is a 100-fold more potent blocker for TRPV5 than TRPV6 ($\text{IC}_{50} \sim 9 \mu\text{M}$ for TRPV6 but ~ 100 nM for TRPV5) (Fig. 7*C*). TRPV5 is about four times more sensitive to block by Cd^{2+} than TRPV6 ($\text{IC}_{50} \sim 70$ nM for TRPV5 but ~ 260 nM for TRPV6) (182).

2. Pore properties

TRPV5 and TRPV6 are so far the only known highly Ca^{2+} -selective channels in the TRP superfamily. This unique permeation property is also not conserved in the TRPV subfamily, which shares the highest homology with TRPV5/6. TRPV1-4 are, however, all Ca^{2+} and Mg^{2+} permeable, but discriminate much less between divalent and monovalent cations, e.g., the relative selectivity for Ca^{2+} and Mg^{2+} over Na^+ is between $P_{\text{Ca}}/P_{\text{Na}} = 1-10$ (TRPV1-TRPV4) and $P_{\text{Mg}}/P_{\text{Na}} = 2-3$ (only measured for TRPV4) (32, 155, 287, 411). TRPV5/6 display $P_{\text{Ca}}/P_{\text{Na}}$ values of >100 . Permeation of monovalent cations is $\text{Na}^+ > \text{Li}^+ > \text{K}^+ > \text{Cs}^+$ (181, 285, 286, 404, 406). This refers to an Eisenman sequence X for a strong field-strength binding

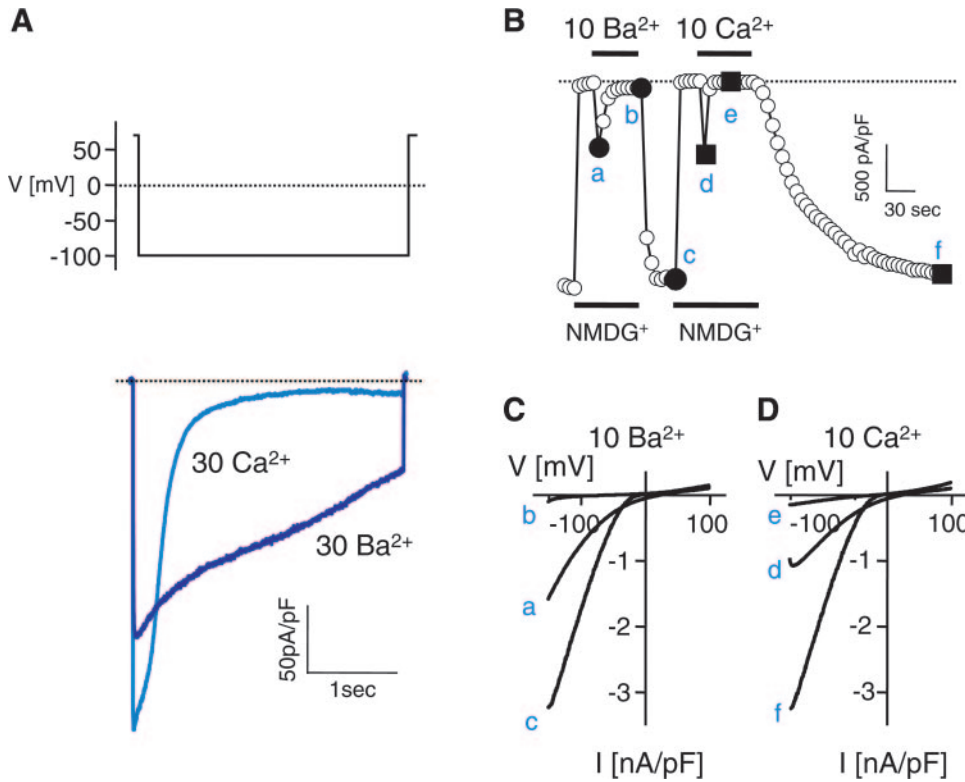


FIG. 6. Ca^{2+} and Ba^{2+} currents through TRPV5 and recovery from inactivation. *A*: during 3-s hyperpolarizing pulses from +70 to -100 mV, large currents are activated in the presence of 30 mM Ca^{2+} and Ba^{2+} as the only charge carrier. Note that Ca^{2+} currents inactivate much faster than Ba^{2+} currents. *B*: inactivation can also be monitored by application of 400-ms voltage ramps from -100 to +100 mV, with 5-s intervals between the ramps. Currents were measured at -100 mV. If Ba^{2+} and Ca^{2+} are the only charge carriers (all monovalent cations substituted by NMDG⁺), currents decay rapidly and much faster in the presence of Ca^{2+} . However, recovery from inactivation monitored by the monovalent currents in the absence of divalent cations is much slower when Ca^{2+} was the charge carrier than with Ba^{2+} . *C*: *I-V* curve obtained from the protocol shown in *B* measured at the times indicated in *B*. Charge carrier is Ba^{2+} . Note the large monovalent currents and rightward shift of the reversal potential when Ba^{2+} is the charge carrier. *D*: same protocol as in *B* and *C*. However, Ca^{2+} is the charge carrier. Although *I-V* curves are very similar in *C* and *D*, the recovery from inactivation is strikingly different (Nilius et al., unpublished data). Letters refer to the time course shown in *B* and indicated by the same letters.

site (181, 285, 286, 406). For TRPV6, a sequence of $\text{K}^+ > \text{Na}^+ > \text{Li}^+$, e.g., Eisenman V or VI (304), has been reported which, however, seems to be unlikely given the identical pores of TRPV5/6. For divalent cations, a permeation sequence of $\text{Ca}^{2+} > \text{Ba}^{2+} > \text{Sr}^{2+} > \text{Mn}^{2+}$ has been reported (181, 305, 404, 406).

A striking and important feature of TRPV5/6 channels is the open pore blockage by intracellular Mg^{2+} (Fig. 9) (409, 410). In the absence of extracellular Ca^{2+} , hyperpolarizing voltage steps (prestep, Fig. 9A) activate inward currents with a slowly rising phase (“gating”) (Fig. 9B). If

after complete opening of the channels at negative potentials steps are applied to different test potentials, inward, but not outward, currents can be observed, indicating that TRPV5/6 channels nearly completely rectify. The typical current-voltage relationships, shown in Figure 9D, indicate that at negative potentials the intracellular Mg^{2+} concentration is ineffective and also an intrinsic rectification remains in the absence of Mg^{2+} . The plot of the instantaneous initial current after the negative test potential against the preceding variable prepotentials defines the fraction of open channels (or the apparent open prob-

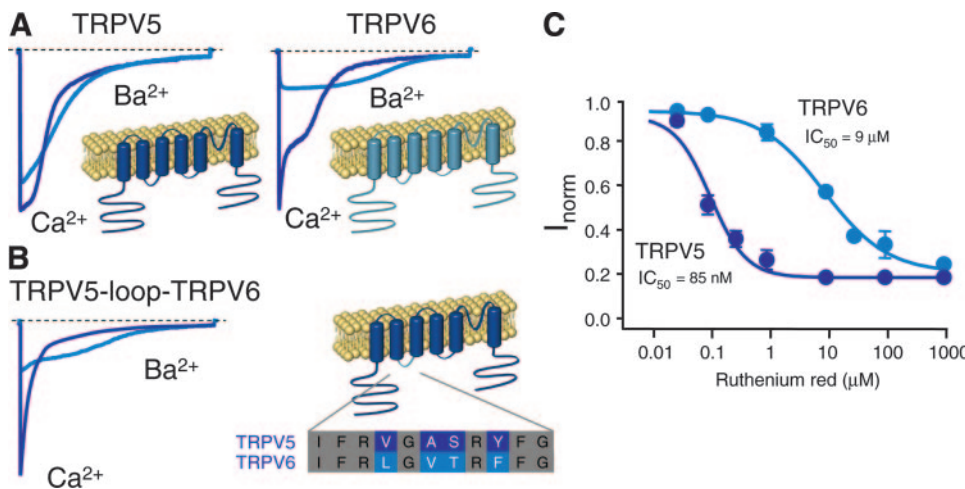


FIG. 7. Determinants of the fast component of inactivation of TRPV6. Functional differences between TRPV5 and TRPV6 include Ca^{2+} -dependent inactivation, Ba^{2+} selectivity (*A*), and ruthenium red block (*C*). Shown is the critical region responsible for the fast Ca^{2+} -dependent inactivation of TRPV6. Alignment depicts the distinctive amino acids within this intracellular loop (*B*).

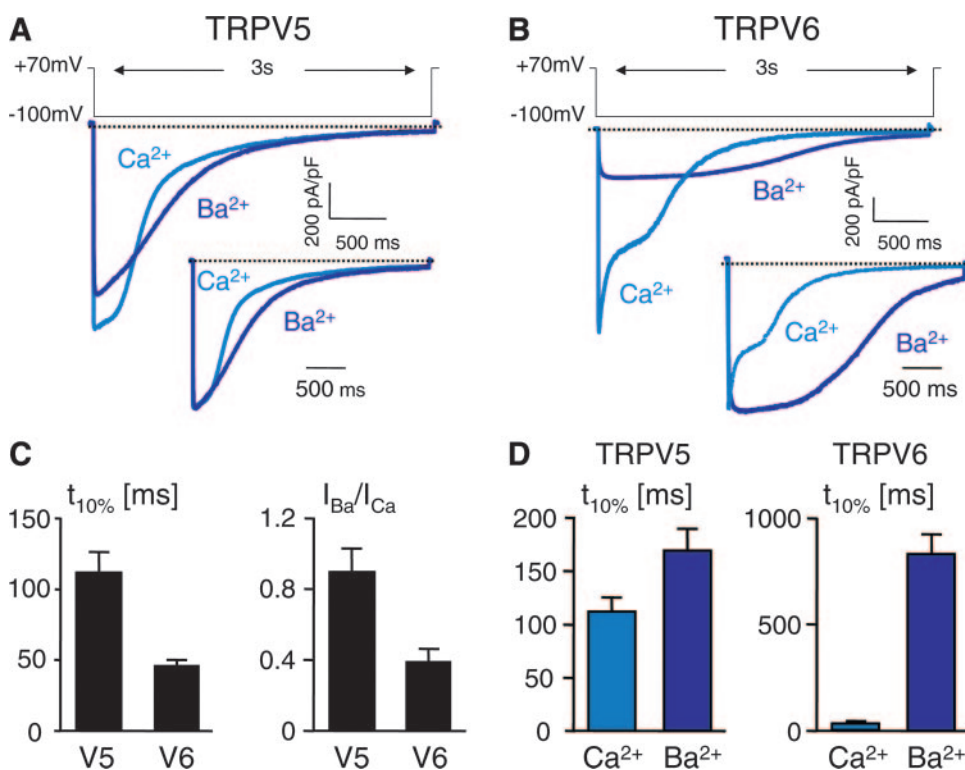


FIG. 8. Comparison of currents through TRPV5 and TRPV6. *A* and *B*: currents through TRPV5 and TRPV6 during a voltage step from +70 to -100 mV. Charge carrier is either Ca²⁺ (30 mM) or Ba²⁺ (30 mM). All of the other cations are substituted by 150 mM NMDG⁺. Cells were loaded with 10 mM BAPTA. *Insets* show currents normalized to the peak. *C*: data compare the time to 10% inactivation ($t_{10\%}$) during a voltage step as in *A* and *B* for currents through TRPV5 and TRPV6. Data compare the times to 10% inactivation when Ca²⁺ or Ba²⁺ is the charge carrier through TRPV5 (*left*) and TRPV6 (*right*). *D*: the time to 10% decay for Ba²⁺ and Ca²⁺ currents through TRPV5 (*left*) and TRPV6 (*right*).

ability, P_o) at the end of the prepotentials. Stepping back from the test potential to the prestep potential unmasks clear voltage dependence: at less negative potentials, partially blocked channels open time dependently due to unblock (voltage dependence). The number of available channels is decreased in a Boltzmann-type voltage dependence, which completely disappears in Mg²⁺-free intracellular solutions (Fig. 9*E*). These three features (i.e., gating, rectification, and voltage dependence) only appear in the presence of intracellular Mg²⁺. In the absence of intracellular Mg²⁺, gating and voltage dependence disappear, whereas rectification is still present, but diminished (Fig. 9*C*). An open pore blockage by intracellular Mg²⁺ explains the following findings: at depolarizing potentials, Mg²⁺ moves towards the pore, thereby plugging the permeation pathway for monovalent ions. Unblock occurs at hyperpolarizing voltages. At very large depolarization, Mg²⁺ is pushed through the pore, which results in a partial unblock of the channels (increased apparent P_o , Fig. 9*E*). These results are crucial to understand the pore properties of TRPV5/6.

Significant progress in the identification of the molecular determinants of TRP channel pores and the understanding of the high selectivity for Ca²⁺ has been particularly achieved for TRPV5 and TRPV6 channels (286, 404, 406, 409, 410). Structural differences in the channel pore explain the striking permeation differences in the TRPV subfamily. Figure 10*A* shows an amino acid sequence alignment of the putative pore regions of the three mammalian TRPV channels. Based on structural

similarity with the selectivity filter of the potassium channel KcsA ("signature sequence" *TTXTXGYGD*) (96), the structural determinant of the low Ca²⁺-selective TRPV1–4 channels is the GM(L/M)GD motif in TRPV1–4 (287, 411, 446). The sequence similarities may indicate conserved pore structures for these cation channels. Importantly, this motif is missing in TRPV5/6. Instead, we have demonstrated that the molecular determinants of the Ca²⁺ selectivity and permeation of TRPV5/6 reside at a single aspartate residue (TRPV5-D542 and TRPV6-D541) present in the pore-forming region (Fig. 10*B*) (286, 409). Neutralization of these residues not only affects the high Ca²⁺ selectivity of TRPV5/6, but also drastically reduces their sensitivity to extracellular Cd²⁺ and abolishes Mg²⁺-dependent voltage-dependent gating of these channels (409, 410, 412). It thus appears that high Ca²⁺ selectivity in TRPV5 and TRPV6 depends on a ring of four aspartate residues in the channel pore, similar to the ring of four negative residues (aspartates and/or glutamates) in the pore of voltage-gated Ca²⁺ channels (Fig. 10*B*). Likely, D542/D541 is the narrowest part of the selectivity filter with a diameter of ~5.2 Å and forms part of the high-affinity binding site for Ca²⁺ and Mg²⁺ (408). A detailed analysis of the structure of the TRPV5 and TRPV6 pores has now been published (94, 407). To obtain insight in the pore architecture of TRPV6, a pore diameter of 5.4 Å was estimated from permeation studies. Mutating D541, a residue involved in high-affinity Ca²⁺ binding, altered the apparent pore diameter, indicating that this residue lines

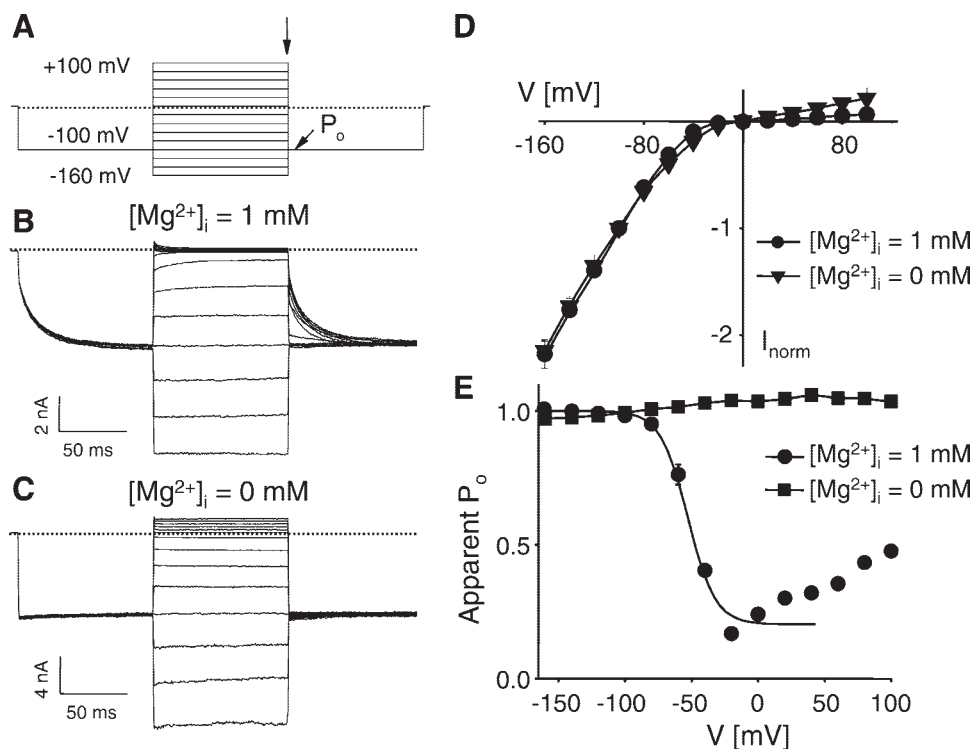


FIG. 9. Block by intracellular Mg^{2+} of monovalent currents through TRPV6. *A*: voltage protocol to activate monovalent currents through TRPV6. Holding potential is 0 mV; a 100-ms prestep to -100 mV is followed by 100-ms test steps to -160 to $+100$ mV (increment 20 mV). The arrows mark the time for measuring of the apparent open probability of TRPV6 dependent on the preceding test potential. *B*: voltage-dependent gating occurs in the presence of intracellular Mg^{2+} (1 mM). Note the strong inward rectification, e.g., almost no outward currents appear. The step back to the prestep potential as indicated in *A* shows a clear voltage dependence, e.g., currents are smaller at depolarized potential in time-dependently increase to the stationary level. *C*: same protocol as in *B*; however, pipette solution contains 10 mM EDTA and no Mg^{2+} . Note that gating and voltage dependence disappear. Rectification is less pronounced. *D*: average I - V relations obtained from this step protocol and normalized to the current at -100 mV. Shown are steady-state currents measured at the end of the test pulse (arrow in *A*). *E*: voltage dependence of the apparent open probability (P_o) is shown in the absence and presence of 1 mM intracellular Mg^{2+} . Apparent P_o of TRPV6 was determined from the inward current immediately after the 100-ms test pulses (arrow in *A*) and was normalized to the maximal inward current. Voltage dependence completely disappeared in the absence of intracellular Mg^{2+} . The solid line represent a Boltzmann fit through the first part of the V - P_o relationship (-160 to 0 mV, half-maximal inactivation at -52 mV, slope 9.5 mV, fraction open channels at $+20$ mV, 0.23). [Modified from Voets et al. (409).]

the narrowest part of the pore and is part of the selectivity filter (407). Pore lining amino acids were determined by cysteine scanning mutagenesis (SCAM). Cysteines introduced in a region preceding D542 for TRPV5 and D541 for TRPV6 displayed a cyclic pattern of reactivity to cysteine reacting agents indicative of a pore helix. The location of the cation-selective filter was identified at the outer part of the pore helix. The pattern of covalent modification of cysteines supports a KcsA homology-based three-dimensional model (96). The external vestibule in TRPV5 and TRPV6 may build up the three structural domains consisting of a coiled structure that is connected to a 15-amino acid pore helix followed by the selectivity filter (probably a coiled structure with D542 and D541 as the narrowest part) and another coiled structure before the beginning of TM6. This is the first structural model of a TRP channel pore.

The pore region of TRPV5/6 contains additional negatively charged amino acids (Fig. 10A) that only have minor effects on the Ca^{2+} permeation properties. In another study, the role of D542 for blockage of monovalent

currents through TRPV5 by Ca^{2+} and Mg^{2+} was supported, however, not for determining Ca^{2+} permeability (196). However, all of our data including recent findings from concatemers and a detailed study of TRPV6 pore properties clearly demonstrated the role of D542/D541 for Ca^{2+} selectivity (182, 286, 408, 409, 412). Another surprising result was the triple pore mutant F534/E535/L536 (84). This mutant has been reported to induce nonfunctional channels. However, any mutation of E535 was without effect for TRPV5 or TRPV6 permeation (196, 286, 408).

3. Mechanism of high Ca^{2+} selectivity

Our understanding of the pore properties of TRPV5/6 refers to the following mechanism of high Ca^{2+} selectivity, which is similar to the mechanisms of permeation by binding as proposed earlier for L-type Ca^{2+} channels (165, 381). Under Ca^{2+} -free conditions, Mg^{2+} will bind at a site within the channels, which is mainly determined by D542/D541. At low driving forces, e.g., less negative membrane

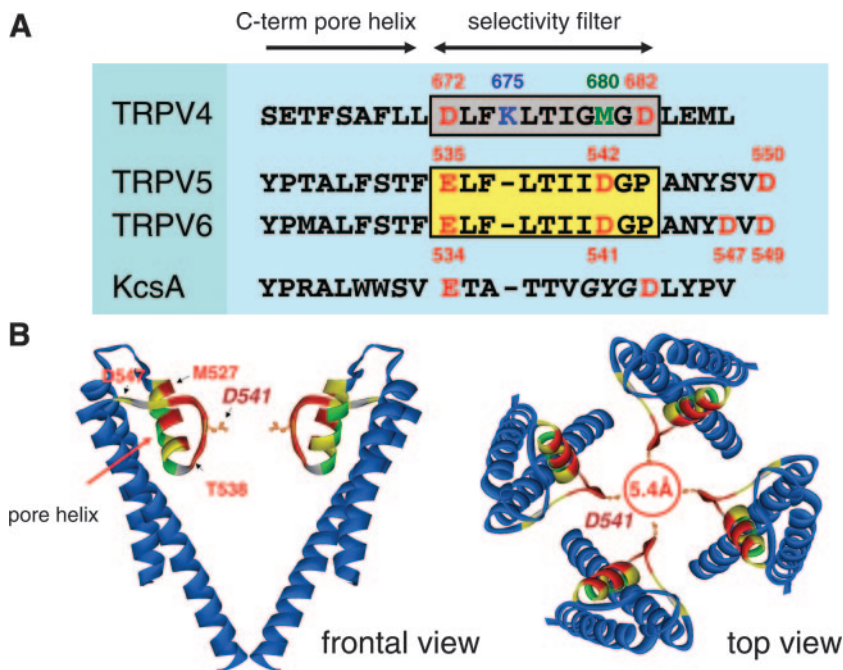


FIG. 10. Structure of the TRPV5/6 pore. *A*: alignment of the pore regions of TRPV4, -5, and -6 and the potassium channel KcsA (accession numbers AAG17543 for TRPV4, CAB40138 for TRPV5, AAD47636 for TRPV6, and S60172 for KcsA). The boxed sequences represent the putative selectivity of all channels. The amino-terminal part of this pore structure likely represents a putative pore helix. *B* and *C*: model for the TRPV6 pore region, based on the KcsA structure. Views of the structure are shown, looking sideways at two opposite subunits (*left*) or looking down from the external solution to the complete homotetrameric channel (*right*). At the narrowest point, formed by the acidic side chain of Asp-541 (orange), the pore has a diameter of 5.4 Å. Blue residues correspond to the residues in TM5 and TM6 (TM1 and TM2 in KcsA), whose accessibility was not tested in this study. Amino acids that were subjected to SCAM analysis (residues P526 to D547) are colored in green, yellow, red, or gray: residues in red reacted rapidly to Ag^+ (reaction rate $>5 \times 10^6 \text{ M}^{-1} \cdot \text{s}^{-1}$), residues in yellow reacted with Ag^+ at a rate $<5 \times 10^6 \text{ M}^{-1} \cdot \text{s}^{-1}$, and residues in green did not show significant reactivity to Ag^+ . Residues where cysteine substitution resulted in nonfunctional channels are marked in gray. The figure was prepared using DS ViewerPro 5.0 (Accelrys), based on the coordinates of KcsA.

potentials, the driving force is not sufficient to move Mg^{2+} out of this binding well and the channel is blocked. At hyperpolarization, Mg^{2+} will be moved from this high-affinity site, thereby allowing monovalent cations to permeate the channels. Vice versa, at very positive membrane potentials, Mg^{2+} will move through the pore towards the extracellular space. Because of the higher affinity of the binding site for Ca^{2+} versus Mg^{2+} , Ca^{2+} will outnumber Mg^{2+} at this site and is now blocking the pore for a movement of monovalent cations. If the inward driving force is high enough to remove Ca^{2+} from the high-affinity site, a fast inward permeation occurs supported by the low-affinity sites, which flank the high-affinity Ca^{2+} binding site. All our data so far support a crucial role of D542/D541 for establishing this functionally important site in the channel pore. The same mechanism has been reevaluated for tetrameric channels (182). Importantly, mutation of only one aspartate residue in the tetrameric channels already results in loss of Ca^{2+} selectivity and voltage dependence. Obviously, D542/D541 reflects a dominant effect on the unique pore properties of these Ca^{2+} channels.

4. Rectification

A nearly complete inward rectification is a further hallmark of the TRPV5/6 channels in addition to the high Ca^{2+} selectivity. This inward rectification is only partially due to blockage by Mg^{2+} , which is removed by hyperpolarization. Thus the most prominent part of rectification remains in the absence of intracellular Mg^{2+} and is not due to blockage by endogenous polyamines. This intrinsic

rectification of the channels is, however, dramatically reduced by neutralization of D542/D541, indicating that this site is also involved in rectification (409).

5. Gating

In the generally used overexpression systems, TRPV5/6 are constitutively open at a low intracellular Ca^{2+} concentration and negative voltage. The above-described mechanism of removing channel blockage by Ca^{2+} or Mg^{2+} is necessarily part of the gating mechanism. We cannot exclude other mechanisms that might influence gating of TRPV5/6. However, essential prerequisites of channel opening are 1) low intracellular Ca^{2+} to remove Ca^{2+} -dependent inactivation; 2) hyperpolarization, e.g., an increased driving force for the permeating cation which must be sufficient to move Ca^{2+} from the high affinity site; and 3) removal of the open pore blockage by Ca^{2+} and Mg^{2+} .

C. Modulation of Channel Activity

1. Intracellular Ca^{2+}

TRPV5 and TRPV6 are subject to Ca^{2+} -dependent feedback inhibition (282, 404). Both channels rapidly inactivate during hyperpolarizing voltage steps, and this inactivation is reduced when Ba^{2+} or Sr^{2+} was used as charge carriers. This inhibition was dependent on the extracellular Ca^{2+} concentration and occurred also in cells buffered intracellularly with 10 mM BAPTA. Currents also disappeared during repetitive activation by

short hyperpolarizing pulses. This decay of the current was significantly diminished when Ca^{2+} was replaced by Ba^{2+} as charge carrier and abolished when extracellular Ca^{2+} was lowered to 1 nM, again indicating that a Ca^{2+} -operated process inhibits TRPV5/6 activity. These regulatory processes were strongly influenced by the surrounding Ca^{2+} concentrations. Elevation of the extracellular Ca^{2+} concentration significantly increased the rate of current decay. Ca^{2+} influx is a prerequisite for this phenomenon because the Ca^{2+} -impermeable D542A mutant lacks a monovalent current decay in response to repetitive stimulation (282). These data suggest that the TRPV5/6 channels are downregulated by Ca^{2+} influx through the channel and thus likely by increasing the Ca^{2+} concentration in a microdomain near the pore region, thereby inducing feedback inhibition of the channel. This could be a crucial mechanism for regulation of TRPV5/6 under physiological conditions. It was shown that this inhibition is highly Ca^{2+} sensitive with calculated affinity values down to 100 nM. When measured directly in inside-out patches, half-maximal inhibition of TRPV5 currents occurred at ~ 200 nM (282). With the consideration of the high-affinity mechanism of Ca^{2+} -dependent TRPV5/6 inhibition, the presence of intracellular Ca^{2+} buffer proteins such as calbindins will play an important role in the regulation of channel activity (173, 175, 181).

Recovery from inhibition upon washout of extracellular Ca^{2+} (whole cell configuration) or removal of Ca^{2+} from the inner side of the channel (inside-out patches) is slow in both conditions. Half-maximal recovery was reached after 100–135 s (282). The slow recovery of TRPV5 (and to a lesser extent TRPV6) from their Ca^{2+} -induced inhibited state is an intriguing feature of both TRPV5/6. Surprisingly, recovery is much slower than the inhibition, although this putative microdomain is accessible for intracellular Ca^{2+} , and it does not correlate with the removal of intracellular Ca^{2+} either, since full recovery occurs much later than restoration of the basal Ca^{2+} level in non- Ca^{2+} -buffered cells, or after removing Ca^{2+} from the inner side of excised membrane patches (282). The similar rates of recovery in whole cell and excised patch experiments might indicate that it is controlled by a complex consisting of pore and microdomain. Furthermore, these data suggest that other processes than rapid binding and slow dissociation of Ca^{2+} could be involved and might hint to interaction with other regulatory proteins.

The molecular mechanism of this feedback inhibition remains, however, unclear at the moment. The first mechanistic insight into Ca^{2+} -dependent inactivation of TRPV6 included a Ca^{2+} -dependent binding of CaM to the carboxy terminus (Fig. 11, A and B). (276). A CaM binding site was identified which seemed to be responsible for Ca^{2+} -dependent inactivation in TRPV6. The minimal structure of this site comprises an arginine-rich motif between the

positions 691 and 711, *NWERLRQGTLRRDLRGIINR*, which includes a conserved PKC phosphorylation site *RQGTLRR*. Phosphorylation of this site inhibited Ca^{2+} -dependent inactivation of TRPV6. This sequence, however, is only partially conserved in TRPV6. Truncation of TRPV6, N696X, in which most of the CaM binding motif is removed, also exhibited a decreased inhibition of TRPV6 by the intracellular Ca^{2+} concentration (229, 281).

Other carboxy-terminal truncations and mutants modulated Ca^{2+} -dependent inactivation of TRPV5 (Fig. 11C). Deletion of the last 30 amino acids of the carboxy terminus of TRPV5, G701X, decreased significantly the Ca^{2+} sensitivity. This carboxy-terminal part of TRPV5 does not comprise the Ca^{2+} -CaM binding site of TRPV6. Another critical stretch for Ca^{2+} -dependent inactivation of TRPV5 was found upstream in the carboxy terminus. Analysis of truncations at amino acid 635, 639, 646, 649, and 653 disclosed a critical stretch involved in Ca^{2+} -dependent inactivation between position 649 and 653 (Fig. 11D). Detailed mutation analysis revealed that mutation of A650 and F651 decreased already the Ca^{2+} sensitivity of TRPV5. C653X showed a decreased Ca^{2+} sensitivity, comparable to G701X, while E649X lacked Ca^{2+} -dependent inactivation (Fig. 11C). Likely, cells expressing truncations shorter than E649 do not survive and could only be restored in the presence of the high-affinity blocker ruthenium red, suggesting that these truncations exhibited a deleterious Ca^{2+} influx (288).

2. pH

It is well known that acidification of the apical medium inhibits transcellular Ca^{2+} absorption across primary cultures of rabbit CNT and CCD cells (37). It was, therefore, interesting to evaluate modulation of TRPV5 by pH. $^{45}\text{Ca}^{2+}$ uptake in TRPV5 expressing *Xenopus laevis* oocytes is inhibited by acidification of the incubation medium (179). Indeed, extracellular acidification reduced currents through TRPV5 carried by either monovalent or divalent cations, which was confirmed by Peng et al. (303). Additionally, extracellular pH also affected current kinetics, extracellular Mg^{2+} blockage, and Ca^{2+} affinity. The gating component of monovalent cation currents through TRPV5 was delayed at alkaline pH and as well as blockage by extracellular Mg^{2+} . Mg^{2+} blockage of monovalent currents was shifted from an IC_{50} of ~ 62 at pH 7.4 to ~ 300 μM at pH 6.0 and ~ 40 μM at pH 8.5, indicating that blockage of TRPV5 by extracellular Mg^{2+} is reduced under more alkaline conditions. Blockage of monovalent cation currents through TRPV5 by Ca^{2+} is less efficient at low pH (in the presence of 100 μM extracellular Ca^{2+} ~ 160 nM at pH 7.4 and ~ 5 μM at pH 6.0) (405). Both results indicate that Ca^{2+} and Mg^{2+} binding in the channel are weakened at higher proton concentrations. For L-type Ca^{2+} channels and cyclic nucleotide-gated channels, it

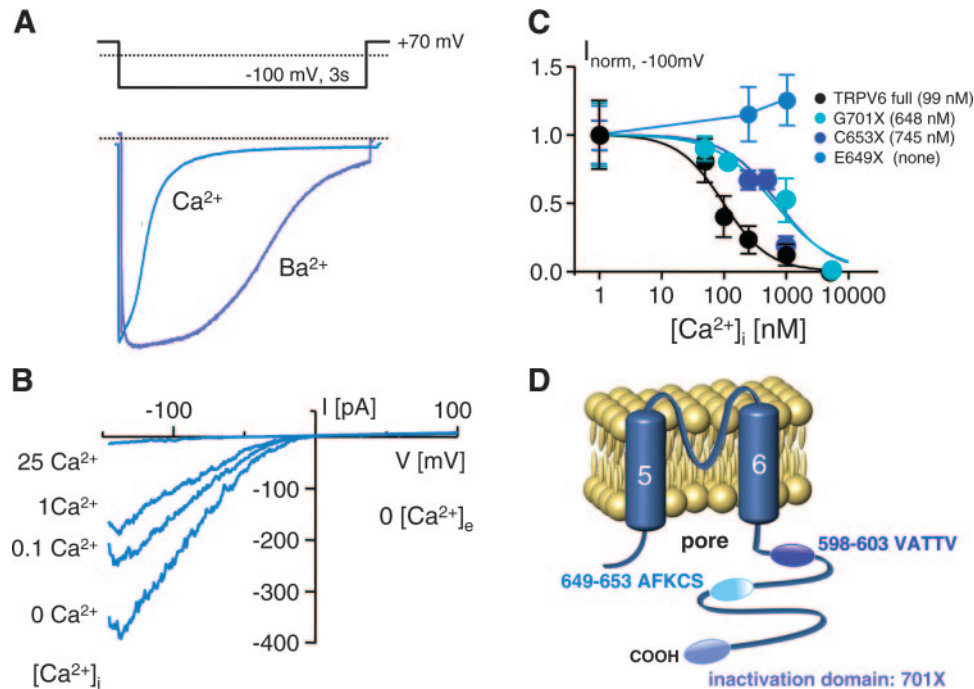


FIG. 11. Ca^{2+} -dependent inactivation of TRPV5 and structural determinants. *A*: step protocols for Ca^{2+} currents through TRPV5. Holding potentials at +70 mV, test potential is always -100 mV. Currents are scaled to the size of the current in 30 mM Ca^{2+} . The Ba^{2+} and Ca^{2+} trace are from the same cell. Differences for Ca^{2+} and Ba^{2+} are typical for Ca^{2+} -dependent inactivation. Traces are superimposed from cell expressing various carboxy-terminal truncations as indicated by the numbers. Slow inactivation for Ba^{2+} as the charge carrier compared with Ca^{2+} is typical for Ca^{2+} -dependent inactivation (see text for details). *B*: monovalent currents in excised inside patches obtained from voltage ramps. All currents are from the same cell. At the inner side of the patch, the intracellular Ca^{2+} concentration is changed as indicated (concentrations in μM). Note that half-maximal inhibition is close to 100 nM. *C*: current-voltage relationship for different carboxy-terminal truncation mutants. Currents at -100 mV are normalized to the controls at an intracellular Ca^{2+} concentration ($[\text{Ca}^{2+}]_i$) of 1 nM (288). Note the absence of block by the $[\text{Ca}^{2+}]_i$ for E649X Ca^{2+} . *D*: scheme of various carboxy-terminal truncation mutants. Numbers indicate the truncation at the indicated site. Representative currents are depicted in *A* (for detailed explanation, see text).

was suggested that protonation of a single glutamate residue in the pore region is responsible for the dramatic changes in divalent cation affinity for the channel with respect to variations in the extracellular pH (316, 328, 376). This could be analogous for TRPV5 in which a single aspartate residue determines the Ca^{2+} permeation and Mg^{2+} blockage of the channel. Extrapolating the pH influence to the in vivo situation, this effect could at least in part provide the molecular basis of acidosis-induced calciuresis. Interestingly, the molecular mechanism of TRPV5 blockage by protons is mechanistically understood taking into account the pore structure described above. Mutation of the glutamate at position 522 to glutamine (E522Q) preceding the pore helix decreases inhibition of the channel by extracellular protons. Thus pH sensitivity is mainly mediated by glutamate at position 522 and may act as the "pH sensor" of TRPV5 (438).

3. Pharmacology

Little is known about effective pharmacological tools to modulate TRPV5/6. Ruthenium red and econazole appeared to be the most effective inhibitors. TRPV5/6 are efficiently blocked by inorganic cations. The profile of

TRPV5 blockage is $\text{Pb}^{2+} = \text{Cu}^{2+} = \text{Gd}^{3+} > \text{Cd}^{2+} > \text{Zn}^{2+} > \text{La}^{3+} > \text{Co}^{2+} > \text{Fe}^{2+} \gg \text{Fe}^{3+}$, with IC_{50} values between 1 and $\sim 10 \mu\text{M}$ (283, 303–305, 406). The inorganic polycationic dye ruthenium red, which binds to phospholipids, inhibits TRPV5 and TRPV6 in a voltage-dependent manner. Blockage is attenuated at depolarizing potentials. Currents of monovalent cations through TRPV5 are blocked with an IC_{50} of $\sim 100 \text{ nM}$ at -100 mV. Transcellular Ca^{2+} transport in primary cultures of immunodissected rabbit CNT and CCD is inhibited in the same concentration range (283). Antimycotic imidazoles such as econazole and miconazole are highly effective inhibitors with IC_{50} values of $\sim 1\text{--}2 \mu\text{M}$. These compounds block, however, voltage independent (283). Blockers of store-operated Ca^{2+} entry channels (SOC), e.g., SKF96365 and 2-aminoethoxydiphenylborate (2-APB), are nearly ineffective for TRPV5 and TRPV6 (283, 336, 410). Another SOC blocker, the adenylyl cyclase inhibitor MDL 12330A (399), exerts a half-maximal inhibition of TRPV5 at $\sim 20 \mu\text{M}$ (283). Xestospongin, a noncompetitive inositol 1,4,5-trisphosphate receptor antagonist, seems, however, to block TRPV6 (402). TRPV5 is not or very weakly affected by capsaizepine, a selective blocker of capsaicin receptor

TRPV1. Arginine-rich peptides, such as dynorphins, inhibit currents through TRPV1 (311). TRPV5 is, however, resistant to both dynorphin A and the fragment 10 consisting of the first 10 amino acid residues of dynorphin A. Also, blockers of protein tyrosine kinases such as tyrphostin B46 and genistein, CaM antagonists calmidazolium R24571 and trifluoperazine, and channel blockers such as mibefradil, quinidine, nifedipine, niflumic acid, and verapamil, have only small or no effects on TRPV5 activity (283). Interestingly, some pharmacological tools differentiate between TRPV5 and TRPV6. Blockage by ruthenium red and Cd^{2+} is much more sensitive for TRPV5 than TRPV6 (181, 182). Blockage of TRPV6 by capsaicin has been described (84) that is ineffective for TRPV5 (Nilius, unpublished data).

D. CRAC and TRPV6

One of the still unsolved problems in channel physiology is the nature and the mechanism of activation of SOC. Twenty-four years ago Casteels and Droogmans (68) showed that depletion of agonist-sensitive intracellular stores stimulates the rate of Ca^{2+} uptake from the extracellular solution in vascular smooth muscle cells. The first electrical measurement of SOC was achieved in mast cells, and this current was referred to as "calcium release-activated calcium current" (CRAC) (189). CRAC is still the best-characterized SOC. It is a highly Ca^{2+} -selective, inwardly rectifying channel; permeable to Ca^{2+} , Sr^{2+} , Ba^{2+} , but not Mg^{2+} ; exhibits anomalous mole fraction behavior; becomes permeable for monovalent cations in the absence of extracellular divalent cations; and is inactivated by an increase in the intracellular Ca^{2+} concentration (300). These properties are reminiscent to the above-described biophysical properties of TRPV5/6 except the activation by depletion of intracellular Ca^{2+} stores. Recently, Yue et al. (444) reported that TRPV6 was activated by store depletion and manifests the pore properties of CRAC in RBL cells and might, therefore, be CRAC or at least part of the CRAC pore (444). This store-operated mode could, however, only be observed in COS cells in a restricted posttransfection time window when the current density was lower than in other studies. A strong argument for TRPV6 being CRAC was at that time apparent identical single-channel conductance for monovalent cations (208). It has also been reported in several forthcoming studies that a correlation between CRAC and TRPV6 exists: 1) an upregulation of CRAC channel was observed in RBL cells by transfection with TRPV6 (336); 2) in prostate cancer cells, which express TRPV6, antisense oligonucleotides downregulated TRPV6 and CRAC and antiandrogens unregulated both TRPV6 and CRAC (395); and 3) expression of a "dominant negative" pore mutant of TRPV6 in Jurkat cells, the already mentioned triple

mutant F534A/E535A/L536A, attenuated endogenous CRAC (84). However, several features are incompatible with the proposed equality of the TRPV6 and CRAC or CRAC pores. Open pore blockage by intracellular Mg^{2+} , which is a hallmark of TRPV5/6 gating (409, 410, 412), is completely absent in CRAC. In fact, CRAC behaves like TRPV5/6 in the absence of intracellular Mg^{2+} even when a high free intracellular Mg^{2+} concentration is present (also Fig. 4). As explained, this Mg^{2+} blockage is caused by binding of Mg^{2+} at the aspartate residue D541/542. Mutation of this residue attenuated intracellular Mg^{2+} blockage and Ca^{2+} selectivity of TRPV5/6 and decreased the inward rectification. Interestingly, Mg^{2+} blockage and high Ca^{2+} selectivity was also abolished if a single aspartate is mutated in a concatemeric homotetramer of TRPV6, indicating that this site is dominant for regulation of these important pore properties (182, 408–410). Recently, TRPV6 antisense and siRNA knockdown approaches inhibited TRPV6-derived currents in mast cells, but failed to inhibit CRAC currents. These results render it improbable that TRPV6 is a component of native CRAC channels in mast cells (203). It seems, therefore, unlikely that even heteromultimers containing TRPV6 form the highly Ca^{2+} -selective CRAC pore.

More striking evidence against TRPV5/6 being CRAC comes now surprisingly from single-channel measurements. It has been recently shown that in extracellular solutions that are free of divalent cations and under conditions of reduced intracellular Mg^{2+} , the dominant cation current in Jurkat and RBL cells is through a channel first termed MagNuM (magnesium-nucleotide-regulated metal cation current), which is conducted by the LTRPC7 channel (162) or also called MIC (Mg^{2+} inhibited cation channels) (314). These channels have a single-channel conductance for monovalent cations of ~ 45 pS as reported for TRPV6 by Yue et al. (444). Because most of the studies on CRAC have used divalent-free solutions on either side of the membrane to study selectivity, the single-channel conductance of CRAC was misinterpreted by the one of MagNuM/MIC/TRPM7 which are activated by a decrease in intracellular Mg^{2+} /Mg-ATP (162). CRAC has indeed a single-channel conductance of ~ 0.2 pS (209, 220) rather than ~ 45 pS as TRPV6 (see also Refs. 16, 73, 313). Interestingly, estimation of the pore diameter also resulted in rather different values. TRPV6 has a diameter of ~ 5.2 Å (408), whereas for CRAC a diameter of ~ 3.8 Å was estimated (313).

However, other differences also exist including the striking permeation difference of CRAC and TRPV5/6 for Cs^+ (Cs^+ is much less permeable through CRAC than through TRPV5/6), the different time course of the monovalent currents through CRAC (inactivating) and TRPV5/6 (sustained), the striking differences in rectification (much less rectification for monovalent currents in CRAC than TRPV5/6) and effects of extracellular 2-APB (blockage of

CRAC but even light potentiation of TRPV6) (for a review see Refs. 280, 410). In addition, we have never observed any store-operated activation for TRPV5 or TRPV6. However, TRPV6 expression in HEK293 cells does result in a constitutive open channel, is not activated by ionomycin-induced store depletion, and is inhibited by a rise in cytosolic Ca^{2+} concentration independently of the post-transfection time (410). Furthermore, TRPV6 seems not to be expressed in Jurkat cells, one of the preferred cells to study CRAC, and expression of TRPV6 in these cells does not reveal store-dependent properties (47). CRAC is obviously not TRPV5/6. A modulator role for store-operated Ca^{2+} influx cannot be excluded (75). As a bottom line, all Ca^{2+} -permeable TRP channels contribute to changes in the intracellular Ca^{2+} concentration and may, therefore, also affect store-operated processes. There is so far no TRP channels for which a consensus for being CRAC has been settled and at least TRPV5 or TRPV6 are very unlikely CRAC/SOC (74, 75).

E. Molecular Structure of TRPV5 and TRPV6

The oligomerization of TRPV5 and TRPV6 channels has recently been unraveled (182). Cross-linking studies, coimmunoprecipitations, and molecular mass determination of TRPV5/6 complexes using sucrose gradient sedimentation showed that TRPV5 and TRPV6 form homo- and heterotetrameric channel complexes. As described in section v, TRPV5 and TRPV6 are coexpressed in some tissues, which allows oligomerization of these channels in vivo. For instance, immunohistochemical data in kidney clearly demonstrated coexpression of TRPV5 and TRPV6 in the DCT (182). However, coexpression of TRPV5 and TRPV6 in these tissues is until now only quantified at the mRNA level, indicating that TRPV6 is 100–10,000 more expressed than TRPV5. Quantification at the protein level of both channels is certainly important to address the stoichiometry in vivo. Heteromeric complex formation can modify the activity of members of the TRP family. The *Drosophila* TRP and TRPL members were identified first, and it has been shown that these proteins form heteromultimeric channels associated in a supramolecular signaling complex with receptors and regulators including PKC, CaM, and the scaffolding PDZ domain containing protein InaD (13, 233). Moreover, it has been shown for TRPC1 and TRPC3 that hetero-oligomers of these channels possess more distinctive properties than that of either channel alone (237). In addition, Strubing et al. (370) demonstrated that TRPC1 and TRPC5 are subunits of a heteromeric neuronal channel. Both TRPC proteins have overlapping distributions in the hippocampus. Coexpression of TRPC1 and TRPC5 in HEK293 cells resulted in a novel nonselective cation channel with a voltage dependence similar to *N*-methyl-D-aspartate (NMDA) receptor

channels, but unlike that of any reported TRPC channel. Other TRPCs exclusively assemble into homo- or heterotetramers within the confines of TRPC subfamilies, e.g., TRPC4/5 and TRPC3/6/7 (187). Based on the ability of the TRPC channels to form functional homo- and heteromultimeric complexes, Tsiokas et al. (382) provided evidence that PKD2, which is functionally related to the TRPC proteins, interacts with TRPC1, suggesting a possible role of this protein in modulating Ca^{2+} entry in response to G protein-coupled receptor activation and/or store depletion (382). Within the TRPV family, the oligomeric structure of TRPV1 was studied by biochemical cross-linking, and the predominant existence of tetramers was suggested (207). The principles of TRP channel formation provide the conceptual framework to address the physiological role of distinct TRP members. Likewise, hetero-oligomerization of TRPV5 and TRPV6 might influence the functional properties of the formed Ca^{2+} channel. As TRPV5 and TRPV6 exhibit different channel kinetics with respect to Ca^{2+} -dependent inactivation, Ba^{2+} selectivity and sensitivity for inhibition by ruthenium red, the influence of the heterotetramer composition on channel properties was investigated (Fig. 7). Concatemers were constructed consisting of four TRPV5 and/or TRPV6 subunits configured in a head-to-tail fashion (182). A different ratio of TRPV5 and TRPV6 subunits in these concatemers showed that the phenotype resembles the mixed properties of TRPV5 and TRPV6. An increased number of TRPV5 subunits in such a concatemer displayed more TRPV5-like properties, indicating that the stoichiometry of TRPV5/6 heterotetramers influences the channel properties. Consequently, regulation of the relative expression levels of TRPV5 and TRPV6 may be a mechanism to fine-tune the Ca^{2+} transport kinetics in kidney or other TRPV5/6-coexpressing tissues. The tetrameric organization of TRPV5/6 resembles that of the *Shaker* potassium channel, which is composed of four tandemly associated homologous domains (221, 234). The clustering of four subunits is assumed to create an aqueous pore centered at the fourfold symmetry axis (Fig. 10B) (234). This tetrameric architecture of TRPV5/6 implies that four of the aspartic residues [D542 (286), D541 (408)] form a negatively charged ring that functions as a selectivity filter for Ca^{2+} in analogy with voltage-gated Ca^{2+} channels (182). Interestingly, Niemeyer and co-workers (102) identified the third ankyrin repeat being a stringent requirement for physical assembly of TRPV6 subunits. Deletion of this repeat or mutation of critical residues within this repeat renders nonfunctional channels that do not coimmunoprecipitate or form tetramers. It was proposed that the third ankyrin repeat initiates a molecular zipper process that proceeds past the fifth ankyrin repeat and creates an intracellular anchor that is necessary for functional subunit assembly (102). Protein crystallography of these channels will be the most chal-

lenging approach to determine the molecular structure in the near future.

V. SITES OF EPITHELIAL CALCIUM TRANSPORT

The exchange of Ca^{2+} between higher organisms and the environment takes place across epithelia, including the gastrointestinal tract, bone, kidney, and gills. Ca^{2+} transport occurring in these Ca^{2+} -absorbing epithelial tissues is realized by paracellular and transcellular Ca^{2+} transport as outlined in sections II and III.

A. Kidney

The renal handling of Ca^{2+} has been the subject of intensive investigation over the last years. The kidney plays an essential role in the maintenance of the Ca^{2+} balance by regulating the Ca^{2+} excretion of the body. On a daily basis, ~ 8 g of Ca^{2+} is filtered at the glomeruli of which $<2\%$ is excreted into the urine. As a consequence, filtered Ca^{2+} is extensively absorbed as it passes through the individual nephron segments.

1. Proximal tubule

The proximal tubules, including proximal convoluted (PCT) and proximal straight (PST) tubules, are responsible for absorbing the majority of Ca^{2+} . Micropuncture studies have demonstrated that $\sim 70\%$ of the Ca^{2+} is absorbed in these segments (99, 122, 374, 385). Ca^{2+} transport along the proximal tubule proceeds essentially as an isosmotic process that is based on early micropuncture studies demonstrating that Ca^{2+} , Na^+ , and water are absorbed in parallel (reviewed in Ref. 371). This means that the majority of Ca^{2+} reabsorption in these segments is energetically passive and follows the local Na^+ reabsorption.

2. Limb of Henle

In the thin descending and ascending limbs of Henle, the permeability for Ca^{2+} is very low, and basically we can conclude that significant net Ca^{2+} transport does not occur in this segment (318, 331). This low Ca^{2+} permeability is particularly striking in view of the comparatively high permeability to Na^+ and Cl^- (331). Because these thin limbs of Henle do not transport Ca^{2+} , the thick ascending limb of Henle (TALH) is responsible for the Ca^{2+} reabsorption between the bend of the loop and the start of the DCT (14, 53, 56, 92, 93, 120, 129, 192, 274, 331, 372, 373, 432). Approximately 20% of the Ca^{2+} filtered at the glomeruli is absorbed in Henle's loop (371). In several studies Ca^{2+} reabsorption in cortical TALH was examined. Bourdeau and Burg (54) provided evidence that

Ca^{2+} transport was driven by the electrochemical gradient, indicative of a passive absorption process. Similar findings were described by Shareghi and Agus (343), who concluded that Ca^{2+} reabsorption in the TALH is passive and driven by the large lumen-positive membrane potential. In contrast, Imai (192) postulated an active Ca^{2+} transport component in cortical TALH segments, whereas his studies in medullary TALH segments are more consistent with a passive mechanism. These findings were confirmed in mouse kidney by Friedman (120), whereas Wittner et al. (433) demonstrated that Ca^{2+} transport in the mouse cortical TALH is entirely passive. Interestingly, Ca^{2+} transport in cortical segments was stimulated by PTH without an increase in the transepithelial potential difference (120). At variance, Wittner et al. (433) showed that PTH-stimulated passive Ca^{2+} transport by increasing the electrical driving force and, therefore, the permeability for the paracellular pathway. Immunohistochemical studies on mouse and rat kidney sections did not provide evidence for the presence of the identified Ca^{2+} transport proteins including TRPV5, TRPV6, calbindins, NCX1, and PMCA1b in TALH segments (171, 240). Interestingly, a new protein, named paracellin 1 (PCLN-1), expressed in human TALH tight junctions, possibly plays a critical role in the control of passive Ca^{2+} , and also Mg^{2+} , reabsorption, since mutations of PCLN-1 are present in patients with the hypomagnesemia hypercalciuria syndrome (HHS) (43). In these patients, renal Ca^{2+} reabsorption is impaired as expected. This study was the first to demonstrate that homozygous mutations of PCLN-1 result in a selective defect in paracellular divalent cation reabsorption in the TALH, with intact sodium chloride reabsorption ability in this segment. Altogether, this segment definitely plays a significant role in the process of Ca^{2+} reabsorption, mainly due to paracellular Ca^{2+} transport. The contribution of active Ca^{2+} transport is, however, questionable (264).

3. DCT and CNT

The fine-tuning of Ca^{2+} excretion in the kidney occurs in the distal part of the nephron and amounts to 15% of the filtered load of Ca^{2+} (79). This section consists of DCT and CNT. The CNT lies just distal to the DCT, arising abruptly in rabbits and gradually in most other species (63, 80, 204, 240). The CNT contains, in contrast to DCT, in addition to principal cells also intercalated cells. The relative contribution of these two segments to active Ca^{2+} reabsorption appears to differ between the various species (38, 346–349, 371). In these nephron segments, Ca^{2+} reabsorption occurs against the existing electrochemical gradient. Together with the fact that the tight junctions are relatively impermeable for Ca^{2+} , this substantiates that Ca^{2+} is reabsorbed in these segments through an active transcellular pathway. By comparing the fractional

Ca²⁺ delivery at the beginning of the DCT and the final urine, early studies indicated Ca²⁺ reabsorption in these segments (385). Over the last years, several studies indicated that in most mammalian species the DCT is the primary nephron segment of active Ca²⁺ transport. However, the exact sites for transcellular Ca²⁺ reabsorption along the distal part of the nephron are still being questioned. Extensive studies revealed that the localization of the Ca²⁺ transport proteins, including TRPV5, TRPV6, calbindins, NCX, and PMCA, is restricted to the late distal part of the DCT (DCT2) and the CNT (171, 240). Micropuncture investigations of Ca²⁺ transport in the rat distal convolution (comprising DCT1, DCT2, CNT, and the initial CCD) aimed to distinguish between the first two (including DCT1, -2) and last two (including CNT and initial CCD) segments. Micropuncture studies by Costanzo and Windhager (78) showed similar Ca²⁺ transport rates in these segments, whereas experiments by Greger et al. (154) suggested that transcellular Ca²⁺ transport occurs predominately in CNT.

Transepithelial Ca²⁺ transport depends on the activity of Ca²⁺-transporting proteins in the apical and basolateral plasma membranes and the cytosol of the epithelial cells. Loffing et al. (240) and several studies by Hoenderop and Bindels and co-workers (171, 279) demonstrated in the mouse coexpression of the Ca²⁺ transport proteins including TRPV5, TRPV6, PMCA1b, NCX1, and calbindin-D_{28K} in DCT2 and CNT, with the highest immunochemical abundance in DCT2, and a gradual decrease along CNT (Fig. 12A). The parallel axial reduction of apical TRPV5 and of basolateral Ca²⁺ extru-

sion machinery, i.e., PMCA1b and NCX1, indicates a progressive decrease of transcellular Ca²⁺ transport rates along CNT. TRPV5, PMCA1b, and NCX1 abruptly disappeared at the transition to the CCD, consistent with the notion that transcellular Ca²⁺ transport is negligible in CCD (240). A minority of cells along CNT lacked immunopositive staining for TRPV5 and the other Ca²⁺-transporting proteins. These negative cells were identified as intercalated cells (171, 240). Taken together, these findings strongly suggest that, in the mouse, the major sites of transcellular Ca²⁺ transport are DCT2 and, probably to a lesser extent, CNT. Whether Ca²⁺ transport occurs in DCT1 of mice, and if so at which rate is unknown. The occurrence of weak immunostaining for NCX1 and PMCA1b would be in line with active Ca²⁺ transport in this segment. At variance with the presence of these basolateral Ca²⁺-transporting proteins, TRPV5 and TRPV6 were not detectable in DCT1 (171, 240, 279). This raises the question whether other apical Ca²⁺ entry pathways might play a role in transcellular Ca²⁺ transport in DCT1 or confirms the absence of an active transport process. The existence of such pathways in DCT has been suggested by RT-PCR data obtained from isolated rat tubules (443) and an immortalized mouse DCT cell line (12). However, these cell preparations do not represent solely DCT1, and the corresponding findings should, therefore, be interpreted with great care. Combined micropuncture experiments, immunohistochemistry of the Ca²⁺ transport proteins, and corresponding nephron-specific mouse knockout models are needed to investigate whether active Ca²⁺ transport occurs in DCT1.

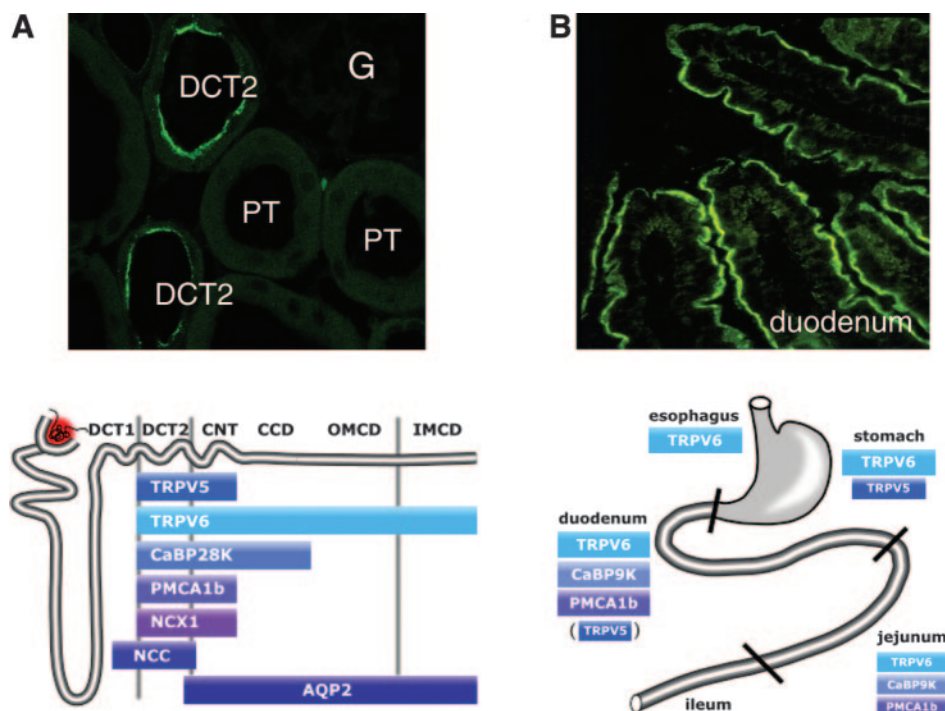


FIG. 12. Localization of TRPV5 and TRPV6 in kidney and small intestine. *A*: immunopositive staining for TRPV5 that is predominantly found along the apical membrane of the distal tubule in the mouse. Schematic overview of the expression of the Ca²⁺ transport proteins in the kidney (*bottom*). *B*: immunopositive staining for TRPV6 that is typically observed along the mouse brush-border membrane of the duodenum. Schematic overview expression of the Ca²⁺ transport proteins in the intestine is shown (*bottom*).

4. Collecting duct

The collecting duct is the last segment of the nephron and extends from the connecting tubule in the cortex through the outer and inner medulla to the tip of the papilla. It can be divided into at least three regions, based primarily on their localization in the kidney. These include CCD, the outer medullary collecting duct (OMCD), and the inner medullary collecting duct (IMCD). The collecting duct consists of principal cells that are responsible for salt and water reabsorption and intercalated cells that play a major role in H^+ and HCO_3^- secretion. These latter cells constitute $\sim 30\%$ of the cells in the CCD, OMCD, and IMCD and lack the typical Ca^{2+} transport proteins (Fig. 12A) (171). Based on differences between the fractional Ca^{2+} delivery at the last accessible segment in the distal part of the nephron on the surface of the cortex and in the final urine, it was suggested that $\sim 3\%$ of the filtered Ca^{2+} is absorbed by the CCD (385). Because net transport occurs against the electrochemical gradient in the absence of water transport, the mechanism is thought to be active. In isolated perfused rabbit CCD, Shareghi et al. (344) and Bourdeau and Hellstrom-Stein (55) reported a low Ca^{2+} permeability and an insignificant net flux that is driven by the membrane potential and not affected by PTH and $1,25-(OH)_2D_3$. However, other groups demonstrated a significant Ca^{2+} transport in this segment. Limited Ca^{2+} transport studies are performed in IMCD tubules. Lechene and co-workers (31) measured Ca^{2+} transport along the IMCD in rats by the microcatheterization technique. In this study, net Ca^{2+} reabsorption occurs along the IMCD and the fractional Ca^{2+} reabsorption is not altered by thyroparathyroidectomy (31). Ca^{2+} transport by the IMCD of normal rats was also studied using the in vitro microperfusion technique. Net fluxes of Ca^{2+} were measured using ^{45}Ca as a tracer, and Ca^{2+} influx was independent of Na^+ transport, was not blocked by verapamil, but was increased by Ca^{2+} transtubular gradient (244). In this respect, it is interesting to discuss a recent study that addresses the localization of TRPV6 in the mouse nephron. TRPV6 expression was also detected in OMCD and IMCD and displayed a distinct apical localization (279). However, the absence of supportive Ca^{2+} transport proteins, as confirmed by the lack of immunopositive staining for calbindins, questioned the involvement of these cells in Ca^{2+} reabsorption. Second, intercalated cells also expressed TRPV6. The consistent apical localization would imply that TRPV6 has a functional role as apical Ca^{2+} entry channel. Hypothetically, TRPV6-mediated Ca^{2+} influx could affect transport processes in these segments, for instance, as part of a hormonal signaling cascade. In particular, vasopressin was shown to induce Ca^{2+} influx across the apical membrane of collecting duct cells, and alterations in intracellular Ca^{2+} levels are known to affect Na^+ reabsorption in these tubules

(130, 364, 390). Taken together, the present data suggest that Ca^{2+} reabsorption in the collecting duct is primarily located in the CCD that accounts for maximally 3% of the total amount of Ca^{2+} filtered at the glomerulus.

B. Gastrointestinal Tract

The small intestine is the largest part of the gastrointestinal tract and is composed of the duodenum, jejunum, and ileum. The large intestine starts after the small intestine in the digestive track and consists of cecum, colon, and rectum. The mechanisms of Ca^{2+} absorption belong to the best studied processes, deficiencies of which cause significant health problems throughout the world. Intestinal Ca^{2+} absorption is a crucial control system in the regulation of Ca^{2+} homeostasis, because it facilitates the entry of dietary Ca^{2+} into the extracellular compartment. Ca^{2+} is absorbed by two distinct mechanisms including passive (paracellular) and active (transcellular) transport as outlined in sections II and III, and their relative magnitude of importance is set by the dietary Ca^{2+} content. Active transcellular Ca^{2+} absorption is located largely in the duodenum and upper jejunum, whereas paracellular Ca^{2+} absorption occurs throughout the entire length of the intestine (60). Chyme moves down the intestinal lumen in ~ 3 h, spending only a short time in the duodenum, but over 2 h in the distal part of the small intestine. In the situation that dietary Ca^{2+} intake is low, transcellular Ca^{2+} transport accounts for a substantial fraction of the absorbed Ca^{2+} , and vice versa, when Ca^{2+} intake is high (58, 59).

Transcellular Ca^{2+} absorption can be described in three sequential cellular steps: entry, intracellular diffusion, and extrusion (see sect. III). The Ca^{2+} -binding protein calbindin- D_{9K} is responsible for intracellular diffusion of Ca^{2+} in the enterocyte, and its gastrointestinal expression has been studied in many species. Yamagishi et al. (436) examined the calbindin- D_{9K} mRNA expression in the gastrointestinal tract of cattle by Northern blot analysis. Studies in several animal models have shown that calbindin- D_{9K} and PMCA1b are both expressed in patterns that are compatible with roles in Ca^{2+} absorption, being found in villous cells of the proximal duodenum and gradually decreased distally, demonstrating vitamin D dependence and decreased expression with aging (Fig. 12B) (7, 117, 190, 379, 436, 445). The expression was highest at the most proximal region. In addition, NCX1 is expressed in the basolateral membrane of mammalian enterocytes (164). In fish enterocytes, NCX1 appears to be the main mechanism by which transcellular fluxes of Ca^{2+} are extruded from the cells at the basolateral surface (115). In contrast, in mammalian enterocytes, Ca^{2+} extrusion is predominantly dependent on PMCA1b activity (398).

Recent studies addressed the expression of TRPV5 and TRPV6 in the gastrointestinal tract (Fig. 12B). Ini-

tially, Northern blot analysis showed expression of rabbit TRPV5 in duodenum and jejunum, whereas ileum was negative. However, these hybridizations were performed before the identification of the TRPV6 member using a full-length cDNA as a probe that does not discriminate between the two homologous members (178). Subsequent studies using isoform-specific probes, quantitative PCR analysis, and immunohistochemical analysis determined the expression of both channels in the gut. These studies showed that TRPV6 is at the mRNA level at least three orders of magnitude higher expressed than TRPV5 (301, 387, 392). However, at the protein and functional level, it is not clear whether TRPV5 plays a significant role in the intestine, but in line with the observed quantitative mRNA data, a predominant role of TRPV6 is expected in the intestine. Initial characterization of TRPV5 knockout mice that exhibit Ca^{2+} hyperabsorption, probably mediated by the increased TRPV6 and calbindin- $\text{D}_{9\text{K}}$ expression levels, is in agreement with this notion (see sect. VII) (180). Additional immunohistochemical and functional studies are needed to address a possible role of TRPV5 in the small intestine. In the intestine, TRPV6 expression was found in duodenum, jejunum, and cecum where it colocalizes with calbindin- $\text{D}_{9\text{K}}$ and PMCA1b (Fig. 12B) (181, 304, 305). A comparable study by Hediger and co-workers (305) demonstrated expression of TRPV6 throughout the entire digestive tract from esophagus to colon. For unknown reasons, Flockerzi and co-workers (430) failed to detect TRPV6 (CaT-L) expression in the small intestine and colon.

Recently, TRPV6 and TRPV5 mRNA levels were quantified in mouse by quantitative PCR analysis and normalized for cDNA input. This study demonstrated that TRPV6 mRNA in order of decreasing expression is present in duodenum, cecum > colon >> ileum. Likewise, TRPV5 was expressed in kidney >>> duodenum, cecum, whereas ileum and colon were negative (279). Variation in TRPV5 and TRPV6 expression patterns found in different studies in intestine, esophagus, ileum, and colon might be caused by the low abundance of either TRPV5 or TRPV6 in these tissues or differences between species resulting in failure of detection. Immunocytochemical techniques have been used to examine the distribution of TRPV6, TRPV5, calbindin- $\text{D}_{9\text{K}}$, and PMCA1b protein in enterocytes (171). TRPV6 and TRPV5 were localized along the brush-border membrane, whereas calbindin- $\text{D}_{9\text{K}}$ and PMCA1b were expressed cytosolic and at the basolateral membrane, respectively (394, 447). However, at the mRNA level, TRPV6 is 100 times more abundant in the intestine compared with TRPV5. Detailed immunohistochemical studies by Zhuang et al. (447) indicated expression of TRPV6 on the brush-border apical surface of intestinal villi in the entire small intestine and colon. Taken together, these findings are consistent with the postulated role of the epithelial Ca^{2+} channel TRPV6 as the major

transcellular mediator of Ca^{2+} uptake from the intestinal lumen.

1. Stomach

A contribution of the stomach in Ca^{2+} absorption from the gastrointestinal tract has been postulated from *in vivo* and *in vitro* studies in different ruminant species, although this organ is not generally considered to play a major role (339). Unidirectional flux rates of Ca^{2+} across rumen wall epithelia of sheep were measured *in vitro* by applying the Ussing-chamber technique in the absence of electrochemical gradients. Under these conditions, significant unidirectional Ca^{2+} flux rates suggest the presence of active mechanisms for Ca^{2+} transport (339). Interestingly, quantitative PCR analyses demonstrated a significant expression of TRPV6 in the stomach, whereas a lower expression of TRPV5 was observed (181, 279). These data were confirmed at the protein level in which strong labeling of TRPV6 was observed. TRPV6 expression was predominantly expressed in the upper segments of the gastric glands compared with the lower fragments (447). In this study, it was suggested that TRPV6 plays a role in these mucus-secreting cells in maintaining the intracellular Ca^{2+} balance after mucus secretion to refill the depleted cellular Ca^{2+} stores (444, 447). Functional studies showed that the voltage-operated Ca^{2+} channel blocker verapamil had no significant effect on Ca^{2+} transport in rumen that is in line with the insensitivity of the epithelial Ca^{2+} channels for this inhibitor (178, 303, 339). In this study a $\text{Ca}^{2+}/\text{H}^{+}$ exchange mechanism in the apical membrane of rumen epithelial cells was postulated that does not seem to be under the control of $1,25\text{-(OH)}_2\text{D}_3$. Because vanadate did not affect Ca^{2+} absorption, basolateral Ca^{2+} extrusion occurs independently from the Ca^{2+} pump activity and may be accomplished via $\text{Na}^{+}/\text{Ca}^{2+}$ exchange (339). Future studies using isolated mucus-secreting cells from TRPV6 and TRPV5 knockout mice should address the physiological role of these channels in more detail.

C. Others

1. Placenta

During pregnancy Ca^{2+} absorption in the placenta is solely responsible for the nutrient supply to the developing fetus. The Ca^{2+} needs of the fetus increase progressively throughout the pregnancy. Ca^{2+} is actively transported across the placenta from the maternal to the fetal circulation in late gestation to meet the requirements of the rapidly mineralizing skeleton and to maintain an extracellular level of Ca^{2+} that is physiologically appropriate for the development of fetal tissues (27–29, 62, 132, 227, 258–261, 310). Ca^{2+} is transported by the syncytiotro-

phoblasts, cells that line the chorionic villi tissue and correspond to the epithelial layer separating the maternal and fetal circulation (105). In analogy to Ca^{2+} transfer across the intestinal and renal distal tubular cells (see sect. III), it has been postulated that Ca^{2+} enters the Ca^{2+} -transporting cells through maternal-facing basement membranes. Subsequently, Ca^{2+} diffuses across these cells by calbindin- $\text{D}_{9\text{K}}$ and calbindin- $\text{D}_{28\text{K}}$ and is actively extruded at the fetal-facing basement membranes by a Ca^{2+} -ATPase (28, 29). With the use of animal models, it was demonstrated that the placental expression of calbindin- $\text{D}_{9\text{K}}$ increases more than 100-fold over the last 7 days of gestation, whereas the expression of the Ca^{2+} -ATPase increases twofold over the same interval (146). Interestingly, initial Northern blot analysis indicated that TRPV5 and TRPV6 are both expressed in placenta (178, 304). Quantitative PCR analysis in human placenta revealed a robust mRNA expression of TRPV6, whereas TRPV5 was expressed at a very low level (301). Lafond and co-workers (260) demonstrated the expression of TRPV5 and TRPV6 by RT-PCR in cytotrophoblasts freshly isolated from human term placenta. Again, a higher mRNA expression of TRPV6 compared with TRPV5 was measured. This study indicated that the pattern of TRPV6 and TRPV5 expression correlates with the Ca^{2+} uptake potential along the human trophoblasts isolated from term placenta. These studies provided evidence for a role of the epithelial Ca^{2+} channels in basal Ca^{2+} influx during active Ca^{2+} transport by the syncytiotrophoblast.

2. Bone

Bone, the major Ca^{2+} store of the body, is an important tissue involved in Ca^{2+} homeostasis. Ca^{2+} removal from and redistribution in bone is mediated by specific bone cells, namely, osteoblasts and osteoclasts. The translocation of Ca^{2+} from the extracellular fluid compartment into the mineralizing matrix is not well understood at the molecular level. Knowledge on how bone directly contributes to serum Ca^{2+} homeostasis is virtually absent. It can be via bone resorption and formation, but these processes are relatively slow for rapid responses to changes in serum Ca^{2+} . To understand Ca^{2+} movement in bone and Ca^{2+} homeostasis, it is crucial to identify and characterize the Ca^{2+} transport processes in bone. The osteoclast is a cell unique in its ability to resorb bone and becomes exposed to high Ca^{2+} concentrations in the millimolar range (42). It is generally accepted that, during resorption, osteoclasts can sense changes in their ambient Ca^{2+} concentration. An increased ambient Ca^{2+} concentration triggers a sharp cytosolic Ca^{2+} increase through both Ca^{2+} release and Ca^{2+} influx. The bone-forming osteoblasts form a layer that later calcifies. Several reports have described calbindin- $\text{D}_{9\text{K}}$ expression in rat and human osteoblast-like cells (17, 104, 420). In these

studies, immunoreactive calbindin- $\text{D}_{9\text{K}}$ was localized in the cytoplasm of osteoblasts. Moreover, calbindin- $\text{D}_{28\text{K}}$ was expressed at low levels in several osteoblastic cell lines and at high levels in primary cultures of murine osteoblastic cells. Its localization in osteoblasts involved in bone formation and in their cell processes suggests a role in Ca^{2+} transport from these cells toward the sites of active bone mineralization. Interestingly, TRPV5 and TRPV6 mRNA have been detected in bone cells isolated from mouse femurs (279). To date, information on expression and localization of these proteins in bone cells is limited, and their functions in matrix mineralization are unclear.

3. Exocrine tissues

Exocrine tissues such as pancreas, testis, prostate, mammary gland, sweat gland, and salivary gland are not primarily implicated in transepithelial Ca^{2+} transport. Interestingly, several studies have demonstrated expression of Ca^{2+} -transporting proteins in these exocrine tissues by Northern blot, PCR analysis, or immunohistochemistry. In pancreas, TRPV5 was observed in secretory granules of the β -cells where it colocalized with calbindin- $\text{D}_{28\text{K}}$ and insulin (194). This study suggested a role for TRPV5 in insulin secretion, although such a role could not be confirmed in studies on the pancreas of Zucker diabetic fatty (ZDF) rats, an animal model for type 2 diabetes mellitus. Interestingly, insulin secretion is impaired in vitamin D-deficient rats (202) but restored by vitamin D treatment (193). Sooy et al. (362) suggested that calbindin- $\text{D}_{28\text{K}}$ could control the rate of insulin release via regulation of the intracellular Ca^{2+} concentration. Like in kidney, in pancreatic β -cell NCX, PTH-related peptide (PTHrP), calbindin- $\text{D}_{28\text{K}}$ and receptors for $1,25\text{-(OH)}_2\text{D}_3$ have been detected (76, 97, 198, 396). In contrast to TRPV5, TRPV6 mRNA is found in the exocrine acinar cell of the pancreas, but not in pancreatic duct and β -cells (430, 447). In the human pancreas, acinar cells showed a granular and apical membrane staining of TRPV6 (447). In addition, a weak signal was found along the basolateral membrane that could be involved in Ca^{2+} entry from the circulation. Ca^{2+} extrusion in the acinar pancreatic cell has been studied in great detail. With the use of confocal microscopy and Ca^{2+} -sensitive fluorescent probes, it was shown that the secretory pole of the acinar cell is the major Ca^{2+} extrusion site following agonist stimulation (25, 26). It is well known that intracellular Ca^{2+} plays an essential role in exocytosis. Localization of Ca^{2+} influx through TRPV6 and Ca^{2+} extrusion at the luminal membrane would be important to direct physiological Ca^{2+} signals to the apical compartment of the acinar cell. Altogether, this indicates that in the pancreatic cell the Ca^{2+} homeostasis is a complex process in which many Ca^{2+} transport proteins might play a role and functional studies are needed to

investigate the function of the Ca^{2+} transport proteins in the pancreas.

Several studies demonstrated a robust TRPV6 expression in prostate. Recently, quantitative PCR measurements and immunohistochemical studies indicated that the prostate contains the highest TRPV6 expression levels of all tested tissues (111, 176, 265, 279, 305, 306, 430, 447). Although the exact function in this organ remains to be elucidated, previous reports have suggested that TRPV6 expression correlates with prostate carcinoma tumor grade (111, 306). The first indication of TRPV6 as tumor progression marker came from expression studies in human prostate cancer cell lines (306). Expression of TRPV6 was elevated in prostate cancer samples compared with benign prostatic hyperplasia specimens and positively correlated with Gleason grade in prostate cancer. TRPV6 mRNA was downregulated by androgen and induced by a specific androgen receptor antagonist in LNCaP cells, suggesting that the expression of this channel is negatively regulated by androgen. Flockerzi and co-workers (430) identified a transcript from rat duodenum, named CaT-L, which was expressed in locally advanced prostate cancer and metastatic and androgen-insensitive prostatic lesions, but was undetectable in healthy prostate tissue (430). Detailed characterization of CaT-L demonstrated that this gene is identical to TRPV6. Recently, it was reported that CaT-L or TRPV6 is not expressed in benign prostate tissues including benign prostate hyperplasia, but is upregulated in prostate cancer. Other reports indicated that TRPV6 mRNA (279) and protein (447) are also expressed in normal prostate tissue. In prostatectomy specimens from 97 clinically organ-confined tumors, TRPV6 expression correlated significantly with the Gleason score, pathological stage, and extraprostatic extension (111). Together these findings indicate that TRPV6 expression is associated with prostate cancer progression and, therefore, represents a prognostic marker and a promising target for new therapeutic strategies to treat advanced prostate cancer.

Interestingly, several exocrine glands including sweat, salivary, and mammary glands do express one or both of the epithelial Ca^{2+} channels. Freeman and co-workers (447) demonstrated that TRPV6 is localized in the mammary gland along the luminal membrane of the epithelial cells in contrast to localization in the sweat gland where the channel was detected on both the luminal and basolateral membrane surfaces. Differences in the localization of TRPV6 may reflect diverse physiological functions in these exocrine glands. To date, TRPV5 expression in these exocrine glands remains to be established. In addition, functional studies are needed to examine the physiological function of the epithelial Ca^{2+} channels in these tissues.

VI. REGULATION OF EPITHELIAL CALCIUM TRANSPORT

A. Regulation by 1,25-(OH) $_2$ D $_3$

It is commonly accepted that vitamin D $_3$ is one of the main hormones controlling Ca^{2+} balance (322). There are two sources of vitamin D $_3$ in the body. It is either ingested from the diet or synthesized in the skin from its precursor 7-dehydrocholesterol in the presence of sunlight (271). Vitamin D $_3$ itself is physiologically inactive. It will undergo an activation process, involving 25-hydroxylation in the liver followed by 1 α -hydroxylation in the kidney to synthesize the biologically active 1,25-(OH) $_2$ D $_3$. The latter reaction step occurs in mitochondria of the renal proximal tubule (116). Whether these proximal tubular cells produce 1,25-(OH) $_2$ D $_3$ depends on the Ca^{2+} status of the body. In the situation that Ca^{2+} is sufficient with adequate dietary Ca^{2+} intake and normal plasma Ca^{2+} concentration, 1 α -OHase activity is low because there is no need for additional Ca^{2+} . However, when Ca^{2+} is insufficient, with a low dietary Ca^{2+} intake and decreased plasma Ca^{2+} concentration, the activity of this enzyme increases to produce 1,25-(OH) $_2$ D $_3$ to ensure that additional Ca^{2+} will be absorbed from the gastrointestinal tract.

From a historical point of view, the biological role of 1,25-(OH) $_2$ D $_3$ in active intestinal Ca^{2+} absorption is most studied. Orr and co-workers (141, 350) discovered many decades ago that vitamin D $_3$ is required for intestinal Ca^{2+} absorption. Ample studies confirmed this initial study that established the role of 1,25-(OH) $_2$ D $_3$ in active Ca^{2+} absorption. More recently, a similar role in the distal part of the nephron was demonstrated as discussed in section v (38, 175). The effects underlying at least part of these processes are mediated by the interaction of 1,25-(OH) $_2$ D $_3$ with the nuclear VDR in a ligand-dependent manner (159). This genomic mechanism of action is similar to that of other steroid hormones and is mediated by stereospecific interaction of 1,25-(OH) $_2$ D $_3$ with the VDR which heterodimerizes with the retinoid X receptor (RXR) (211). After interaction with the vitamin D response element (VDRE) in the promoter of target genes, transcription proceeds through the interaction of VDR with coactivators and with the transcription machinery. Importantly, VDR is expressed in epithelia that play a role in Ca^{2+} (re)absorption. The functional significance of target proteins as well as the functional significance of proteins involved in the transport and metabolism of vitamin D is also of major importance. In general, transcellular Ca^{2+} transport in the small intestine and the distal part of the nephron is facilitated by the Ca^{2+} transport proteins, namely, TRPV5, TRPV6, the calbindins, NCX1 and PMCA1b, and stimulated by 1,25-(OH) $_2$ D $_3$ primarily via a genomic action. The contribution of each individual trans-

porter to the overall stimulatory action of $1,25\text{-(OH)}_2\text{D}_3$ has been addressed in several studies as described in the following section.

1. Calbindins

Early studies demonstrated that $1,25\text{-(OH)}_2\text{D}_3$ stimulates the expression of calbindin- $\text{D}_{9\text{K}}$ and calbindin- $\text{D}_{28\text{K}}$ in humans and many animal models. Promoter studies on these mammalian calbindin genes have demonstrated functional VDREs that interact with nuclear factors and may mediate, at least in part, the enhanced expression of these genes by $1,25\text{-(OH)}_2\text{D}_3$ (88, 140). The appearance of calbindin- $\text{D}_{9\text{K}}$ protein in the gut and Ca^{2+} transport coincide as a function of time in response to $1,25\text{-(OH)}_2\text{D}_3$ (200). However, situations are reported in which Ca^{2+} absorption diminishes while calbindin remains high in the small intestine (158, 363). Apparently, a tight correlation between calbindin expression and Ca^{2+} transport is not always present. It is not known whether the expression of TRPV6 is affected under this condition, but these observations suggest that calbindin- $\text{D}_{9\text{K}}$ is not the rate-limiting step in Ca^{2+} absorption. Previous studies have indicated that other proteins play an additional role in transcellular Ca^{2+} (re)absorption which led to an analysis of the basolateral efflux and apical influx Ca^{2+} transporters.

2. Basolateral extrusion mechanisms

The effect of $1,25\text{-(OH)}_2\text{D}_3$ on the basolateral extrusion systems, NCX1 and PMCA1b, is less clear and remains controversial. Although NCX1 plays a dominant role in the extrusion process in renal cells (121, 184, 243, 427), many studies failed to establish a direct regulation by vitamin D. Exposure of $1,25\text{-(OH)}_2\text{D}_3$ to primary cultures of rabbit DCT and CNT did not noticeably alter NCX1 expression (391). However, repletion studies with vitamin D-deficient animal models consistently demonstrated a vitamin D-dependent regulation of renal NCX1 and duodenal PMCA1b (see sect. vi). Importantly, these studies in mice indicated that renal PMCA1b expression and intestinal NCX1 expression were not significantly regulated by vitamin D. PMCA1b is the only isoform predominantly expressed in small intestine and kidney (8, 391). In kidney, it has been shown experimentally that during variable circumstances the extrusion capacity of PMCA1b is more than adequate, suggesting that the Ca^{2+} exit step is not necessarily a prime target for regulation by $1,25\text{-(OH)}_2\text{D}_3$ (391). This could perhaps explain the difficulty to observe a consistent stimulatory effect of $1,25\text{-(OH)}_2\text{D}_3$ on renal PMCA1b (169, 392). Recently, Kip and Strehler (214) demonstrated that $1,25\text{-(OH)}_2\text{D}_3$ is a positive regulator of PMCA in MDCK cells. Interestingly, $1,25\text{-(OH)}_2\text{D}_3$ caused a decrease of PMCA protein content in the apical membrane fraction and a concomitant increase of the pumps in the basolateral membrane (214). In addition,

these authors could demonstrate a significant increase in the expression of PMCA upon stimulation by $1,25\text{-(OH)}_2\text{D}_3$ that correlated with the magnitude of transcellular Ca^{2+} transport. In small intestine, many groups have shown that $1,25\text{-(OH)}_2\text{D}_3$ upregulates PMCA1b protein expression (8, 9, 387, 392). Furthermore, $1,25\text{-(OH)}_2\text{D}_3$ enhanced PMCA1b mRNA stability and activity (147, 148). However, other reports in which primary cultures of renal cells and animal models were used failed to show significant regulation of renal PMCA1b expression level by $1,25\text{-(OH)}_2\text{D}_3$ (391, 392). Conversely, run-off reporter gene assays using 1.7 kb of the human PMCA1 promoter expressed in distal tubular cell lines demonstrated mRNA downregulation by $1,25\text{-(OH)}_2\text{D}_3$ (149). Taken together, a consistent stimulatory effect of $1,25\text{-(OH)}_2\text{D}_3$ on NCX1, but not on PMCA1b, in the kidney has been established. In the small intestine, however, PMCA1b is the vitamin D-regulated extrusion system.

3. Epithelial Ca^{2+} channels

Recent studies consistently indicated that the expression of TRPV5 and TRPV6 is tightly controlled by $1,25\text{-(OH)}_2\text{D}_3$ (51, 61, 112–114, 169, 174, 279, 359, 387, 392, 435). The first evidence for this vitamin D sensitivity was obtained in *in vivo* studies in which vitamin D_3 -depleted rats were repleted (174). This was accompanied by normalization of the plasma Ca^{2+} concentration and an increase in the amount of TRPV5 mRNA and protein expression in the kidney. As a different approach to elicit vitamin D genomic responses, a single dose of $1,25\text{-(OH)}_2\text{D}_3$ was administered to mice (392). Quantitative PCR data demonstrated an upregulation of TRPV5 in kidney (3-fold) and TRPV6 in duodenum (6-fold). Recently, Nijenhuis et al. (279) addressed the localization and $1,25\text{-(OH)}_2\text{D}_3$ -dependent regulation of TRPV6 in the kidney. Intraperitoneal injection of 100 ng $1,25\text{-(OH)}_2\text{D}_3$ in mice resulted in an increase in TRPV6 mRNA (2-fold) and protein (3-fold) expression in the kidney. Although renal TRPV6 expression was upregulated by $1,25\text{-(OH)}_2\text{D}_3$, the effect of this hormone on TRPV5 expression was more impressive. Analysis of putative promoter regions of human and murine TRPV5/6 genes revealed potential vitamin D response elements in line with the previously observed functional data (174, 279). Song et al. (359) also examined the expression of TRPV5 and TRPV6 mRNA in duodenum and kidney of mice. Following a single dose of $1,25\text{-(OH)}_2\text{D}_3$, induction of duodenal TRPV6 mRNA occurred within 3–6 h and preceded the induction of intestinal Ca^{2+} absorption. In addition, this study described that the intestinal TRPV6 mRNA level increased 30-fold at weaning, coincident with the induction of calbindin- $\text{D}_{9\text{K}}$ expression. In contrast, renal TRPV6 and TRPV5 mRNA expression was equal until weaning when TRPV5 mRNA is induced and TRPV6 mRNA levels drop 70% (359). The observed vita-

min D-dependent regulation of TRPV5 and TRPV6 was subsequently extensively studied using many different cell lines and animal (knockout) models as discussed in the next paragraph.

4. Vitamin D-dependent regulation of Ca^{2+} transport in animal models

Powerful tools to investigate the vitamin D dependency of target proteins are knockout mice. Within the past few years a wealth of new information has been obtained from studies using knockout and transgenic mice. Several genetically modified mouse models including VDR (392, 440) and 1α -OHase (86, 298) knockout mice, in which the vitamin D system has been inactivated, have been created to systematically dissect the genetic regulation of Ca^{2+} transport genes and their functional consequences on transcellular Ca^{2+} transport. St-Arnaud and co-workers (86) generated 1α -OHase knockout mice that represent a unique animal model for pseudovitamin D-deficiency rickets (PDDR), since these mice display undetectable $1,25\text{-(OH)}_2\text{D}_3$ concentrations, hypocalcemia, secondary hyperparathyroidism, and failure to thrive (86). In addition, the 1α -OHase^{-/-} mice developed distinct histological evidence of rickets and osteomalacia. Interestingly, there was a correlative relationship between the expression level of TRPV5, calbindin- $\text{D}_{28\text{K}}$, and NCX1 proteins in kidney; TRPV6, calbindin- $\text{D}_{9\text{K}}$, and PMCA1b in duodenum; and the serum Ca^{2+} concentration (169, 386, 387). Normalization of the plasma Ca^{2+} concentration by $1,25\text{-(OH)}_2\text{D}_3$ was associated with a restoration of the expression level of the Ca^{2+} transporters, confirming the essential role of these proteins in active $1,25\text{-(OH)}_2\text{D}_3$ -mediated Ca^{2+} (re)absorption. The concerted regulation of TRPV5/6 and the other Ca^{2+} -transporting proteins guarantees sufficient capacity during high transport rates. Calbindin-D regulates the Ca^{2+} influx across the apical membrane by buffering intracellular Ca^{2+} and thus controlling feedback inhibition of TRPV5/6 channel activity (404).

Analogous observations were made from experiments performed with VDR knockout mice (392, 423). In these hypocalcemic mice, urinary Ca^{2+} excretion is inappropriately high, suggesting renal Ca^{2+} wasting due to disturbed Ca^{2+} reabsorption. It has been demonstrated in this mouse model that duodenal TRPV6 levels are dramatically and consistently downregulated (392, 423). Intriguingly, the observed expression pattern indicated that, among the candidate Ca^{2+} -transporting genes, mainly TRPV6 is severely impaired in VDR-knockout mice.

In addition, the correlation between vitamin D and the expression level of the Ca^{2+} transport proteins has been addressed in several cell models. Wood and co-workers (113, 435) studied in detail the vitamin D sensitivity of TRPV6, calbindin- $\text{D}_{9\text{K}}$, and PMCA1b in Caco-2

cells. A clear correlation between the $1,25\text{-(OH)}_2\text{D}_3$ -induced expression of TRPV6, calbindin- $\text{D}_{9\text{K}}$, and PMCA1b and transcellular Ca^{2+} transport was established in this intestinal cell line. In contrast, Barley et al. (20) could not confirm the generally observed vitamin D-dependent sensitivity of TRPV6 in duodenal biopsies from 20 normal volunteers. However, there was a 10-fold variation between the lowest and the highest level of TRPV6 expression. In addition, the subjects used were a mixed population of men and women of age 25–71 years, which made it hard to disclose a relationship between TRPV6 expression and vitamin D metabolites. Likewise, cell lines and primary cultures have been established from the distal part of the nephron including DCT and CNT (38, 91, 391). Measurements of calbindin- $\text{D}_{28\text{K}}$ expression in control and $1,25\text{-(OH)}_2\text{D}_3$ -treated renal epithelial cells indicated a direct relationship between $1,25\text{-(OH)}_2\text{D}_3$ -induced calbindin expression and transcellular Ca^{2+} transport (391). Taken together, vitamin D-deficient animal models and epithelial cell lines demonstrated a consistent $1,25\text{-(OH)}_2\text{D}_3$ sensitivity of TRPV5, TRPV6, and the calbindins and to a lesser extent the basolateral extrusion systems NCX1 and PMCA1b.

B. Regulation by PTH

The parathyroid glands play a key role in maintaining the extracellular Ca^{2+} concentration through their capacity to sense even minute changes in the level of blood Ca^{2+} from its normal level. The Ca^{2+} -sensing receptor (CaSR) is the mechanism through which the parathyroid chief cells sense variations in the Ca^{2+} concentration and release PTH. In response to low blood Ca^{2+} levels, PTH is secreted into the circulation and then acts primarily on kidney and bone, where it activates the PTH/PTHrP receptor. This receptor directly enhances the tubular Ca^{2+} reabsorption, and it stimulates the activity of 1α -OHase and, thereby, increases the $1,25\text{-(OH)}_2\text{D}_3$ -dependent absorption of Ca^{2+} from the intestine. Several groups localized PTH/PTHrP receptor mRNA in rat kidney to glomerular podocytes, PCT, PST, cortical thick ascending limb, and DCT, but the receptor was not detected in the thin limb of Henle's loop or in CD (231, 437). PTH stimulates active Ca^{2+} reabsorption in the distal part of the nephron (154). As outlined in section III, Bindels et al. (38) and Gesek and Friedman (124) have used immunodissected cell lines from rabbit DCT and CNT and mouse DCT, respectively, to investigate PTH-stimulated Ca^{2+} transport. These studies demonstrated equivocally that PTH increases transepithelial Ca^{2+} transport via a dual signaling mechanism involving PKA- and PKC-dependent processes (124, 170). Various mechanisms of PTH action have been postulated including membrane insertion of apical Ca^{2+} channels (12), opening of basolateral chloride

channels resulting in cellular hyperpolarization (127), and modulation of PMCA activity (383). Friedman and colleagues (12) examined Ca^{2+} influx in single cultured cells from distal renal tubules sensitive to PTH by measuring intracellular Ca^{2+} . Their results demonstrated that PTH activates dihydropyridine-sensitive channels responsible for Ca^{2+} entry. Once inserted or activated, these dihydropyridine-sensitive channels could mediate Ca^{2+} entry into these Ca^{2+} -transporting epithelial cells (12). This finding is in contrast to the channel characteristics of TRPV5 that is dihydropyridine insensitive (178). It is well possible that these dihydropyridine-sensitive Ca^{2+} channels play a role in signal transduction processes to maintain the cellular Ca^{2+} homeostasis. Recently, it was reported that parathyroidectomy in rats resulted in decreased serum PTH levels and hypocalcemia, which was accompanied by decreased levels of TRPV5, calbindin- $\text{D}_{28\text{K}}$, and NCX1 (388). Supplementation with PTH restored serum Ca^{2+} concentrations and abundance of these Ca^{2+} transporters in kidney. These data suggest that PTH affects renal Ca^{2+} handling through the regulation of the expression of the active renal Ca^{2+} transport proteins, including the epithelial Ca^{2+} channel TRPV5. Furthermore, it was demonstrated that PTH stimulates the PMCA activity by increasing the affinity for Ca^{2+} in the distal tubule, which is in contrast to $1,25\text{-(OH)}_2\text{D}_3$ that did not directly affect the basolateral membrane PMCA activity (383).

Immunohistochemical analysis of rat duodenal sections showed localization of the PTH/PTHrP receptor in epithelial cells along the villus with intense staining of brush-border and basolateral membranes and cytoplasm (135). Interestingly, the receptor was absent in goblet cells. Direct effects of PTH have been reported on Ca^{2+} uptake by isolated rat duodenal cell preparations enriched in enterocytes. The first indication of a direct effect of PTH on the intestine was accomplished by perfusion experiments of isolated duodenal loops with PTH that increased Ca^{2+} transport (272, 273). These findings were confirmed by Picotto et al. (309) who demonstrated that PTH significantly stimulates enterocyte Ca^{2+} influx. This Ca^{2+} influx was blocked by the Ca^{2+} channel antagonists verapamil and nitrendipine.

In bone, PTH can induce a rapid release of Ca^{2+} from the bone matrix, but it also mediates long-term changes in Ca^{2+} metabolism by acting directly on the bone-forming osteoblasts and indirectly on bone-resorbing osteoclasts by increasing their number and activity. However, molecular mechanisms of PTH action in mediating Ca^{2+} transport in bone and intestine remain poorly understood.

C. Regulation by Calcitonin

Calcitonin, a 32-amino acid peptide hormone produced primarily by the thyroid, and its receptor are well

known for their ability to regulate osteoclast-mediated bone resorption (186). Calcitonin has been suggested to be a renal Ca^{2+} -conserving hormone and may share similar signaling mechanisms with PTH. Previously, this peptide was infused into groups of acutely thyroparathyroidectomized rats that had been treated with calcitonin for 12 days resulting in a marked inhibitory effect on renal Ca^{2+} excretion (67). The hypocalcemic and hypophosphatemic calcitonin is secreted by mammalian thyroid parafollicular cells. It has been reported that calcitonin increases Ca^{2+} reabsorption in mouse DCT cells, but the molecular mechanism is not known yet. It was postulated that calcitonin increases Cl^- conductance in DCT cells, resulting in membrane hyperpolarization and activation of Ca^{2+} entry through Ca^{2+} channels (139). Interestingly, renal $1\alpha\text{-OHase}$ gene expression is strictly upregulated at the transcriptional level through its gene promoter by PTH and calcitonin, whereas $1,25\text{-(OH)}_2\text{D}_3$ itself has a negative effect on gene expression (205). Consequently, increased $1\alpha\text{-OHase}$ gene activity results in elevated $1,25\text{-(OH)}_2\text{D}_3$ levels and enhanced intestinal and renal Ca^{2+} (re)absorption. Previous experiments demonstrated that calcitonin inhibits bone resorption and decreases Ca^{2+} efflux from isolated cat tibiae that underlies its widespread clinical use for the treatment of bone disorders, including Paget's disease, osteoporosis, and hypercalcemia of malignancy.

D. Regulation by Stanniocalcin

Stanniocalcin is another hypocalcemic hormone that is originally identified in fish (414). In these animals stanniocalcin exerts its antihypercalcemic effect by regulating Ca^{2+} and phosphate transporters in the gills, intestine, and kidney (136a). Interestingly, this hormone has also been recently identified in humans (415). In mammals, stanniocalcin is expressed in multiple organs including Ca^{2+} -transporting epithelia like intestine, colon, kidney, and placenta (70, 71). It is released by specialized organs, the corpuscles of Stannius that are located adjacent to the kidney and scattered throughout the kidney (415). Immunoreactivity for stanniocalcin was detected in the limb of Henle, macular densa cells, DCT, and CCD (297). Stanniocalcin acts locally in kidney and gut to modulate Ca^{2+} and phosphate excretion, and its overexpression in mice results in high serum phosphate, dwarfism, and increased metabolic rate (109, 401). The main function of stanniocalcin, similar to that of calcitonin, appears to be the prevention of hypercalcemia. Importantly, stanniocalcin was upregulated by $1,25\text{-(OH)}_2\text{D}_3$ treatment (188, 297). Nevertheless, the true physiological role for stanniocalcin in mammals is less clear, and future studies are needed to establish the functional importance of this hormone.

E. Regulation by Estrogens

Estrogen deficiency results in a negative Ca^{2+} balance and bone loss in postmenopausal women (289, 441, 442). Estrogen deficiency after menopause results in bone loss, which is associated with a rise in plasma and urinary Ca^{2+} (442). It has been generally described that the rise in plasma and urine Ca^{2+} are secondary to an increase in bone resorption. However, some studies have shown that the rise in urinary Ca^{2+} at menopause is not due to an increase in filtered load, suggesting that estrogen also has an effect on renal Ca^{2+} handling (1). In addition to bone, the intestine and kidney are also potential sites for estrogen action and involved in Ca^{2+} handling and regulation. There is increasing evidence that estrogen exerts a physiological role in the regulation of renal and intestinal Ca^{2+} (re)absorption. In vivo studies showed that estrogen deficiency is associated with increased renal Ca^{2+} loss, which can be corrected by estrogen replacement therapy (290, 315). Furthermore, estrogen receptors also reside in proximal and distal tubules of the kidney and in duodenum and colon. However, the underlying mechanism by which estrogen may act on Ca^{2+} (re)absorption is still poorly understood. In addition, it has not been conclusively established whether there is a direct effect of estrogen on Ca^{2+} transport or indirectly mediated by an effect on vitamin D metabolism. It was demonstrated that estrogen upregulates the expression of TRPV5 in kidney in a $1,25\text{-(OH)}_2\text{D}_3$ -independent manner (386). In ovariectomized $1\alpha\text{-OHase}$ knockout mice, 17β -estradiol replacement therapy resulted in upregulation of renal TRPV5, but not the other Ca^{2+} transporters, mRNA, and protein levels, leading to normalization of plasma Ca^{2+} levels (386). Thus renal TRPV5 expression is, independent of vitamin D, transcriptionally controlled by estrogen. By upregulating TRPV5 expression, estrogen could be positively involved in Ca^{2+} reabsorption. Recent findings suggest that also TRPV6 expression is regulated by estrogen, as duodenal expression of TRPV6 mRNA of $1\alpha\text{-OHase}$ knockout mice and ovariectomized rats is upregulated after 17β -estradiol administration (387). Van Cromphaut et al. (393) reported that renal TRPV5 and duodenal TRPV6 expression are reduced in estrogen receptor α ($\text{ER}\alpha$) knockout mice and upregulated by estrogen treatment. In this study, TRPV6 expression was enhanced in both pregnant VDR knockout mice and wild-type littermates. Furthermore, in lactating mice, renal TRPV5 mRNA and duodenal TRPV6 expression levels increased 2 and 13 times, respectively. It is clear that the expression of both epithelial Ca^{2+} channels is influenced by the estrogen status. Estrogens, hormonal changes during pregnancy, and lactation have distinct, vitamin D-independent effects at the genomic level on active duodenal Ca^{2+} absorption mechanisms, mainly through a major upregulation of TRPV6. The estrogen effects seem to be mediated solely by $\text{ER}\alpha$. Nevertheless,

it remains to be clarified whether these changes have functional implications on Ca^{2+} (re)absorption. These data confirm that estrogens and vitamin D are independent potent regulators of the expression of TRPV6, which is involved in active intestinal Ca^{2+} absorption. Together, these data indicate that the function of estrogen in maintenance of the Ca^{2+} balance might be at least in part fulfilled by regulation of TRPV5 and TRPV6 levels, thereby controlling (re)absorption of the amount of Ca^{2+} that is needed for bone calcification.

The mechanism of estrogen-controlled upregulation of epithelial Ca^{2+} channel mRNA remains to be elucidated. Interestingly, Weber et al. (423) recently described an estrogen-responsive element in the promoter sequence of the mouse TRPV6 gene, which was absent in the mouse TRPV5 gene. Alternatively, transcriptional activation by the estrogen-liganded estrogen receptor can be mediated through other elements including activator protein 1 (AP-1) binding sites and GC-rich stimulatory protein (Sp1) binding sites (224, 334). Importantly, the human TRPV5 promoter contains several of these AP-1 and Sp1 sites (174). In the 5'-upstream region of the translational initiation site in the mouse TRPV5 gene, several of these AP-1 and Sp1 binding sites can be found that could be involved in the positive effect observed on TRPV5 mRNA expression by 17β -estradiol treatment. Detailed promoter analysis is necessary to identify the regulatory sites involved in this estrogen-mediated regulation of TRPV5 and TRPV6.

F. Regulation by Thyroid Hormone

There is ample evidence that thyroid dysfunction is associated with disturbances of Ca^{2+} and phosphate homeostasis (81–83, 222, 223, 263). Hypercalcemia is frequently observed in humans with thyrotoxicosis, and similar observations were made in animals (103, 160, 223, 333). It is interesting that long-term hyperthyroid state is associated with Ca^{2+} malabsorption and increased bone resorption. Several effects of thyroid hormone on the kidney, intestine, and bone resemble those of $1,25\text{-(OH)}_2\text{D}_3$. Actions at the cellular level constituting their function as Ca^{2+} -regulating hormones have not been addressed until recently. Kumar and Prasad (223) demonstrated that Ca^{2+} uptake into brush-border membrane vesicles and Ca^{2+} efflux from the basolateral membrane of enterocytes was significantly increased in hyperthyroid rats and decreased in hypothyroid animals. Comparable observations were made in the kidney by these investigators (222). It was postulated that thyroid hormone increases the affinity of TRPV6 for Ca^{2+} in the brush-border membrane of the enterocyte. However, experiments to confirm this hypothesis remain to be performed.

G. Regulation by Dietary Ca^{2+}

Dietary Ca^{2+} is one nutrient that has been the focus of multiple studies in an effort to discover its preventive actions. It has been implicated in the reduction of risk in osteoporosis, whereas a low- Ca^{2+} diet avoids kidney stone formation. Obesity, hypertension, and even cancer are less well-known areas in which increasing dietary Ca^{2+} has a positive outcome (232). A significant link between Ca^{2+} intake and bone mass has been reported. Although recommended daily allowance of calcium is 600 mg/day for adults, ~850 mg/day or more is recommended later in life.

The power of Ca^{2+} supplementation is best illustrated by the use of VDR and 1α -hydroxylase knockout models. The bone phenotype of VDR-ablated mice can be completely rescued by feeding the animals a high- Ca^{2+} , high-phosphorus, high-lactose diet. In addition, the PDDR phenotype of mice deficient for the 1α -OHase gene has been rescued by feeding them with the high- Ca^{2+} diet. The rescue regimen consisted of feeding a diet containing 2% (wt/wt) Ca^{2+} from 3 wk of age until death at 8.5 wk of age. Serum analysis revealed that the rescue diet corrected the hypocalcemia and secondary hyperparathyroidism (87, 168, 169).

Subsequently, the expression level of the Ca^{2+} transport proteins was studied in the knockout mice models described above. Several aforementioned studies provided evidence that the Ca^{2+} transport proteins, including TRPV5 and TRPV6 channels, are regulated by $1,25(\text{OH})_2\text{D}_3$. It is, however, difficult to distinguish the effects of hypocalcemia from those of vitamin D deficiency. Therefore, studies were performed in VDR and 1α -OHase knockout mice fed a normal and high- Ca^{2+} rescue diet (169, 392). Importantly, the reduced expression level of renal TRPV5, calbindin- $\text{D}_{28\text{K}}$, and NCX1 in the 1α -OHase^{-/-} mice was restored by high dietary Ca^{2+} intake and accompanied by normalization of the plasma Ca^{2+} concentration. In line with the $1,25(\text{OH})_2\text{D}_3$ -dependent regulation, dietary Ca^{2+} controls also the other Ca^{2+} transport proteins. In contrast, this Ca^{2+} -enriched rescue diet reduced the expression of renal TRPV5 and calbindin- $\text{D}_{28\text{K}}$ in 1α -OHase^{+/-} mice that exhibit normal serum vitamin D and Ca^{2+} levels. It is known that under physiological conditions, plasma Ca^{2+} acts via a negative-feedback mechanism that eventually leads to suppression of the 1α -OHase-activity that decreases Ca^{2+} reabsorption and expression of Ca^{2+} transport proteins. Likewise, the expression of the intestinal Ca^{2+} transport proteins, TRPV6, calbindin- $\text{D}_{9\text{K}}$, and PMCA1b, were normalized by this rescuing Ca^{2+} diet (387).

Comparable observations were made in VDR knockout mice where duodenal TRPV5 and TRPV6 mRNA levels were upregulated by dietary Ca^{2+} (392). Studies with VDR^{-/-} and 1α -OHase^{-/-} mice revealed that Ca^{2+} sup-

plementation can upregulate gene transcription encoding for Ca^{2+} transporters in the absence of circulating $1,25(\text{OH})_2\text{D}_3$, but the molecular mechanism of this vitamin D-independent Ca^{2+} -sensitive pathway remains elusive. It is, however, likely that in addition to the identified $1,25(\text{OH})_2\text{D}_3$ response elements in the promoter regions of TRPV5/6 and calbindin-D genes also Ca^{2+} -responsive elements are present. Several elements have been proposed to function as Ca^{2+} -sensitive transcriptional regulators including the serum responsive element and the cAMP/ Ca^{2+} -responsive element (133). Of interest is the identification of a Purkinje cell expression specific element in the calbindin- $\text{D}_{28\text{K}}$ gene that functions as a Ca^{2+} -sensitive transcriptional regulatory mechanism (10). This mechanism may play a role in fine-tuning the Ca^{2+} buffer capacity of Purkinje cells. Detailed promoter analysis is needed to investigate if these domains are also present in the promoter of the Ca^{2+} transport genes.

H. Regulation by the Ca^{2+} -Sensing Receptor

The CaSR plays a pivotal role in the regulation of Ca^{2+} homeostasis by sensing subtle changes in circulating Ca^{2+} concentration (185). In the parathyroid gland, the CaSR represents the molecular mechanism by which parathyroid cells detect changes in blood ionized Ca^{2+} concentration, modulate PTH secretion accordingly, and thus maintain serum Ca^{2+} levels within a narrow physiological range. Interestingly, in the kidney, the CaSR regulates renal Ca^{2+} excretion and influences the transepithelial movement of water and other electrolytes. The CaSR is expressed at numerous sites along the nephron including the apical membrane of the PT, the basolateral membrane of the medullary and cortical TAL and DCT, in some cells of CCD, and at the apical membrane of the IMCD. Thus CaSR can apparently be trafficked either to the apical or to the basolateral membrane depending on the tubule cell type. The receptor is located in the epithelial cells of the PT, where it is located in close proximity to the numerous apical transporters of various nutrients and electrolytes that reside within this portion of the nephron (329). There is evidence that the CaSR in the PT antagonizes or limits the effects of PTH as stimulator of $1,25(\text{OH})_2\text{D}_3$ production and phosphate excretion (11). The water-impermeable TAL is responsible for the reabsorption of ~20–25% of filtered Ca^{2+} . The extracellular Ca^{2+} concentration at the basolateral side of these cells will increase as Ca^{2+} reabsorption occurs. Elevation of plasma Ca^{2+} or Mg^{2+} levels modulates mineral ion transport in the loop of Henle. The observations can be explained by the action of the CaSR, which permits the reabsorbed Ca^{2+} to feed back onto the cell decreasing $\text{Ca}^{2+}/\text{Mg}^{2+}$ reabsorption and, thereby, preventing hypercalcaemia (421). Motoyama and Friedman (264) demon-

strated that CaSR activation in cortical TAL by the agonist NPS R-467 or Gd^{3+} indirectly inhibits passive Ca^{2+} transport and directly suppresses PTH-induced transcellular Ca^{2+} transport. Immunohistochemical investigation of rat kidney reveals CaSR immunostaining at the basolateral and occasionally apical membranes of DCT (329). However, the extent to which CaSR expression overlaps with the Ca^{2+} transport proteins including TRPV5 is not known. In MDCK cells, basolateral exposure to CaSR-stimulatory concentrations of extracellular Ca^{2+} or neomycin inhibits unidirectional Ca^{2+} reabsorption across these cells, possibly via the inhibition of PMCA (44). Studies in immortalized mDCT cells showed that $1,25-(OH)_2D_3$ -induced Mg^{2+} influx is also inhibited upon exposure to elevated extracellular Ca^{2+} concentrations, an effect that was blocked by an anti-CaSR monoclonal antibody or by transfection with antisense CaSR oligodeoxynucleotides (330). Furthermore, it has been demonstrated that a high luminal Ca^{2+} concentration activates the CaSR receptor in the apical membrane of the IMCD. As a consequence, the vasopressin-elicited water permeability is blunted by a PKC-mediated aquaporin-2 retrieval mechanism to reduce water reabsorption and prevent a further rise in urinary Ca^{2+} concentration (335). These data are the first analyses of hypercalcemia-induced alterations in arginine vasopressin-regulated water permeability and membrane transporters in IMCD. It is hypothesized that alterations in IMCD transport occur during hypercalcemia, allowing the body to dispose of excess Ca^{2+} without forming Ca^{2+} -containing renal stones.

CaSR forms a unique molecular target for drugs that can directly alter the activity of the receptor, thereby manipulating the extracellular Ca^{2+} balance. Several calcimimetic compounds, like NPS R-467, have been described that activate CaSRs on parathyroid cells and suppresses serum levels of PTH and Ca^{2+} . However, the involvement of intestinal and renal Ca^{2+} (re)absorption in the NPS R-467-induced hypocalcaemia is not clear. A recent study by van Abel et al. (388) investigated the effect of NPS R-467 on the expression of intestinal and renal Ca^{2+} transport proteins, including the epithelial Ca^{2+} channels TRPV5 and TRPV6. To this end, mice were infused with NPS R-467 via osmotic minipumps for 7 days. Treatment with NPS R-467 reduced serum PTH levels in a dose-dependent manner, which was accompanied by a significant decrease in serum Ca^{2+} concentration. Quantitative PCR and biochemical analysis of duodenal and renal samples demonstrated an overall downregulation of mRNA expression levels and proteins involved in active transcellular Ca^{2+} (re)absorption. The effects of the treatment with NPS R-467 on the expression of Ca^{2+} transporters could involve a direct action of CaSRs in kidney and/or intestine; however, previous studies have also indicated that the acute hypocalcemic response to calcimi-

metic compounds results from the inhibition of PTH secretion (388).

I. Regulation by Associated Proteins

To date, little information is available concerning the molecular players responsible for regulating the activity of TRPV5 and TRPV6. A number of regulatory proteins have recently been described that modify the biophysical, pharmacological, and expression properties of ion channels and transporters by direct interactions (233). These newly identified associated proteins have facilitated the elucidation of important molecular pathways modulating transport activity. Until now three regulatory proteins, i.e., calmodulin, S100A10-annexin 2, and 80K-H, have been described that associate with TRPV5 and/or TRPV6 (145, 276, 394).

1. Calmodulin

CaM was identified as a TRPV6-interacting member and is a ubiquitous cytosolic protein known to regulate the activity of different ion channels, Ca^{2+} pumps, and other proteins in a Ca^{2+} -dependent manner (276). CaM consists of four Ca^{2+} -binding EF-hand structures, which are localized in the amino and carboxy terminus. Ca^{2+} binding to CaM is highly cooperative with Ca^{2+} binding first to the carboxy-terminal EF-hands, which have the highest affinity for Ca^{2+} , followed by Ca^{2+} binding to lower affinity sites located in the amino terminus (418). At rest, when Ca^{2+} concentrations are low, Ca^{2+} entry through voltage-gated Ca^{2+} channels, cyclic nucleotide-gated channels, and NMDA receptors is enabled. Upon Ca^{2+} influx, activated Ca^{2+} -CaM inactivates the above-mentioned influx pathways as well as TRPL-mediated currents in *Drosophila* photoreceptors (341). In addition, other members of the TRP family are possibly regulated by CaM. CaM binding to TRPV1 was restricted to a 35-amino acid segment in the carboxy terminus, and deletion of this CaM binding segment prevented TRPV1 desensitization (293). Members of the TRPC family have been shown to bind CaM (52, 225, 439). CaM acts as a Ca^{2+} sensor in the Ca^{2+} -dependent feedback inhibition of TRPC1 as demonstrated using Ca^{2+} -insensitive CaM mutants (356). Another study using CaM inhibitors described that TRPC6 is regulated by CaM (52).

There is a rapid Ca^{2+} -dependent inactivation of TRPV6 channels that seems to be independent of CaM binding and could be due to a local effect of Ca^{2+} on the intracellular pore-forming region (276). This conclusion was based on the observation that the inactivation behavior of TRPV6 was altered in mutants that do not bind CaM. In addition, there was a slower inactivation that was found to be Ca^{2+} /CaM dependent. Although CaM does not bind to TRPV6 at Ca^{2+} concentrations normally present in

cells at rest, binding was observed at increased Ca^{2+} concentrations with maximal binding at a concentration of 60 μM . Ca^{2+} /CaM binding inactivates TRPV6 channels, although additional Ca^{2+} -dependent and -independent inactivation or rundown mechanisms must exist. Removal of CaM binding does not affect the initial rapid phase of inactivation, nor does it affect the slow inactivation.

Interestingly, binding of Ca^{2+} /CaM, however, can be prevented by PKC-mediated phosphorylation of a threonine residue within the CaM binding site. Niemeyer et al. (276) concluded that PKC activity thus may act as a switch that can regulate the amount of Ca^{2+} influx through TRPV6 channels by altering their inactivation behavior. These results suggest a model in which TRPV6-expressing cells can have a substantial Ca^{2+} influx, where phosphorylation of TRPV6 can act as a positive-feedback system, delaying the inactivation process. The described mechanism of competitive regulation of TRPV6 by PKC and CaM is, however, restricted to human TRPV6, since this particular PKC site in the CaM-binding motif is not conserved in the other species (276). Recently, the corresponding region in mouse TRPV6 was shown to bind CaM (167). Detailed analysis of the binding region predicted a casein kinase motif, but no significant phosphorylation could be detected in this particular domain. The regulation of TRPV6 by CaM was recently confirmed by Lambers et al. (229). By combination of pull-down assays and coimmunoprecipitations, it was demonstrated that CaM binds to both TRPV5 and TRPV6 in a Ca^{2+} -dependent fashion. The binding of CaM to mouse TRPV6 was localized to the transmembrane domain and consensus CaM-binding motifs located in the amino [1–5–10 motif, TRPV6 (88–97)] and carboxy termini [1–8–14 motif, TRPV6 (643–656)], suggesting a mechanism of regulation involving multiple interaction sites (229). Electrophysiological experiments demonstrated that HEK293 cells heterologously expressing TRPV5 or TRPV6 and CaM mutants revealed that TRPV6, but not TRPV5, is negatively regulated by an inactive CaM mutant. This finding is remarkable given the high homology between both channels, similar Ca^{2+} -dependent regulation of channel activity, and binding of CaM to both channels. Furthermore, the effect of CaM was mediated by the high Ca^{2+} affinity EF-hand structures 3 and 4 present in the carboxy terminus of CaM (229).

2. S100A10-annexin 2

Recently, an auxiliary protein of TRPV5 and TRPV6 was identified by screening a mouse kidney cDNA library using the yeast two-hybrid system. A bait was constructed with the cytoplasmic carboxy-terminal region of TRPV5. This study described the identification of the first auxiliary protein for TRPV5 and TRPV6, named S100A10, which specifically associates with the carboxy termini of

these epithelial Ca^{2+} channels (394). S100A10 is a 97-amino acid protein member of the S100 superfamily that is present in a large number of organisms including vertebrates, insects, nematodes, and plants. S100A10 is predominantly present as a heterotetrameric complex with annexin 2, which has been implicated in numerous biological processes including endocytosis, exocytosis, and membrane-cytoskeleton interactions (136). Annexin 2 interacts with actin and is postulated to bind to the cytoplasmic face of membrane rafts to stabilize these domains, thereby providing a link to the actin cytoskeleton. Several members of the S100 protein family form heteromeric complexes with annexins: S100A11 with annexin 1 (247), S100A6 with annexin 2 (380), and S100A10 is often found tightly associated with annexin 2 to form a tetrameric complex (326). Van de Graaf et al. (394) provided the first evidence of a regulatory role for the S100A10-annexin 2 heterotetramer in vitamin D-mediated Ca^{2+} (re)absorption in general and in particular in TRPV5 and TRPV6 functioning. The association of S100A10 with TRPV5 and TRPV6 was restricted to a short peptide sequence VATTV located in the carboxy termini of these channels. This stretch is conserved among all identified species of TRPV5 and TRPV6 (394). Interestingly, the TTV sequence in the S100A10 binding motif resembles an internal type I PDZ consensus binding sequence, which is S/TXV (360). However, S100A10 does not contain PDZ domains, indicating that the TRPV5-S100A10 interaction has a different nature. The first threonine of the S100A10 interaction motif was identified as a crucial determinant for binding. Furthermore, the activity of TRPV5 and TRPV6 was abolished when this particular threonine was mutated, demonstrating that this motif is essential for channel function. Malfunctioning of these mutant channels was accompanied by a major disturbance in their subcellular localization, indicating that the S100A10-annexin 2 heterotetramer facilitates the translocation of TRPV5 and TRPV6 channels to the plasma membrane. The importance of annexin 2 in this process was demonstrated by a siRNA-based downregulation of annexin 2 that significantly inhibited the currents through TRPV5 and TRPV6, indicating that annexin 2 in conjunction with S100A10 is crucial for TRPV5 activity. In line with the cortical localization of annexin 2 and its postulated function in organizing certain plasma membrane domains, these findings provided the first functional evidence for a regulatory role of annexin 2 controlling Ca^{2+} channel trafficking. Interestingly, previous studies indicated that the background K^+ channel (TASK1) is associated with S100A10 via its carboxy-terminal sequence SSV (142). The S100A10 interaction promoted the translocation of TASK1 to the plasma membrane producing functional K^+ channels. This sequence resembles the binding motif in TRPV5 and TRPV6 identified in the present study, suggesting a shared structural S100A10 binding pocket. However, this

motif is absent in the tetrodotoxin-insensitive voltage-gated Na^+ channel (Nav1.8), which has been shown to bind S100A10 via its amino terminus and essential for plasma membrane trafficking (296). Interestingly, in line with the epithelial Ca^{2+} channels, S100A10 expression was found to be vitamin D sensitive (394). In addition, annexin 2 expression levels have been shown to increase upon prolonged incubation with $1,25\text{-(OH)}_2\text{D}_3$ (252). Coregulation of TRPV5/6, S100A10, and annexin 2 could fulfill the essential control of trafficking of these channels to the plasma membrane. $1,25\text{-(OH)}_2\text{D}_3$ has been shown to exert its effects by slow and rapid mechanisms. The slower genomic effects are mediated by interaction with the nuclear VDR. Recently, it was reported that annexin 2 serves as a membrane receptor for $1,25\text{-(OH)}_2\text{D}_3$ and mediates the rapid effect of the hormone on intracellular Ca^{2+} . It has been demonstrated that $1,25\text{-(OH)}_2\text{D}_3$ is specifically bound to annexin 2 in the plasma membrane of rat osteoblast-like cells (18, 19). Partially purified plasma membrane proteins and purified annexin 2 exhibited specific and saturable binding for $1,25\text{-}[^3\text{H}]\text{(OH)}_2\text{D}_3$. The results suggest that annexin 2 may serve as a receptor for rapid actions of $1,25\text{-(OH)}_2\text{D}_3$. However, there is still a debate whether there is functional interaction between $1,25\text{-(OH)}_2\text{D}_3$ and annexin 2 (253a). Taken together, these findings show that the S100A10-annexin 2 complex is a significant component for the trafficking of ion channels to the plasma membrane in general and in particular a major regulator of TRPV5 and TRPV6 function and, therefore, the Ca^{2+} homeostasis.

3. 80K-H

By the use of cDNA microarrays, Gkika et al. (145) identified 80K-H as a protein involved in the Ca^{2+} -dependent control of TRPV5 (145). 80K-H was initially identified as a PKC substrate, but its biological function remains to be established (166). This recent study demonstrated a specific interaction between 80K-H and TRPV5, colocalization of both proteins in the kidney, and similar transcriptional regulation by $1,25\text{-(OH)}_2\text{D}_3$ and dietary Ca^{2+} (145). Furthermore, 80K-H directly bound Ca^{2+} , and inactivation of its two EF-hand structures totally abolished Ca^{2+} binding. Electrophysiological studies using 80K-H mutants showed that three domains of 80K-H (the two EF-hand structures, the highly acidic glutamic stretch, and the His-Asp-Glu-Leu sequence) are critical determinants for TRPV5 activity. Importantly, inactivation of the EF-hand pair reduced the TRPV5-mediated Ca^{2+} current and increased the TRPV5 sensitivity to intracellular Ca^{2+} , accelerating the feedback inhibition of the channel. None of the 80K-H mutants altered the TRPV5 plasma membrane localization nor the association of 80K-H with TRPV5, suggesting that 80K-H has a direct effect on

TRPV5 activity (145). Taken together, 80K-H acts as a novel Ca^{2+} sensor controlling TRPV5 channel activity.

J. Diuretics

Diuretics such as furosemide and thiazides are frequently used in the clinical practice and are known to alter Ca^{2+} metabolism. All of them are usually administered alone or in a combination of diuretics over a long period of time and are known to disturb Ca^{2+} reabsorption leading to various symptoms including alterations in structure and stability of bone (422). However, despite the widespread use of these diuretics, the molecular mechanism underlying their action on Ca^{2+} reabsorption remains incompletely understood.

1. Furosemide

Loop diuretics, such as furosemide, inhibit the $\text{Na}^+\text{-K}^+\text{-2Cl}^-$ (NKCC2) transporter present in the apical membrane of the TALH resulting in a reduction in NaCl reabsorption and K^+ recycling across the apical membrane. This action diminishes the lumen-positive potential, which is the driving force for paracellular Ca^{2+} reabsorption in this particular nephron segment and explains the hypercalciuric effect of furosemide (123). The calciuric effect of furosemide enhances the delivery of Ca^{2+} to DCT and CNT, which are the primary sites of active Ca^{2+} reabsorption. It is at present unknown whether these latter nephron segments partly compensate the hypercalciuric effect of the loop diuretics. In this respect, it is interesting to study the effect of furosemide on the expression and activity of the Ca^{2+} transport proteins. This knowledge could also provide a rationale for TRPV5 or calbindin- $\text{D}_{28\text{K}}$ activating treatment during furosemide application to reduce the side effect caused by the hypercalciuric action of furosemide. Until now, data about the molecular regulation of these proteins during furosemide treatment were not available.

2. Thiazides

Thiazides are the most widely prescribed drugs today, particularly by being the mainstay of first-line therapy in hypertension. In addition, these diuretics have, in contrast to loop diuretics, the unique characteristic of decreasing Na^+ reabsorption while increasing Ca^{2+} reabsorption (79). Their hypocalciuric effect provides therapeutic opportunities in, for instance, idiopathic hypercalciuria and nephrolithiasis. Furthermore, thiazides have been shown to increase bone mineral density and decrease fracture risk, spiking interest in the favorable long-term effects of these diuretics in counteracting osteoporosis (321). However, the exact molecular mechanism

responsible for this thiazide-induced hypocalciuria has been a subject of discussion.

Thiazides increase renal Na^+ excretion by inhibiting the $\text{Na}^+\text{-Cl}^-$ cotransporter (NCC) present in the apical membrane of DCT cells (255). This inhibition of Na^+ reabsorption results in increased renal salt and water loss and thereby decreases extracellular volume (255). Costanzo and Windhager (79) showed in pioneering micropuncture and microperfusion experiments that chlorothiazide can stimulate Ca^{2+} transport in DCT in situ. Their data are restricted to the acute effects of these diuretics on electrolyte transport and are difficult to translate to chronic thiazide treatment. Several theories, emphasizing an activation of transcellular Ca^{2+} transport processes in DCT, were subsequently advanced to explain the hypocalciuria during thiazide administration. Stimulation of apical Ca^{2+} entry has been suggested, mediated by hyperpolarization of the plasma membrane secondary to NCC inhibition (138). Alternatively, enhanced basolateral $\text{Na}^+/\text{Ca}^{2+}$ exchange by upregulation of NCX1 secondary to decreased intracellular Na^+ concentration has also been suggested as the principal responsible mechanism (101, 121, 123). However, the significant downregulation of NCX1 transcripts during thiazide treatment shown in this latter study is hard to reconcile with the proposed stimulation of $\text{Na}^+/\text{Ca}^{2+}$ exchange activity. Furthermore, calbindin- $\text{D}_{28\text{K}}$ mRNA and protein abundance were also decreased during thiazide treatment (278). Calbindin- $\text{D}_{28\text{K}}$ facilitates diffusion of Ca^{2+} through the cytosol and simultaneously serves as an intracellular Ca^{2+} buffer to protect the cell from toxic Ca^{2+} levels (107). This substantial decrease of the Ca^{2+} diffusion and buffering capacity would be detrimental in the presence of increased apical Ca^{2+} entry and increased transcellular Ca^{2+} transport. The above-described hypotheses rely on substantial colocalization in DCT of NCC and the proteins involved in active Ca^{2+} transport. Extensive immunohistochemical studies demonstrated only minor overlap, whereas the Ca^{2+} transporters (i.e., TRPV5, calbindin- $\text{D}_{28\text{K}}$, NCX1, and PMCA1b) completely colocalized (171, 240, 278). Interestingly, Loffing et al. (239) demonstrated that the DCT epithelium had lost the structural characteristics of electrolyte transporting epithelia after chronic thiazide treatment and the cells were in different stages of apoptosis. In apoptotic cells, calbindin- $\text{D}_{28\text{K}}$ and PMCA1b were strongly decreased, and the NCC protein was shifted from the luminal membrane to the basal membrane and was found additionally in small membrane vesicles in intercellular and peritubular spaces. The consistently decreased expression of the Ca^{2+} transporters during thiazide treatment strongly argues against stimulation of active Ca^{2+} transport processes in chronic thiazide treatment. Furthermore, transcripts of NCC were drastically reduced in homogenates of kidney cortex and almost absent in dam-

aged DCT cells (278). All other tubular segments were unaffected by the treatment.

On the other hand, extracellular volume contraction leading to increased proximal Na^+ reabsorption and thereby increasing the electrochemical gradient driving passive Ca^{2+} transport in proximal tubule segments has been suggested as a possible additional effect, further decreasing overall Ca^{2+} excretion. In addition to inhibition of NCC by thiazides, mutations in the gene encoding NCC have been shown to cause Gitelman's syndrome (354). These patients suffer from hypovolemia, hypokalemic alkalosis, hypomagnesemia, and hypocalciuria (254). The mechanism causing the hypocalciuria in Gitelman's syndrome has not been elucidated, but in general, similar hypotheses have been postulated as for the thiazide action (101). Early studies by Weinman and Eknoyan (424) already demonstrated that the escape from the chronic effects of chlorothiazide is due to a decrease in the glomerular filtration rate and to an increase in fractional reabsorption in the proximal tubule. Nijenhuis et al. (278) showed that the HCTZ-induced hypocalciuria was accompanied by a significant decrease in body weight compared with controls, illustrating that extracellular volume contraction occurred. Since Na^+ depletion resulted in a similar hypocalciuria, it is likely that the extracellular fluid volume (ECV) contraction by itself is responsible for the thiazide-induced hypocalciuria. This is further supported by the finding that Na^+ repletion during HCTZ treatment, thereby preventing the ECV contraction, normalized the calciuresis. In literature, volume contraction has merely been suggested as a contributing factor in thiazide-induced hypocalciuria (121, 123). The underlying mechanism is an enhancement of proximal Na^+ reabsorption observed in volume contraction by diuretics and Na^+ restriction (110, 319, 416), which leads to an increase in the electrochemical driving force for passive Ca^{2+} reabsorption (57). Indeed, thiazides are known to decrease lithium clearance, which is generally accepted as an inverse estimation of proximal Na^+ reabsorption (215).

In conclusion, chronic thiazide treatment exerts two major effects. First, thiazides induce a hypovolemia that stimulates the proximal electrolyte reabsorption and explains the hypocalciuria. Second, thiazide exposure leads to structural degeneration of DCT resulting in downregulation of the particular ion transporters. These data inquire revision of the generally postulated hypotheses on hypocalciuria in chronic thiazide treatment and Gitelman's disease, indicating a critical role of ECV contraction and the resulting enhancement of passive Ca^{2+} reabsorption.

K. Immunosuppressants

Immunosuppressants like the calcineurin inhibitors tacrolimus (FK506) and cyclosporin A, next to glucocor-

ticoids, such as dexamethasone, are widely prescribed drugs in various disorders and for organ transplant recipients. Although their immunosuppressive actions are accomplished by distinct mechanisms, FK506 and dexamethasone are both known to induce significant side effects on mineral homeostasis. These drugs are associated with an increased bone turnover, a negative Ca^{2+} balance, and hypercalciuria, perturbations that can ultimately result in osteoporosis (323, 332, 367). Furthermore, hypomagnesemia is a well-known additional consequence of FK506 treatment (6, 251). The kidney is essential to both Ca^{2+} and Mg^{2+} homeostasis by providing the main excretory route for these divalent ions. However, the exact mechanisms by which these immunosuppressants provoke renal divalent wasting are unknown. The hypercalciuria during treatment with these drugs has been attributed to increased bone resorption as well as decreased renal Ca^{2+} reabsorption (242, 323, 324). Until now, the cascade of cellular and molecular events leading to impaired renal Ca^{2+} handling during FK506 and glucocorticoid treatment is largely unknown. In theory, downregulation of Ca^{2+} transport proteins in the distal part of the nephron may be involved in the pathogenesis of hypercalciuria and hypermagnesuria during drug treatment. Previous reports showed reduced calbindin- $\text{D}_{28\text{K}}$ levels during FK506 treatment, suggesting that FK506 could affect active Ca^{2+} transport (2). Recently, it was demonstrated that FK506 treatment significantly increased urinary Ca^{2+} excretion, accompanied by a downregulation of the renal mRNA expression of TRPV5 and calbindin- $\text{D}_{28\text{K}}$, and a specific reduction of the protein abundance of these Ca^{2+} transport proteins in DCT and CNT (277). The fact that serum Ca^{2+} concentrations and glomerular filtration rate did not differ from controls confirmed that impaired Ca^{2+} reabsorption rather than an increased filtered load caused the hypercalciuria. In addition, the expression of the major intestinal Ca^{2+} transport proteins was not increased by FK506 treatment, excluding that hypercalciuria is secondary to upregulation of active Ca^{2+} absorption. These data strongly supported the hypothesis that FK506 induces a primary defect of renal active Ca^{2+} reabsorption by specifically downregulating the proteins involved in active Ca^{2+} transport.

The molecular mechanism underlying the downregulation of the Ca^{2+} transport proteins by FK506 remains elusive. In previous studies, plasma $1,25\text{-(OH)}_2\text{D}_3$ was either unaltered or moderately increased, while plasma PTH was not affected by similar doses of FK506, which excludes that the reduced Ca^{2+} transport protein expression levels are secondary to decreased circulating levels of these calciotropic hormones (2, 241). Interestingly, several groups demonstrated that the immunosuppressive action of FK506 depends on the inhibition of the Ca^{2+} -dependent phosphatase calcineurin in T-lymphocytes (131, 238, 295). Calcineurin is not known to be involved in renal

Ca^{2+} reabsorption, but the calcineurin inhibitor cyclosporin A increased urinary Ca^{2+} excretion and decreased calbindin- $\text{D}_{28\text{K}}$ protein levels, suggesting that calcineurin inhibition may play a role in the impairment of Ca^{2+} reabsorption by these drugs (2, 366). In addition, FK506 binds to intracellular immunophilins called FK506-binding proteins (FKBPs), which have been implicated as ion channel regulators (157, 338, 352). In particular, FKBP4 was shown to bind and regulate the Ca^{2+} -permeable *Drosophila* TRPL channel, and this binding was disrupted by the addition of FK506 (150). Site-directed mutagenesis showed that mutations of P702Q or P709Q in the highly conserved TRPL sequence "701LPPPFNVLP709" eliminated interaction of the TRPL with the FK506-binding protein of *Drosophila* (dFKBP59). Detailed sequence alignment of TRPV5/6 species indicated that this domain is not conserved in the TRPV subfamily. Furthermore, several intracellular Ca^{2+} release channels were shown to be modulated by binding of FKBPs (250). Therefore, it is tempting to speculate that FKBPs are potential associated proteins regulating epithelial Ca^{2+} channel expression or activity.

VII. CHARACTERIZATION OF EPITHELIAL CALCIUM CHANNEL KNOCKOUT MICE

A. TRPV5 Knockout Mice

The characterization of TRPV5 and TRPV6 knockout mice should reveal the diseases that are associated with epithelial Ca^{2+} channel dysfunction. Recently, Hoenderop et al. (180) generated TRPV5 null ($\text{TRPV5}^{-/-}$) mice by genetic ablation of TRPV5 to investigate the requirement of TRPV5 functioning in renal and intestinal Ca^{2+} (re)absorption. Interestingly, metabolic studies demonstrated that $\text{TRPV5}^{-/-}$ mice exhibit a robust calciuresis, since significantly more Ca^{2+} was excreted in the urine compared with wild-type ($\text{TRPV5}^{+/+}$) littermates. The urinary Ca^{2+} concentration of the knockout mice reached values of 20 mM compared with 6 mM for $\text{TRPV5}^{+/+}$ littermates. Serum analysis showed that $\text{TRPV5}^{-/-}$ mice have normal plasma Ca^{2+} concentrations, but significantly elevated $1,25\text{-(OH)}_2\text{D}_3$ levels compared with $\text{TRPV5}^{+/-}$ and $\text{TRPV5}^{+/+}$ mice. To pinpoint the defective site of the Ca^{2+} reabsorption along the nephron in vivo, micropuncture studies were performed in these transgenic mice that combine classical and new research tools in a way that promises to yield important new insights into single-nephron function. Quantitative free-flow collections of tubular fluid revealed unaffected Ca^{2+} reabsorption in $\text{TRPV5}^{-/-}$ mice up to the last surface loop of the late proximal tubule (LPT) (Fig. 13A). In contrast, mean Ca^{2+} delivery to puncturing sites within distal convolution (DC; DCT and CNT), was significantly enhanced in $\text{TRPV5}^{-/-}$

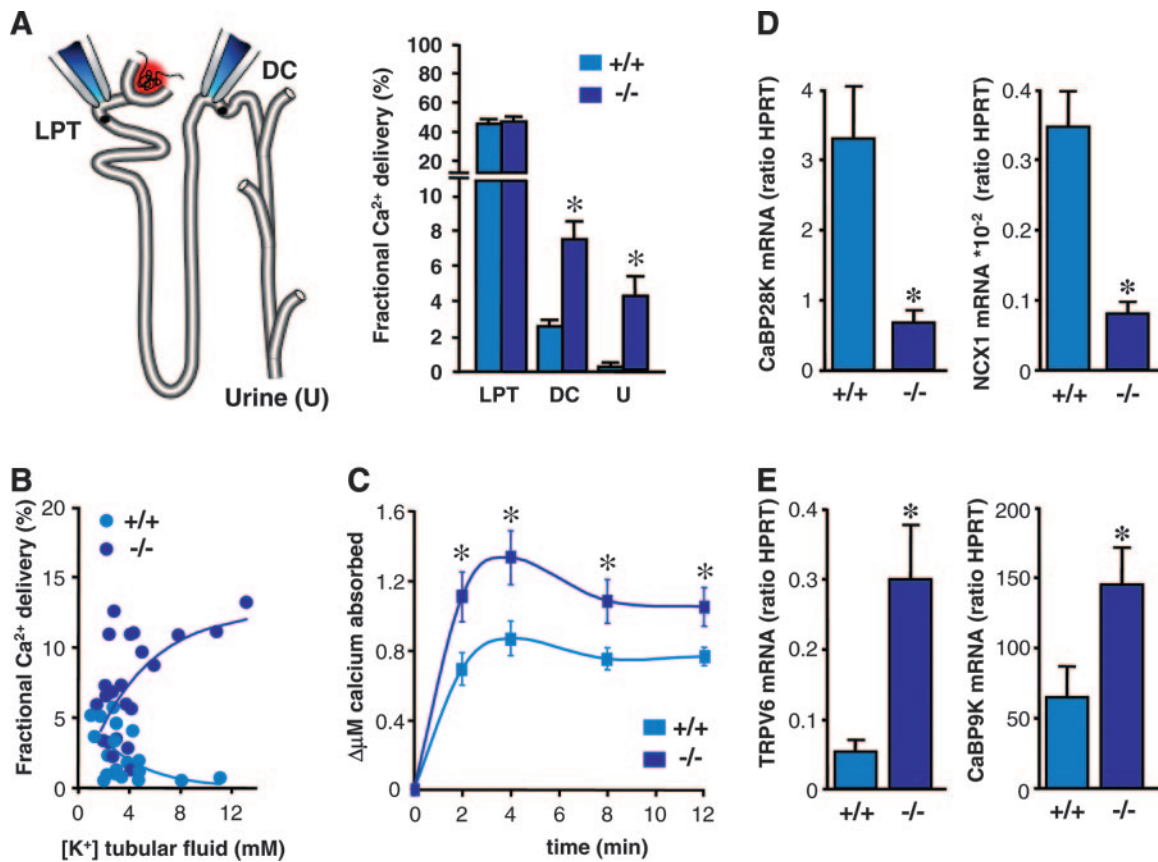


FIG. 13. Characterization of TRPV5^{-/-} mice. *A*: fractional Ca²⁺ delivery to the last surface loop of proximal tubule (LPT), to distal convoluted tubule (DC) and to urine (U) measured by micropuncture experiments in TRPV5^{+/+} and TRPV5^{-/-} mice. *B*: relation between K⁺ concentration in tubular fluid of distal convoluted tubule and fractional Ca²⁺ delivery to these sites. Low K⁺ concentrations indicate early aspects and high K⁺ concentrations late aspects of distal convoluted tubule (2). Values are means \pm SE of 6 mice/group for urine data and of 19–24 nephrons/group for late proximal tubule (LPT) and DCT and CNT (DC) collections. **P* < 0.05 vs. TRPV5^{+/+}. *C*: changes in serum Ca²⁺ ($\Delta\mu\text{M}$) within 10 min after administration of ⁴⁵Ca²⁺ by oral gavage in TRPV5^{+/+} and TRPV5^{-/-} mice (*n* = 12). Data are averaged values \pm SE from mice at 8 wk old. Asterisks (*) indicate significant difference from wild-type mice (*P* < 0.05). *D*: mRNA expression of calbindin-D_{28K} and the Na⁺/Ca²⁺ exchanger (NCX1) in kidney cortex of TRPV5^{+/+} and TRPV5^{-/-} mice (*n* = 9), assessed by quantitative PCR analysis, is calculated as a ratio to the HPRT mRNA. *E*: mRNA expression of TRPV6 and calbindin-D_{9K} in duodenum of TRPV5^{+/+} and TRPV5^{-/-} mice, assessed by quantitative PCR analysis, is calculated as a ratio to the HPRT mRNA (*n* = 9). [Modified from Hoenderop et al. (180).]

mice. Because K⁺ secretion occurs along the distal nephron sites accessible to micropuncture (together with water reabsorption in CNT and CCD), the distal luminal potassium concentration was used as an indicator of the distal collection site (Fig. 13*B*). Based on the shape of the relationship between distal luminal K⁺ concentration and fractional Ca²⁺ delivery, it is evident that in contrast to TRPV5^{+/+} mice, fractional Ca²⁺ delivery increases with a higher K⁺ concentration, indicating a defect in Ca²⁺ reabsorption along the DCT and CNT which is consistent with the localization of TRPV5.

Interestingly, polyuria and polydipsia were consistently observed in TRPV5^{-/-} mice compared with TRPV5^{+/-} and TRPV5^{+/+} littermates. Polyuria facilitates the excretion of large quantities of Ca²⁺ by reducing the potential risk of Ca²⁺ precipitations. It is known that a high luminal Ca²⁺ concentration activates the CaSR in the apical membrane of the IMCD. As a consequence, the

arginine vasopressin-elicited water permeability is blunted by a PKC-mediated aquaporin-2 retrieval mechanism to reduce water reabsorption and prevent a further rise in urinary Ca²⁺ concentration and possibly stone formation (335). The hypercalciuria-induced polyuria has been observed in humans (253) and animal models (119, 317). Furthermore, TRPV5^{-/-} mice produced urine that was significantly more acidic compared with TRPV5^{+/+} and TRPV5^{+/-} littermates. Acidification of the urine is also known to prevent renal stone formation in hypercalciuria, since Ca²⁺ precipitates will not be formed at pH 5–6 (24).

In general, Ca²⁺ hyperabsorption by the small intestine is favored as compensation for renal Ca²⁺ wasting. Ca²⁺ absorption was assessed in preliminary experiments by measuring serum ⁴⁵Ca²⁺ at early time points after oral gavage. A significant increase in the rate of ⁴⁵Ca²⁺ absorption was observed in TRPV5^{-/-} mice compared with wild-

type littermates, indicating a compensatory role of the small intestine (Fig. 13C). TRPV6 and calbindin-D_{9K} expression levels were significantly upregulated in TRPV5^{-/-} mice consistent with this increased Ca²⁺ absorption (Fig. 13E) (180).

Surprisingly, inactivation of the *TRPV5* gene was accompanied by a decrease in the renal calbindin-D_{28K} and NCX1 mRNA expression (Fig. 13D). Because transcellular Ca²⁺ reabsorption in DCT and CNT was abolished in TRPV5^{-/-} mice, the simultaneous decrease in calbindin-D_{28K} and NCX1 mRNA levels, in the presence of elevated 1,25-(OH)₂D₃ levels, suggests a regulatory mechanism primarily controlled by TRPV5. This means that TRPV5 or the Ca²⁺ influx through TRPV5 possibly controls the transcription of the other Ca²⁺ transport genes including calbindin-D_{28K} and NCX1. Although downregulation of renal calbindin-D_{28K} is secondary to TRPV5 ablation in the TRPV5^{-/-} mice, the reduced calbindin-D_{28K} level may further augment the severity of the hypercalciuria. In this respect, it is interesting to compare the hypercalciuria in calbindin-D_{28K} and TRPV5 knockout mice. Calbindin-D_{28K} knockout mice fed a regular Ca²⁺ diet displayed an approximately twofold increase in the urinary Ca²⁺ excretion compared with wild-type littermates, whereas TRPV5^{-/-} mice fed the same Ca²⁺ diet excreted approximately six times more Ca²⁺ in the urine compared with their littermates (180, 361). These findings underscore the gatekeeper function of TRPV5 in the process of Ca²⁺ reabsorption.

Furthermore, microcomputed tomography analyses of the femur demonstrated that trabecular thickness in the femoral head of TRPV5^{-/-} mice was significantly reduced compared with TRPV5^{+/+} mice (Fig. 14). Trabecular bone volume, tissue volume, and bone fraction were not different between the genotypes (180). This could not be explained by a difference in trabecular number. Alternatively, it is possible that the trabeculae are longer, i.e., protrude further into the bone marrow cavity and thereby compensate for reduced trabecular thickness. Analyses of the diaphysis showed that cortical bone volume, cortical volume fraction, and cortical bone thickness were re-

duced in TRPV5^{-/-} versus TRPV5^{+/+} mice. These initial data from TRPV5^{-/-} mice demonstrated that TRPV5 is the gatekeeper in active Ca²⁺ reabsorption. Ablation of the TRPV5 gene seriously disturbs renal Ca²⁺ handling, causing increased 1,25-(OH)₂D₃ plasma levels, Ca²⁺ hyperabsorption, and reduced bone formation. All of these deficiencies have been reported frequently in patients with idiopathic hypercalciuria, although the molecular basis for this disorder remains unknown.

B. TRPV6 Knockout Mice

Hediger and co-workers (34) addressed the functional role of TRPV6 in Ca²⁺ absorption by inactivation of the mouse TRPV6 gene. These TRPV6 null (TRPV6^{-/-}) mice were placed on a Ca²⁺-deficient diet and subsequently challenged in a ⁴⁵Ca²⁺ absorption assay. TRPV6^{-/-} mice showed a consistent decrease in Ca²⁺ absorption over time. From these initial data it was concluded that TRPV6^{-/-} mice show a significant Ca²⁺ malabsorption, suggesting that TRPV6 is indeed the rate-limiting step in 1,25-OH₂D₃-dependent Ca²⁺ absorption. However, future studies are needed to address the functions of TRPV6 in detail.

VIII. OUTLOOK

Ca²⁺ play a fundamental role in many cellular processes, and its extracellular concentration is kept under strict control to allow proper physiological functions. The transepithelial Ca²⁺ (re)absorption determines the influx and efflux of Ca²⁺ to the extracellular Ca²⁺ pool and is controlled by several hormones. This review has focused on the identification, function, and regulation of the Ca²⁺ transport proteins. Over the last years significant advances were achieved in the Ca²⁺ homeostasis field. The picture that emerges from the recent data pointed to a cellular model for transepithelial Ca²⁺ transport in which distinct players execute an essential role. The identification of the new epithelial Ca²⁺ channels, TRPV5 and

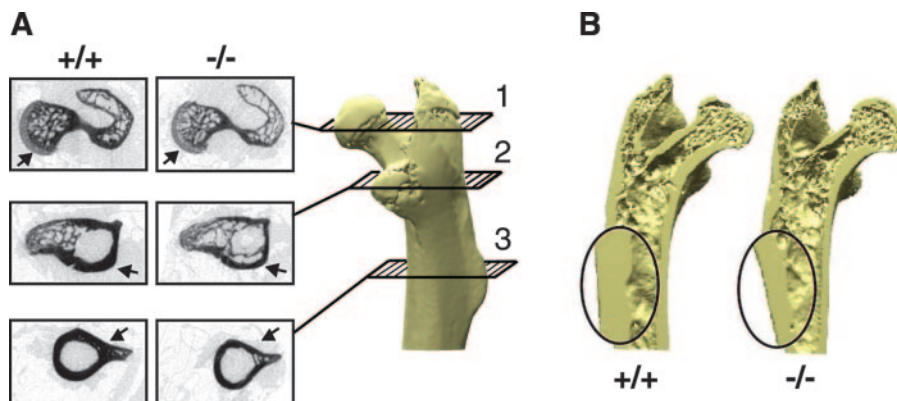


FIG. 14. Bone analysis of TRPV5^{-/-} mice. Bone phenotype of female and male TRPV5^{+/+} and TRPV5^{-/-} mice. *A*: representative cross-section X-ray images of the femoral head (1), the lesser trochanter (2), and the diaphysis (3) in TRPV5^{+/+} and TRPV5^{-/-} mice. Note the decreased cortical bone width in the trochanter and diaphysis (arrows). *B*: 3-dimensional reconstruction of femurs from TRPV5^{+/+} and TRPV5^{-/-} mice. Note the reduced cortical and trabecular thickness in the TRPV5^{-/-} mice. [Modified from Hoenderop et al. (180).]

TRPV6, gave insights in a new molecular concept of Ca^{2+} influx. Unique physiological functions important for body Ca^{2+} homeostasis have been attributed to these gatekeeper channels, and many key questions in the study of transepithelial Ca^{2+} transport can now be addressed. What is the three-dimensional structure of these Ca^{2+} channels? Valuable information can be deduced from a structural models of TRPV5/6 channels. Future work should develop computational approaches to construct and refine three-dimensional models of these gatekeeper channels by incorporating and integrating available and new experimental data. How do intracellular Ca^{2+} control epithelial Ca^{2+} channel activity to allow sufficient Ca^{2+} uptake and subsequent transcellular Ca^{2+} movement? How is this Ca^{2+} movement organized in the absorbing epithelial cell, and which signaling pathways are involved? What is the underlying mechanism of the stimulatory effect of the calciotropic hormones? In this respect, it will be important to identify regulatory domains in the epithelial Ca^{2+} channels, binding partners of TRPV5/6 that participate in the channel complex and the signaling pathways controlling channel activity. Furthermore, what is the function of TRPV5/6 in unexplored tissues as testis, brain, exocrine tissues, stomach, and bone? Tissue-specific knockout mice models will help us to address these key functions of the Ca^{2+} -transporting proteins. We have seen that ablation of the TRPV5 gene seriously disturbs renal Ca^{2+} handling resulting in compensatory intestinal hyperabsorption and bone abnormalities. These deficiencies in Ca^{2+} handling have been reported frequently in patients with idiopathic hypercalciuria, although the molecular basis is unknown and genetic defects in TRPV5, and/or TRPV6 remain to be identified. It is clear that despite considerable advances, much remains to be learned, and the field of Ca^{2+} homeostasis will remain active for many more years.

We thank the members of our laboratories for valuable discussion, advice, and critical reading of this manuscript.

This work was supported by Dutch Organization of Scientific Research Grants Zon-Mw 016.006.001, Zon-Mw 902.18.298, NWO-ALW 810.38.004, NWO-ALW 805-09.042, NWO-ALW 814-02.001, and NWO 812-08.002; Stomach Liver Intestine Foundation Grant MWO 03-19; Human Frontiers Science Program Grant RGP32/2004; Dutch Kidney Foundation Grants C10.1881 and C03.6017; the Belgian Federal Government; the Flemish Government; Onderzoeksraad Katholieke Universiteit Leuven (Leuven, Belgium) Grants GOA 99/07, FWO G.0237.95, FWO G.0214.99, FWO G.0136.00, and FWO G.0172.03; and the Belgian Prime Minister's Office Interuniversity Poles of Attraction Program.

Address for reprint requests and other correspondence: R. J. M. Bindels, 160 Cell Physiology, University Medical Center Nijmegen, PO Box 9101, NL-6500 HB Nijmegen, The Netherlands (E-mail: R.Bindels@ncmls.ru.nl).

REFERENCES

1. **Adami S, Gatti D, Bertoldo F, Rossini M, Fratta-Pasini A, Zamberlan N, Facci E, and Lo Cascio V.** The effects of menopause and estrogen replacement therapy on the renal handling of calcium. *Osteoporos Int* 2: 180-185, 1992.
2. **Aicher L, Meier G, Norcross AJ, Jakubowski J, Varela MC, Cordier A, and Steiner S.** Decrease in kidney calbindin-D28kDa as a possible mechanism mediating cyclosporine A- and FK-506-induced calciuria and tubular mineralization. *Biochem Pharmacol* 53: 723-731, 1997.
3. **Airaksinen MS, Eilers J, Garaschuk O, Thoenen H, Konnerth A, and Meyer M.** Ataxia and altered dendritic calcium signaling in mice carrying a targeted null mutation of the calbindin D28k gene. *Proc Natl Acad Sci USA* 94: 1488-1493, 1997.
4. **Almers W and McCleskey EW.** Non-selective conductance in calcium channels of frog muscle: calcium selectivity in a single-file pore. *J Physiol* 353: 585-608, 1984.
5. **Anderson JM.** Molecular structure of tight junctions and their role in epithelial transport. *News Physiol Sci* 16: 126-130, 2001.
6. **Andoh TF, Burdmann EA, Fransechini N, Houghton DC, and Bennett WM.** Comparison of acute rapamycin nephrotoxicity with cyclosporine and FK506. *Kidney Int* 50: 1110-1117, 1996.
7. **Armbrecht HJ, Boltz MA, and Bruns ME.** Effect of age and dietary calcium on intestinal calbindin D-9k expression in the rat. *Arch Biochem Biophys* 420: 194-200, 2003.
8. **Armbrecht HJ, Boltz MA, and Kumar VB.** Intestinal plasma membrane calcium pump protein and its induction by $1,25(\text{OH})_2\text{D}_3$ decrease with age. *Am J Physiol Gastrointest Liver Physiol* 277: G41-G47, 1999.
9. **Armbrecht HJ, Boltz MA, and Wongsurawat N.** Expression of plasma membrane calcium pump mRNA in rat intestine: effect of age and $1,25$ -dihydroxyvitamin D. *Biochim Biophys Acta* 1195: 110-114, 1994.
10. **Arnold DB and Heintz N.** A calcium responsive element that regulates expression of two calcium binding proteins in Purkinje cells. *Proc Natl Acad Sci USA* 94: 8842-8847, 1997.
11. **Ba J, Brown D, and Friedman PA.** Calcium-sensing receptor regulation of PTH-inhibitable proximal tubule phosphate transport. *Am J Physiol Renal Physiol* 285: F1233-F1243, 2003.
12. **Bacskai BJ and Friedman PA.** Activation of latent Ca^{2+} channels in renal epithelial cells by parathyroid hormone. *Nature* 347: 388-391, 1990.
13. **Bahner M, Sander P, Paulsen R, and Huber A.** The visual G protein of fly photoreceptors interacts with the PDZ domain assembled INAD signaling complex via direct binding of activated Galpha(q) to phospholipase Cbeta. *J Biol Chem* 275: 2901-2904, 2000.
14. **Bailly C, Imbert-Teboul M, Roinel N, and Amiel C.** Isoproterenol increases Ca, Mg, and NaCl reabsorption in mouse thick ascending limb. *Am J Physiol Renal Fluid Electrolyte Physiol* 258: F1224-F1231, 1990.
15. **Baker PF, Blaustein MP, Hodgkin AL, and Steinhardt RA.** The influence of calcium on sodium efflux in squid axons. *J Physiol* 200: 431-458, 1969.
16. **Bakowski D and Parekh AB.** Permeation through store-operated CRAC channels in divalent-free solution: potential problems and implications for putative CRAC channel genes. *Cell Calcium* 32: 379-391, 2002.
17. **Balmain N, Bernal A, Hotton D, Cuisinier-Gleizes P, and Mathieu H.** Calbindin-D9K immunolocalization and vitamin D-dependence in the bone of growing and adult rats. *Histochemistry* 92: 359-365, 1989.
18. **Baran DT, Quail JM, Ray R, and Honeyman T.** Binding of $1\alpha,25$ -dihydroxyvitamin D_3 to annexin II: effect of vitamin D metabolites and calcium. *J Cell Biochem* 80: 259-265, 2000.
19. **Baran DT, Quail JM, Ray R, Leszyk J, and Honeyman T.** Annexin II is the membrane receptor that mediates the rapid actions of $1\alpha,25$ -dihydroxyvitamin D_3 . *J Cell Biochem* 78: 34-46, 2000.
20. **Barley NF, Howard A, O'Callaghan D, Legon S, and Walters JR.** Epithelial calcium transporter expression in human duodenum. *Am J Physiol Gastrointest Liver Physiol* 280: G285-G290, 2001.

21. Barry EL, Gesek FA, Froehner SC, and Friedman PA. Multiple calcium channel transcripts in rat osteosarcoma cells: selective activation of alpha 1D isoform by parathyroid hormone. *Proc Natl Acad Sci USA* 92: 10914–10918, 1995.
22. Barry EL, Gesek FA, Yu AS, Lytton J, and Friedman PA. Distinct calcium channel isoforms mediate parathyroid hormone and chlorothiazide-stimulated calcium entry in transporting epithelial cells. *J Membr Biol* 161: 55–64, 1998.
23. Barski JJ, Hartmann J, Rose CR, Hoebeek F, Morl K, Noll-Hussong M, De Zeeuw CI, Konnerth A, and Meyer M. Calbindin in cerebellar Purkinje cells is a critical determinant of the precision of motor coordination. *J Neurosci* 23: 3469–3477, 2003.
24. Baumann JM. Stone prevention: why so little progress? *Urol Res* 26: 77–81, 1998.
25. Belan P, Gerasimenko O, Petersen OH, and Tepikin AV. Distribution of Ca^{2+} extrusion sites on the mouse pancreatic acinar cell surface. *Cell Calcium* 22: 5–10, 1997.
26. Belan PV, Gerasimenko OV, Tepikin AV, and Petersen OH. Localization of Ca^{2+} extrusion sites in pancreatic acinar cells. *J Biol Chem* 271: 7615–7619, 1996.
27. Belkacemi L, Garipey G, Mounier C, Simoneau L, and Lafond J. Expression of calbindin-D28k (CaBP28k) in trophoblasts from human term placenta. *Biol Reprod* 68: 1943–1950, 2003.
28. Belkacemi L, Garipey G, Mounier C, Simoneau L, and Lafond J. Calbindin-D9k (CaBP9k) localization and levels of expression in trophoblast cells from human term placenta. *Cell Tissue Res* 315: 107–117, 2004.
29. Belkacemi L, Simoneau L, and Lafond J. Calcium-binding proteins: distribution and implication in mammalian placenta. *Endocrine* 19: 57–64, 2002.
30. Benais-Pont G, Punn A, Flores-Maldonado C, Eckert J, Raposo G, Fleming TP, Cerejido M, Balda MS, and Matter K. Identification of a tight junction-associated guanine nucleotide exchange factor that activates Rho and regulates paracellular permeability. *J Cell Biol* 160: 729–740, 2003.
31. Bengel HH, Alexander EA, and Lechene CP. Calcium and magnesium transport along the inner medullary collecting duct of the rat. *Am J Physiol Renal Fluid Electrolyte Physiol* 239: F24–F29, 1980.
32. Benham CD, Davis JB, and Randall AD. Vanilloid and TRP channels: a family of lipid-gated cation channels. *Neuropharmacology* 42: 873–888, 2002.
33. Berggard T, Miron S, Onnerfjord P, Thulin E, Akerfeldt KS, Enghild JJ, Akke M, and Linse S. Calbindin D28k exhibits properties characteristic of a Ca^{2+} sensor. *J Biol Chem* 277: 16662–16672, 2002.
34. Bianco S, Peng JB, Takanaga H, Kos CH, Crescenzi A, Brown EM, and Hediger MA. Mice lacking the epithelial calcium channel CaT1 (TRPV6) show a deficiency in intestinal calcium absorption despite high plasma levels of 1,25-dihydroxy vitamin D (Abstract). *FASEB J* 18: A706, 2004.
35. Bindels RJ. Calcium handling by the mammalian kidney. *J Exp Biol* 184: 89–104, 1993.
36. Bindels RJ, Dempster JA, Ramakers PL, Willems PH, and van Os CH. Effect of protein kinase C activation and down-regulation on active calcium transport. *Kidney Int* 43: 295–300, 1993.
37. Bindels RJ, Hartog A, Abrahamse SL, and van Os CH. Effects of pH on apical calcium entry and active calcium transport in rabbit cortical collecting system. *Am J Physiol Renal Fluid Electrolyte Physiol* 266: F620–F627, 1994.
38. Bindels RJ, Hartog A, Timmermans J, and van Os CH. Active Ca^{2+} transport in primary cultures of rabbit kidney CCD: stimulation by 1,25-dihydroxyvitamin D_3 and PTH. *Am J Physiol Renal Fluid Electrolyte Physiol* 261: F799–F807, 1991.
39. Bindels RJ, Ramakers PL, Dempster JA, Hartog A, and van Os CH. Role of $\text{Na}^+/\text{Ca}^{2+}$ exchange in transcellular Ca^{2+} transport across primary cultures of rabbit kidney collecting system. *Pflügers Arch* 420: 566–572, 1992.
40. Biner HL, Arpin-Bott MP, Loffing J, Wang X, Knepper M, Hebert SC, and Kaissling B. Human cortical distal nephron: distribution of electrolyte and water transport pathways. *J Am Soc Nephrol* 13: 836–847, 2002.
41. Birnbaumer L, Yidirim E, and Abramowitz J. A comparison of the genes coding for canonical TRP channels and their M, V and P relatives. *Cell Calcium* 33: 419–432, 2003.
42. Blair HC. How the osteoclast degrades bone. *Bioessays* 20: 837–846, 1998.
43. Blanchard A, Jeunemaitre X, Coudol P, Dechaux M, Froissart M, May A, Demontis R, Fournier A, Paillard M, and Houillier P. Paracellin-1 is critical for magnesium and calcium reabsorption in the human thick ascending limb of Henle. *Kidney Int* 59: 2206–2215, 2001.
44. Blankenship KA, Williams JJ, Lawrence MS, McLeish KR, Dean WL, and Arthur JM. The calcium-sensing receptor regulates calcium absorption in MDCK cells by inhibition of PMCA. *Am J Physiol Renal Physiol* 280: F815–F822, 2001.
45. Blaustein MP, Juhaszova M, Golovina VA, Church PJ, and Stanley EF. Na/Ca exchanger and PMCA localization in neurons and astrocytes: functional implications. *Ann NY Acad Sci* 976: 356–366, 2002.
46. Blaustein MP and Lederer WJ. Sodium/calcium exchange: its physiological implications. *Physiol Rev* 79: 763–854, 1999.
47. Boddling M, Wissenbach U, and Flockerzi V. The recombinant human TRPV6 channel functions as Ca^{2+} sensor in human embryonic kidney and rat basophilic leukemia cells. *J Biol Chem* 277: 36656–36664, 2002.
48. Borke JL, Caride A, Verma AK, Penniston JT, and Kumar R. Plasma membrane calcium pump and 28-kDa calcium binding protein in cells of rat kidney distal tubules. *Am J Physiol Renal Fluid Electrolyte Physiol* 257: F842–F849, 1989.
49. Borke JL, Minami J, Verma A, Penniston JT, and Kumar R. Monoclonal antibodies to human erythrocyte membrane Ca^{2+} - Mg^{2+} adenosine triphosphatase pump recognize an epitope in the basolateral membrane of human kidney distal tubule cells. *J Clin Invest* 80: 1225–1231, 1987.
50. Bosch RR, Hoenderop JG, van der Heijden L, De Pont JJ, Bindels RJ, and Willems PH. Hormonal regulation of phospholipase D activity in Ca^{2+} transporting cells of rabbit connecting tubule and cortical collecting duct. *Biochim Biophys Acta* 1538: 329–338, 2001.
51. Bouillon R, Van Cromphaut S, and Carmeliet G. Intestinal calcium absorption: molecular vitamin D mediated mechanisms. *J Cell Biochem* 88: 332–339, 2003.
52. Boulay G. Ca^{2+} -calmodulin regulates receptor-operated Ca^{2+} entry activity of TRPC6 in HEK-293 cells. *Cell Calcium* 32: 201–207, 2002.
53. Bourdeau JE and Burg MB. Effect of PTH on calcium transport across the cortical thick ascending limb of Henle's loop. *Am J Physiol Renal Fluid Electrolyte Physiol* 239: F121–F126, 1980.
54. Bourdeau JE and Burg MB. Voltage dependence of calcium transport in the thick ascending limb of Henle's loop. *Am J Physiol Renal Fluid Electrolyte Physiol* 236: F357–F364, 1979.
55. Bourdeau JE and Hellstrom-Stein RJ. Voltage-dependent calcium movement across the cortical collecting duct. *Am J Physiol Renal Fluid Electrolyte Physiol* 242: F285–F292, 1982.
56. Bourdeau JE, Langman CB, and Bouillon R. Parathyroid hormone-stimulated calcium absorption in cTAL from vitamin D-deficient rabbits. *Kidney Int* 31: 913–917, 1987.
57. Breslau N, Moses AM, and Weiner IM. The role of volume contraction in the hypocalciuric action of chlorothiazide. *Kidney Int* 10: 164–170, 1976.
58. Bronner F. Mechanisms of intestinal calcium absorption. *J Cell Biochem* 88: 387–393, 2003.
59. Bronner F and Pansu D. Nutritional aspects of calcium absorption. *J Nutr* 129: 9–12, 1999.
60. Bronner F, Pansu D, and Stein WD. An analysis of intestinal calcium transport across the rat intestine. *Am J Physiol Gastrointest Liver Physiol* 250: G561–G569, 1986.
61. Brown AJ, Finch J, and Slatopolsky E. Differential effects of 19-nor-1,25-dihydroxyvitamin D(2) and 1,25-dihydroxyvitamin D(3) on intestinal calcium and phosphate transport. *J Lab Clin Med* 139: 279–284, 2002.
62. Brunette MG. Calcium transport through the placenta. *Can J Physiol Pharmacol* 66: 1261–1269, 1988.

63. **Bulger RE, Tisher CC, Myers CH, and Trump BF.** Human renal ultrastructure. II. The thin limb of Henle's loop and the interstitium in healthy individuals. *Lab Invest* 16: 124–141, 1967.
64. **Cai Q, Chandler JS, Wasserman RH, Kumar R, and Penniston JT.** Vitamin D and adaptation to dietary calcium and phosphate deficiencies increase intestinal plasma membrane calcium pump gene expression. *Proc Natl Acad Sci USA* 90: 1345–1349, 1993.
65. **Cai X and Lytton J.** Molecular cloning of a sixth member of the K^+ -dependent Na^+/Ca^{2+} exchanger gene family, NCKX6. *J Biol Chem* 279: 5867–5876, 2004.
66. **Canessa CM, Schild L, Buell G, Thorens B, Gautschi I, Horisberger JD, and Rossier BC.** Amiloride-sensitive epithelial Na^+ channel is made of three homologous subunits. *Nature* 367: 463–467, 1994.
67. **Carney SL and Thompson L.** Chronic calcitonin administration and renal calcium transport in the rat. *Clin Exp Pharmacol Physiol* 25: 236–239, 1998.
68. **Casteels R and Droogmans G.** Exchange characteristics of the noradrenaline-sensitive calcium store in vascular smooth muscle cells or rabbit ear artery. *J Physiol* 317: 263–279, 1981.
69. **Catterall WA.** Structure and function of voltage-sensitive ion channels. *Science* 242: 50–61, 1988.
70. **Chang AC, Dunham MA, Jeffrey KJ, and Reddel RR.** Molecular cloning and characterization of mouse stanniocalcin cDNA. *Mol Cell Endocrinol* 124: 185–187, 1996.
71. **Chang AC, Janosi J, Hulsbeek M, de Jong D, Jeffrey KJ, Noble JR, and Reddel RR.** A novel human cDNA highly homologous to the fish hormone stanniocalcin. *Mol Cell Endocrinol* 112: 241–247, 1995.
72. **Chantret I, Barbat A, Dussaulx E, Brattain MG, and Zweibaum A.** Epithelial polarity, villin expression, and enterocytic differentiation of cultured human colon carcinoma cells: a survey of twenty cell lines. *Cancer Res* 48: 1936–1942, 1988.
73. **Clapham DE.** Sorting out MIC, TRP, and CRAC ion channels. *J Gen Physiol* 120: 217–220, 2002.
74. **Clapham DE.** TRP channels as cellular sensors. *Nature* 426: 517–524, 2003.
75. **Clapham DE, Montell C, Schultz G, and Julius D.** International Union of Pharmacology. XLIII. Compendium of voltage-gated ion channels: transient receptor potential channels. *Pharmacol Rev* 55: 591–596, 2003.
76. **Clark SA, Stumpf WE, Sar M, DeLuca HF, and Tanaka Y.** Target cells for 1,25 dihydroxyvitamin D_3 in the pancreas. *Cell Tissue Res* 209: 515–520, 1980.
77. **Corey DP.** New TRP channels in hearing and mechanosensation. *Neuron* 39: 585–588, 2003.
78. **Costanzo LS and Windhager EE.** Calcium and sodium transport by the distal convoluted tubule of the rat. *Am J Physiol Renal Fluid Electrolyte Physiol* 235: F492–F506, 1978.
79. **Costanzo LS, Windhager EE, and Ellison DH.** Calcium and sodium transport by the distal convoluted tubule of the rat. *J Am Soc Nephrol* 11: 1562–1580, 2000.
80. **Crayen ML and Thoenes W.** Architecture and cell structures in the distal nephron of the rat kidney. *Cytobiologie* 17: 197–211, 1978.
81. **Cross HS, Debiec H, and Peterlik M.** Thyroid hormone enhances the genomic action of calcitriol in the small intestine. *Prog Clin Biol Res* 332: 163–180, 1990.
82. **Cross HS and Peterlik M.** Cooperative effect of thyroid hormones and vitamin D on intestinal calcium and phosphate transport. *Prog Clin Biol Res* 252: 331–336, 1988.
83. **Cross HS, Polzleitner D, and Peterlik M.** Intestinal phosphate and calcium absorption: joint regulation by thyroid hormones and 1,25-dihydroxyvitamin D_3 . *Acta Endocrinol* 113: 96–103, 1986.
84. **Cui J, Bian JS, Kagan A, and McDonald TV.** CaT1 contributes to the store-operated calcium current in Jurkat T-lymphocytes. *J Biol Chem* 277: 47175–47183, 2002.
85. **Dang TX and McCleskey EW.** Ion channel selectivity through stepwise changes in binding affinity. *J Gen Physiol* 111: 185–193, 1998.
86. **Dardenne O, Prud'homme J, Arabian A, Glorieux FH, and St-Arnaud R.** Targeted inactivation of the 25-hydroxyvitamin D_3 -1 α -hydroxylase gene (CYP27B1) creates an animal model of pseudovitamin D-deficiency rickets. *Endocrinology* 142: 3135–3141, 2001.
87. **Dardenne O, Prud'homme J, Hacking SA, Glorieux FH, and St-Arnaud R.** Correction of the abnormal mineral ion homeostasis with a high-calcium, high-phosphorus, high-lactose diet rescues the PDDR phenotype of mice deficient for the 25-hydroxyvitamin D-1 α -hydroxylase (CYP27B1). *Bone* 32: 332–340, 2003.
88. **Darwish HM, Krisinger J, Strom M, and DeLuca HF.** Molecular cloning of the cDNA and chromosomal gene for vitamin D-dependent calcium-binding protein of rat intestine. *Proc Natl Acad Sci USA* 84: 6108–6111, 1987.
89. **Den Dekker E, Hoenderop JG, Nilius B, and Bindels RJ.** The epithelial calcium channels, TRPV5 and TRPV6: from identification towards regulation. *Cell Calcium* 33: 497–507, 2003.
90. **Dick IM, Liu J, Glendenning P, and Prince RL.** Estrogen and androgen regulation of plasma membrane calcium pump activity in immortalized distal tubule kidney cells. *Mol Cell Endocrinol* 212: 11–18, 2003.
91. **Diepens RJ, Den Dekker E, Bens M, Weidema AF, Vandewalle A, Bindels RJ, and Hoenderop JG.** Characterization of a murine distal convoluted (mpkDCT) cell line to study transcellular calcium transport. *Am J Physiol Renal Physiol* 286: F483–F489, 2003.
92. **Di Stefano A, Wittner M, Nitschke R, Braitsch R, Greger R, Bailly C, Amiel C, Elalouf JM, Roinel N, and de Rouffignac C.** Effects of glucagon on Na^+ , Cl^- , K^+ , Mg^{2+} and Ca^{2+} transports in cortical and medullary thick ascending limbs of mouse kidney. *Pflügers Arch* 414: 640–646, 1989.
93. **Di Stefano A, Wittner M, Nitschke R, Braitsch R, Greger R, Bailly C, Amiel C, Roinel N, and de Rouffignac C.** Effects of parathyroid hormone and calcitonin on Na^+ , Cl^- , K^+ , Mg^{2+} and Ca^{2+} transport in cortical and medullary thick ascending limbs of mouse kidney. *Pflügers Arch* 417: 161–167, 1990.
94. **Dodier Y, Banderali U, Klein H, Topalak O, Dafi O, Simoes M, Bernatchez G, Sauve R, and Parent L.** Outer pore topology of the ECaC-TRPV5 channel by cysteine scan mutagenesis. *J Biol Chem*. In press.
95. **Doucet A and Katz AI.** High-affinity Ca-Mg-ATPase along the rabbit nephron. *Am J Physiol Renal Fluid Electrolyte Physiol* 242: F346–F352, 1982.
96. **Doyle DA, Morais Cabral J, Pfuetzner RA, Kuo A, Gulbis JM, Cohen SL, Chait BT, and MacKinnon R.** The structure of the potassium channel: molecular basis of K^+ conduction and selectivity. *Science* 280: 69–77, 1998.
97. **Drucker DJ, Asa SL, Henderson J, and Goltzman D.** The parathyroid hormone-like peptide gene is expressed in the normal and neoplastic human endocrine pancreas. *Mol Endocrinol* 3: 1589–1595, 1989.
98. **Ebnet K, Aurrand-Lions M, Kuhn A, Kiefer F, Butz S, Zander K, Meyer zu Brickwedde MK, Suzuki A, Imhof BA, and Vestweber D.** The junctional adhesion molecule (JAM) family members JAM-2 and JAM-3 associate with the cell polarity protein PAR-3: a possible role for JAMs in endothelial cell polarity. *J Cell Sci* 116: 3879–3891, 2003.
99. **Edwards BR, Baer PG, Sutton RA, and Dirks JH.** Micropuncture study of diuretic effects on sodium and calcium reabsorption in the dog nephron. *J Clin Invest* 52: 2418–2427, 1973.
100. **Eisenrauch A, Juhaszova M, Ellis-Davies GC, Kaplan JH, Bamberg E, and Blaustein MP.** Electrical currents generated by a partially purified Na/Ca exchanger from lobster muscle reconstituted into liposomes and adsorbed on black lipid membranes: activation by photolysis of Ca^{2+} . *J Membr Biol* 145: 151–164, 1995.
101. **Ellison DH.** Divalent cation transport by the distal nephron: insights from Bartter's and Gitelman's syndromes. *Am J Physiol Renal Physiol* 279: F616–F625, 2000.
102. **Erler I, Hirnet D, Wissenbach U, Flockerzi V, and Niemeyer BA.** Ca^{2+} -selective TRPV channel architecture and function require a specific ankyrin repeat. *J Biol Chem*. In press.
103. **Farnsworth AE and Dobyns BM.** Hypercalcaemia and thyrotoxicosis. *Med J Aust* 2: 782–784, 1974.
104. **Faucheux C, Bareille R, and Amedee J.** Synthesis of calbindin-D28K during mineralization in human bone marrow stromal cells. *Biochem J* 333: 817–823, 1998.

105. **Faulk WP and McIntyre JA.** Immunological studies of human trophoblast: markers, subsets and functions. *Immunol Rev* 75: 139–175, 1983.
106. **Fehler JJ.** Facilitated calcium diffusion by intestinal calcium-binding protein. *Am J Physiol Cell Physiol* 244: C303–C307, 1983.
107. **Fehler JJ, Fuller CS, and Wasserman RH.** Role of facilitated diffusion of calcium by calbindin in intestinal calcium absorption. *Am J Physiol Cell Physiol* 262: C517–C526, 1992.
108. **Fehler JJ and Wasserman RH.** Calcium absorption and intestinal calcium-binding protein: quantitative relationship. *Am J Physiol Endocrinol Metab Gastrointest Physiol* 236: E556–E561, 1979.
109. **Filvaroff EH, Guillet S, Zlot C, Bao M, Ingle G, Steinmetz H, Hoeffel J, Bunting S, Ross J, Carano RA, Powell-Braxton L, Wagner GF, Eckert R, Gerritsen ME, and French DM.** Stanniocalcin 1 alters muscle and bone structure and function in transgenic mice. *Endocrinology* 143: 3681–3690, 2002.
110. **Fisher KA, Lee SH, Walker J, Dileto-Fang C, Ginsberg L, and Stapleton SR.** Regulation of proximal tubule sodium/hydrogen antiporter with chronic volume contraction. *Am J Physiol Renal Physiol* 280: F922–F926, 2001.
111. **Fixemer T, Wissenbach U, Flockerzi V, and Bonkhoff H.** Expression of the Ca^{2+} -selective cation channel TRPV6 in human prostate cancer: a novel prognostic marker for tumor progression. *Oncogene* 22: 7858–7861, 2003.
112. **Fleet JC, Bradley J, Reddy GS, Ray R, and Wood RJ.** $1\alpha,25\text{-(OH)}_2\text{-vitamin D}_3$ analogs with minimal in vivo calcemic activity can stimulate significant transepithelial calcium transport and mRNA expression in vitro. *Arch Biochem Biophys* 329: 228–234, 1996.
113. **Fleet JC, Eksir F, Hance KW, and Wood RJ.** Vitamin D-inducible calcium transport and gene expression in three Caco-2 cell lines. *Am J Physiol Gastrointest Liver Physiol* 283: G618–G625, 2002.
114. **Fleet JC and Wood RJ.** Specific $1,25\text{(OH)}_2\text{D}_3$ -mediated regulation of transcellular calcium transport in Caco-2 cells. *Am J Physiol Gastrointest Liver Physiol* 276: G958–G964, 1999.
115. **Flik G, Schoenmakers TJ, Groot JA, van Os CH, and Wendelaar Bonga SE.** Calcium absorption by fish intestine: the involvement of ATP- and sodium-dependent calcium extrusion mechanisms. *J Membr Biol* 113: 13–22, 1990.
116. **Fraser DR and Kodicek E.** Unique biosynthesis by kidney of a biological active vitamin D metabolite. *Nature* 228: 764–766, 1970.
117. **Freeman TC, Howard A, Bentsen BS, Legon S, and Walters JR.** Cellular and regional expression of transcripts of the plasma membrane calcium pump PMCA1 in rabbit intestine. *Am J Physiol Gastrointest Liver Physiol* 269: G126–G131, 1995.
118. **Freud TS and Christakos S.** *Vitamin D, Chemical, Biochemical and Clinical Endocrinology of Calcium Metabolism: Enzyme Modification by Renal Calcium-Binding Proteins.* Berlin: de Gruyter, 1985.
119. **Frick KK and Bushinsky DA.** Molecular mechanisms of primary hypercalcemia. *J Am Soc Nephrol* 14: 1082–1095, 2003.
120. **Friedman PA.** Basal and hormone-activated calcium absorption in mouse renal thick ascending limbs. *Am J Physiol Renal Fluid Electrolyte Physiol* 254: F62–F70, 1988.
121. **Friedman PA.** Codependence of renal calcium and sodium transport. *Annu Rev Physiol* 60: 179–197, 1998.
122. **Friedman PA.** Calcium transport in the kidney. *Curr Opin Nephrol Hypertens* 8: 589–595, 1999.
123. **Friedman PA and Bushinsky DA.** Diuretic effects on calcium metabolism. *Semin Nephrol* 19: 551–556, 1999.
124. **Friedman PA, Coutermarsh BA, Kennedy SM, and Gesek FA.** Parathyroid hormone stimulation of calcium transport is mediated by dual signaling mechanisms involving protein kinase A and protein kinase C. *Endocrinology* 137: 13–20, 1996.
125. **Friedman PA and Gesek FA.** Calcium transport in renal epithelial cells. *Am J Physiol Renal Fluid Electrolyte Physiol* 264: F181–F198, 1993.
126. **Friedman PA and Gesek FA.** Vitamin D_3 accelerates PTH-dependent calcium transport in distal convoluted tubule cells. *Am J Physiol Renal Fluid Electrolyte Physiol* 265: F300–F308, 1993.
127. **Friedman PA and Gesek FA.** Hormone-responsive Ca^{2+} entry in distal convoluted tubules. *J Am Soc Nephrol* 4: 1396–1404, 1994.
128. **Friedman PA and Gesek FA.** Stimulation of calcium transport by amiloride in mouse distal convoluted tubule cells. *Kidney Int* 48: 1427–1434, 1995.
129. **Friedman PA and Gesek FA.** Cellular calcium transport in renal epithelia: measurement, mechanisms, and regulation. *Physiol Rev* 75: 429–471, 1995.
130. **Frindt G and Windhager EE.** Ca^{2+} -dependent inhibition of sodium transport in rabbit cortical collecting tubules. *Am J Physiol Renal Fluid Electrolyte Physiol* 258: F568–F582, 1990.
131. **Fruman DA, Klee CB, Bierer BE, and Burakoff SJ.** Calcineurin phosphatase activity in T lymphocytes is inhibited by FK 506 and cyclosporin A. *Proc Natl Acad Sci USA* 89: 3686–3690, 1992.
132. **Fukuoka H and Satoh K.** Characterization of the three calcium binding proteins in the human placenta. *Nippon Naibunpi Gakkai Zasshi* 58: 662–678, 1982.
133. **Gallin WJ and Greenberg ME.** Calcium regulation of gene expression in neurons: the mode of entry matters. *Curr Opin Neurobiol* 5: 367–374, 1995.
134. **Garcia NH, Ramsey CR, and Knox FG.** Understanding the role of paracellular transport in the proximal tubule. *News Physiol Sci* 13: 38–43, 1998.
135. **Gentili C, Morelli S, and de Boland AR.** Characterization of PTH/PTHrP receptor in rat duodenum: effects of ageing. *J Cell Biochem* 88: 1157–1167, 2003.
136. **Gerke V and Moss SE.** Annexins: from structure to function. *Physiol Rev* 82: 331–371, 2002.
- 136a. **Gerritsen ME and Wagner GF.** Stanniocalcin: no longer just a fish tale. In: *Vitamins and Hormones*, edited by G. Litwack. New York: Academic, 1994.
137. **Gesek FA and Friedman PA.** On the mechanism of parathyroid hormone stimulation of calcium uptake by mouse distal convoluted tubule cells. *J Clin Invest* 90: 749–758, 1992.
138. **Gesek FA and Friedman PA.** Mechanism of calcium transport stimulated by chlorothiazide in mouse distal convoluted tubule cells. *J Clin Invest* 90: 429–438, 1992.
139. **Gesek FA and Friedman PA.** Calcitonin stimulates calcium transport in distal convoluted tubule cells. *Am J Physiol Renal Fluid Electrolyte Physiol* 264: F744–F751, 1993.
140. **Gill RK and Christakos S.** Identification of sequence elements in mouse calbindin-D28k gene that confer $1,25\text{-dihydroxyvitamin D}_3$ and butyrate-inducible responses. *Proc Natl Acad Sci USA* 90: 2984–2988, 1993.
141. **Gillespie FC, Shimmins JG, and Orr JS.** Use of the occupancy principle in studies of calcium metabolism. *Calcif Tissue Res Suppl*: 89–90, 1970.
142. **Girard C, Tinel N, Terrenoire C, Romey G, Lazdunski M, and Borsotto M.** p11, an annexin II subunit, an auxiliary protein associated with the background K^+ channel, TASK-1. *EMBO J* 21: 4439–4448, 2002.
143. **Giuliano AR, Franceschi RT, and Wood RJ.** Characterization of the vitamin D receptor from the Caco-2 human colon carcinoma cell line: effect of cellular differentiation. *Arch Biochem Biophys* 285: 261–269, 1991.
144. **Giuliano AR and Wood RJ.** Vitamin D-regulated calcium transport in Caco-2 cells: unique in vitro model. *Am J Physiol Gastrointest Liver Physiol* 260: G207–G212, 1991.
145. **Gkika D, Mahieu F, Nilius B, Hoenderop JG, and Bindels RJ.** 80K-H as a new Ca^{2+} sensor regulating the activity of the epithelial Ca^{2+} channel transient receptor potential cation channel V5 (TRPV5). *J Biol Chem* 279: 26351–26357, 2004.
146. **Glazier JD, Atkinson DE, Thornburg KL, Sharpe PT, Edwards D, Boyd RD, and Sibley CP.** Gestational changes in Ca^{2+} transport across rat placenta and mRNA for calbindin9K and Ca^{2+} -ATPase. *Am J Physiol Regul Integr Comp Physiol* 263: R930–R935, 1992.
147. **Glendenning P, Ratajczak T, Dick IM, and Prince RL.** Calcitriol upregulates expression and activity of the 1b isoform of the plasma membrane calcium pump in immortalized distal kidney tubular cells. *Arch Biochem Biophys* 380: 126–132, 2000.
148. **Glendenning P, Ratajczak T, Dick IM, and Prince RL.** Regulation of the 1b isoform of the plasma membrane calcium pump by $1,25\text{-dihydroxyvitamin D}_3$ in rat osteoblast-like cells. *J Bone Miner Res* 16: 525–534, 2001.

149. Glendenning P, Ratajczak T, Prince RL, Garamszegi N, and Strehler EE. The promoter region of the human PMCA1 gene mediates transcriptional downregulation by 1,25-dihydroxyvitamin D₃. *Biochem Biophys Res Commun* 277: 722–728, 2000.
150. Goel M, Garcia R, Estacion M, and Schilling WP. Regulation of *Drosophila* TRPL channels by immunophilin FKBP59. *J Biol Chem* 276: 38762–38773, 2001.
151. Gonzalez-Mariscal L, Betanzos A, Nava P, and Jaramillo BE. Tight junction proteins. *Prog Biophys Mol Biol* 81: 1–44, 2003.
152. Goodenough DA. Plugging the leaks. *Proc Natl Acad Sci USA* 96: 319–321, 1999.
153. Gopalakrishnan S, Dunn KW, and Marrs JA. Rac1, but not RhoA, signaling protects epithelial adherens junction assembly during ATP depletion. *Am J Physiol Cell Physiol* 283: C261–C272, 2002.
154. Greger R, Lang F, and Oberleithner H. Distal site of calcium reabsorption in the rat nephron. *Pflügers Arch* 374: 153–157, 1978.
155. Gunthorpe MJ, Benham CD, Randall A, and Davis JB. The diversity in the vanilloid (TRPV) receptor family of ion channels. *Trends Pharmacol Sci* 23: 183–191, 2002.
156. Hanaoka K, Qian F, Boletta A, Bhumia AK, Piontek K, Tsiokas L, Sukhatme VP, Guggino WB, and Germino GG. Co-assembly of polycystin-1 and -2 produces unique cation-permeable currents. *Nature* 408: 990–994, 2000.
157. Harding MW, Galat A, Uehling DE, and Schreiber SL. A receptor for the immunosuppressant FK506 is a *cis-trans* peptidyl-prolyl isomerase. *Nature* 341: 758–760, 1989.
158. Harmeyer J and Deluca HF. Calcium-binding protein and calcium absorption after vitamin D administration. *Arch Biochem Biophys* 133: 247–254, 1969.
159. Haussler MR, Whitfield GK, Haussler CA, Hsieh JC, Thompson PD, Selznick SH, Dominguez CE, and Jurutka PW. The nuclear vitamin D receptor: biological and molecular regulatory properties revealed. *J Bone Miner Res* 13: 325–349, 1998.
160. Hayes JR and Ritchie CM. Hypercalcaemia due to thyrotoxicosis. *Ir J Med Sci* 152: 422–423, 1983.
161. He S, Ruknudin A, Bambrick LL, Lederer WJ, and Schulze DH. Isoform-specific regulation of the Na⁺/Ca²⁺ exchanger in rat astrocytes and neurons by PKA. *J Neurosci* 18: 4833–4841, 1998.
162. Hermosura MC, Monteilh-Zoller MK, Scharenberg AM, Penner R, and Fleig A. Dissociation of the store-operated calcium current I_{CRAC} and the Mg-nucleotide-regulated metal ion current MagNum. *J Physiol* 539: 445–458, 2002.
163. Hess P, Lansman JB, and Tsien RW. Calcium channel selectivity for divalent and monovalent cations. Voltage and concentration dependence of single channel current in ventricular heart cells. *J Gen Physiol* 88: 293–319, 1986.
164. Hildmann B, Schmidt A, and Murer H. Ca²⁺-transport across basal-lateral plasma membranes from rat small intestinal epithelial cells. *J Membr Biol* 65: 55–62, 1982.
165. Hille B. *Ionic Channels of Excitable Membranes*. Sunderland, MA: Sinauer, 2001.
166. Hirai M and Shimizu N. Purification of two distinct proteins of approximate M_r 80,000 from human epithelial cells and identification as proper substrates for protein kinase C. *Biochem J* 270: 583–589, 1990.
167. Hirnet D, Olausson J, Fecher-Trost C, Boddling M, Nastainczyk W, Wissenbach U, Flockerzi V, and Freichel M. The TRPV6 gene, cDNA and protein. *Cell Calcium* 33: 509–518, 2003.
168. Hoenderop JG, Chon H, Gkika D, Bluysen HA, Holstege FC, St-Arnaud R, Braam B, and Bindels RJ. Regulation of gene expression by dietary Ca²⁺ in kidneys of 25-hydroxyvitamin D₃-1α-hydroxylase knockout mice. *Kidney Int* 65: 531–539, 2004.
169. Hoenderop JG, Dardenne O, Van Abel M, Van Der Kemp AW, van Os CH, St-Arnaud R, and Bindels RJ. Modulation of renal Ca²⁺ transport protein genes by dietary Ca²⁺ and 1,25-dihydroxyvitamin D₃ in 25-hydroxyvitamin D₃-1α-hydroxylase knockout mice. *FASEB J* 16: 1398–1406, 2002.
170. Hoenderop JG, De Pont JJ, Bindels RJ, and Willems PH. Hormone-stimulated Ca²⁺ reabsorption in rabbit kidney cortical collecting system is cAMP-independent and involves a phorbol ester-insensitive PKC isotype. *Kidney Int* 55: 225–233, 1999.
171. Hoenderop JG, Hartog A, Stuiver M, Doucet A, Willems PH, and Bindels RJ. Localization of the epithelial Ca²⁺ channel in rabbit kidney and intestine. *J Am Soc Nephrol* 11: 1171–1178, 2000.
172. Hoenderop JG, Hartog A, Willems PH, and Bindels RJ. Adenosine-stimulated Ca²⁺ reabsorption is mediated by apical A1 receptors in rabbit cortical collecting system. *Am J Physiol Renal Physiol* 274: F736–F743, 1998.
173. Hoenderop JG, Muller D, Suzuki M, van Os CH, and Bindels RJ. Epithelial calcium channel: gate-keeper of active calcium reabsorption. *Curr Opin Nephrol Hypertens* 9: 335–340, 2000.
174. Hoenderop JG, Muller D, Van Der Kemp AW, Hartog A, Suzuki M, Ishibashi K, Imai M, Sweep F, Willems PH, van Os CH, and Bindels RJ. Calcitriol controls the epithelial calcium channel in kidney. *J Am Soc Nephrol* 12: 1342–1349, 2001.
175. Hoenderop JG, Nilius B, and Bindels RJ. Molecular mechanism of active Ca²⁺ reabsorption in the distal nephron. *Annu Rev Physiol* 64: 529–549, 2002.
176. Hoenderop JG, Nilius B, and Bindels RJ. Epithelial calcium channels: from identification to function and regulation. *Pflügers Arch* 446: 304–308, 2003.
177. Hoenderop JG, Vaandrager AB, Dijkink L, Smolenski A, Gambaryan S, Lohmann SM, de Jonge HR, Willems PH, and Bindels RJ. Atrial natriuretic peptide-stimulated Ca²⁺ reabsorption in rabbit kidney requires membrane-targeted, cGMP-dependent protein kinase type II. *Proc Natl Acad Sci USA* 96: 6084–6089, 1999.
178. Hoenderop JG, van der Kemp AW, Hartog A, van de Graaf SF, van Os CH, Willems PH, and Bindels RJ. Molecular identification of the apical Ca²⁺ channel in 1,25-dihydroxyvitamin D₃-responsive epithelia. *J Biol Chem* 274: 8375–8378, 1999.
179. Hoenderop JG, van der Kemp AW, Hartog A, van Os CH, Willems PH, and Bindels RJ. The epithelial calcium channel, ECaC, is activated by hyperpolarization and regulated by cytosolic calcium. *Biochem Biophys Res Commun* 261: 488–492, 1999.
180. Hoenderop JG, van Leeuwen JP, van der Eerden BC, Kersten FF, van der Kemp AW, Merillat AM, Waarsing JH, Rossier BC, Vallon V, Hummler E, and Bindels RJ. Renal Ca²⁺ wasting, hyperabsorption, and reduced bone thickness in mice lacking TRPV5. *J Clin Invest* 112: 1906–1914, 2003.
181. Hoenderop JG, Vennekens R, Muller D, Prenen J, Droogmans G, Bindels RJ, and Nilius B. Function and expression of the epithelial Ca²⁺ channel family: comparison of mammalian ECaC1 and 2. *J Physiol* 537: 747–761, 2001.
182. Hoenderop JG, Voets T, Hoefs S, Weidema AF, Prenen J, Nilius B, and Bindels RJ. Homo- and heterotetrameric architecture of the epithelial Ca²⁺ channels, TRPV5 and TRPV6. *EMBO J* 22: 776–785, 2003.
183. Hoenderop JG, Willems PH, and Bindels RJ. Toward a comprehensive molecular model of active calcium reabsorption. *Am J Physiol Renal Physiol* 278: F352–F360, 2000.
184. Hofer AM and Brown EM. Extracellular calcium sensing and signalling. *Nat Rev Mol Cell Biol* 4: 530–538, 2003.
185. Hoff AO, Catala-Lehnen P, Thomas PM, Priemel M, Rueger JM, Nasonkin I, Bradley A, Hughes MR, Ordenez N, Cote GJ, Amling M, and Gagel RF. Increased bone mass is an unexpected phenotype associated with deletion of the calcitonin gene. *J Clin Invest* 110: 1849–1857, 2002.
186. Hofmann T, Schaefer M, Schultz G, and Gudermann T. Subunit composition of mammalian transient receptor potential channels in living cells. *Proc Natl Acad Sci USA* 99: 7461–7466, 2002.
187. Honda S, Kashiwagi M, Ookata K, Tojo A, and Hirose S. Regulation by 1α,25-dihydroxyvitamin D₃ of expression of stanniocalcin messages in the rat kidney and ovary. *FEBS Lett* 459: 119–122, 1999.
188. Hoth M and Penner R. Depletion of intracellular calcium stores activates a calcium current in mast cells. *Nature* 355: 353–356, 1992.
189. Howard A, Legon S, Spurr NK, and Walters JR. Molecular cloning and chromosomal assignment of human calbindin-D9k. *Biochem Biophys Res Commun* 185: 663–669, 1992.
190. Huo TL and Lytton J. Potential calbindin-D28K associated proteins in rat kidney cortex. *J Am Soc Nephrol* 6: 964, 1995.
191. Imai M. Calcium transport across the rabbit thick ascending limb of Henle's loop perfused in vitro. *Pflügers Arch* 374: 255–263, 1978.

193. **Ishida H, Seino Y, Seino S, Tsuda K, Takemura J, Nishi S, Ishizuka S, and Imura H.** Effect of 1,25-dihydroxyvitamin D₃ on pancreatic B and D cell function. *Life Sci* 33: 1779–1786, 1983.
194. **Janssen SW, Hoenderop JG, Hermus AR, Sweep FC, Martens GJ, and Bindels RJ.** Expression of the novel epithelial Ca²⁺ channel ECaC1 in rat pancreatic islets. *J Histochem Cytochem* 50: 789–798, 2002.
195. **Jayakumar A, Cheng L, Liang CT, and Sacktor B.** Sodium gradient-dependent calcium uptake in renal basolateral membrane vesicles. Effect of parathyroid hormone. *J Biol Chem* 259: 10827–10833, 1984.
196. **Jean K, Bernatchez G, Klein H, Garneau L, Sauvé R, and Parent L.** The role of aspartate residues in Ca²⁺ affinity and permeation of the distal ECaC1 channel. *Am J Physiol Cell Physiol* 282: C665–C672, 2002.
197. **Jenkins SM and Bennett V.** Ankyrin-G coordinates assembly of the spectrin-based membrane skeleton, voltage-gated sodium channels, and L1 CAMs at Purkinje neuron initial segments. *J Cell Biol* 155: 739–746, 2001.
198. **Johnson JA, Grande JP, Roche PC, and Kumar R.** Immunohistochemical localization of the 1,25(OH)₂D₃ receptor and calbindin D28k in human and rat pancreas. *Am J Physiol Endocrinol Metab* 267: E356–E360, 1994.
199. **Johnson JA and Kumar R.** Renal and intestinal calcium transport: roles of vitamin D and vitamin D-dependent calcium binding proteins. *Semin Nephrol* 14: 119–128, 1994.
200. **Jones G, Strugnelli SA, and DeLuca HF.** Current understanding of the molecular actions of vitamin D. *Physiol Rev* 78: 1193–1231, 1998.
201. **Jordt SE, Bautista DM, Chuang HH, McKemy DD, Zygmunt PM, Hogestatt ED, Meng ID, and Julius D.** Mustard oils and cannabinoids excite sensory nerve fibres through the TRP channel ANKTM1. *Nature* 427: 260–265, 2004.
202. **Kadowaki S and Norman AW.** Dietary vitamin D is essential for normal insulin secretion from the perfused rat pancreas. *J Clin Invest* 73: 759–766, 1984.
203. **Kahr H, Schindl R, Fritsch R, Heinze B, Hofbauer M, Hack M, Mortelmaier M, Groschner K, Peng JB, Takanaga H, Hediger MA, and Romanin C.** CaT1 knock-down strategies fail to affect CRAC channels in mucosal-type mast cells. *J Physiol*. In press.
204. **Kaissling B.** Structural aspects of adaptive changes in renal electrolyte excretion. *Am J Physiol Renal Fluid Electrolyte Physiol* 243: F211–F226, 1982.
205. **Kato S.** Genetic mutation in the human 25-hydroxyvitamin D₃ 1 α -hydroxylase gene causes vitamin D-dependent rickets type I. *Mol Cell Endocrinol* 156: 7–12, 1999.
206. **Kawahara K and Matsuzaki K.** Activation of calcium channel by shear-stress in cultured renal distal tubule cells. *Biochem Biophys Res Commun* 184: 198–205, 1992.
207. **Kedei N, Szabo T, Lile JD, Treanor JJ, Olah Z, Iadarola MJ, and Blumberg PM.** Analysis of the native quaternary structure of vanilloid receptor 1. *J Biol Chem* 276: 28613–28619, 2001.
208. **Kerschbaum HH and Cahalan MD.** Single-channel recording of a store-operated Ca²⁺ channel in Jurkat T lymphocytes. *Science* 283: 836–839, 1999.
209. **Kerschbaum HH, Kozak JA, and Cahalan MD.** Polyvalent cations as permeant probes of MIC and TRPM7 pores. *Biophys J* 84: 2293–2305, 2003.
210. **Kikuchi K, Kikuchi T, and Ghishan FK.** Characterization of calcium transport by basolateral membrane vesicles of human small intestine. *Am J Physiol Gastrointest Liver Physiol* 255: G482–G489, 1988.
211. **Kimmel-Jehan C, Jehan F, and DeLuca HF.** Salt concentration determines 1,25-dihydroxyvitamin D₃ dependency of vitamin D receptor-retinoid X receptor-vitamin D-responsive element complex formation. *Arch Biochem Biophys* 341: 75–80, 1997.
212. **Kimura J, Noma A, and Irisawa H.** Na-Ca exchange current in mammalian heart cells. *Nature* 319: 596–597, 1986.
213. **Kip SN and Strehler EE.** Characterization of PMCA isoforms and their contribution to transcellular Ca²⁺ flux in MDCK cells. *Am J Physiol Renal Physiol* 284: F122–F132, 2003.
214. **Kip SN and Strehler EE.** Vitamin D₃ upregulates plasma membrane Ca²⁺-ATPase expression and potentiates apico-basal Ca²⁺ flux in MDCK cells. *Am J Physiol Renal Physiol* 286: F363–F369, 2004.
215. **Kirchner KA.** Effect of diuretic and antidiuretic agents on lithium clearance as a marker for proximal delivery. *Kidney Int Suppl* 28: S22–S25, 1990.
216. **Klockner U and Isenberg G.** Endothelin depolarizes myocytes from porcine coronary and human mesenteric arteries through a Ca-activated chloride current. *Pflügers Arch* 418: 168–175, 1991.
217. **Kordeli E, Lambert S, and Bennett V.** AnkyrinG. A new ankyrin gene with neural-specific isoforms localized at the axonal initial segment and node of Ranvier. *J Biol Chem* 270: 2352–2359, 1995.
218. **Koster HP, Hartog A, van Os CH, and Bindels RJ.** Calbindin-D_{28K} facilitates cytosolic calcium diffusion without interfering with calcium signaling. *Cell Calcium* 18: 187–196, 1995.
219. **Koushik SV, Wang J, Rogers R, Moskopid D, Lambert NA, Creazzo TL, and Conway SJ.** Targeted inactivation of the sodium-calcium exchanger (NCX1) results in the lack of a heartbeat and abnormal myofibrillar organization. *FASEB J* 15: 1209–1211, 2001.
220. **Kozak JA, Kerschbaum HH, and Cahalan MD.** Distinct properties of CRAC and MIC channels in RBL cells. *J Gen Physiol* 120: 221–235, 2002.
221. **Kreusch A, Pfaffinger PJ, Stevens CF, and Choe S.** Crystal structure of the tetramerization domain of the Shaker potassium channel. *Nature* 392: 945–948, 1998.
222. **Kumar V and Prasad R.** Molecular basis of renal handling of calcium in response to thyroid hormone status of rat. *Biochim Biophys Acta* 1586: 331–343, 2002.
223. **Kumar V and Prasad R.** Thyroid hormones stimulate calcium transport systems in rat intestine. *Biochim Biophys Acta* 1639: 185–194, 2003.
224. **Kushner PJ, Agard DA, Greene GL, Scanlan TS, Shiau AK, Uht RM, and Webb P.** Estrogen receptor pathways to AP-1. *J Steroid Biochem Mol Biol* 74: 311–317, 2000.
225. **Kwan HY, Huang Y, and Yao X.** Regulation of canonical transient receptor potential isoform 3 (TRPC3) channel by protein kinase G. *Proc Natl Acad Sci USA*. In press.
226. **Lacerda AE, Kim HS, Ruth P, Perez-Reyes E, Flockerzi V, Hofmann F, Birnbaumer L, and Brown AM.** Normalization of current kinetics by interaction between the α 1 and β 2 subunits of the skeletal muscle dihydropyridine-sensitive Ca²⁺ channel. *Nature* 352: 527–530, 1991.
227. **Lafond J, Leclerc M, and Brunette MG.** Characterization of calcium transport by basal plasma membranes from human placental syncytiotrophoblast. *J Cell Physiol* 148: 17–23, 1991.
228. **Lajeunesse D, Bouhtiauy I, and Brunette MG.** Parathyroid hormone and hydrochlorothiazide increase calcium transport by the luminal membrane of rabbit distal nephron segments through different pathways. *Endocrinology* 134: 35–41, 1994.
229. **Lambers TT, Weidema AF, Nilius B, Hoenderop JG, and Bindels RJ.** Regulation of the mouse epithelial Ca²⁺ channel TRPV6, by the Ca²⁺-sensor calmodulin. *J Biol Chem*. In press.
230. **Larsson D and Nemere I.** Vectorial transcellular calcium transport in intestine: integration of current models. *J Biomed Biotechnol* 2: 117–119, 2002.
231. **Lee K, Brown D, Urena P, Ardaillou N, Ardaillou R, Deeds J, and Segre GV.** Localization of parathyroid hormone/parathyroid hormone-related peptide receptor mRNA in kidney. *Am J Physiol Renal Fluid Electrolyte Physiol* 270: F186–F191, 1996.
232. **Leyva M.** The role of dietary calcium in disease prevention. *J Oklahoma State Med Assoc* 96: 272–275, 2003.
233. **Li HS and Montell C.** TRP and the PDZ protein, INAD, form the core complex required for retention of the signalplex in *Drosophila* photoreceptor cells. *J Cell Biol* 150: 1411–1422, 2000.
234. **Li M, Unwin N, Stauffer KA, Jan YN, and Jan LY.** Images of purified Shaker potassium channels. *Curr Biol* 4: 110–115, 1994.
235. **Li XF, Kraev AS, and Lytton J.** Molecular cloning of a fourth member of the potassium-dependent sodium-calcium exchanger gene family, NCKX4. *J Biol Chem* 277: 48410–48417, 2002.
236. **Li Z, Matsuoka S, Hryshko LV, Nicoll DA, Bersohn MM, Burke EP, Lifton RP, and Philipson KD.** Cloning of the NCX2 isoform of the plasma membrane Na⁺-Ca²⁺ exchanger. *J Biol Chem* 269: 17434–17439, 1994.

237. **Lintschinger B, Balzer-Geldsetzer M, Baskaran T, Graier WF, Romanin C, Zhu MX, and Groschner K.** Coassembly of Trp1 and Trp3 proteins generates diacylglycerol- and Ca^{2+} -sensitive cation channels. *J Biol Chem* 275: 27799–27805, 2000.
238. **Liu J, Farmer JD Jr, Lane WS, Friedman J, Weissman I, and Schreiber SL.** Calcineurin is a common target of cyclophilin-cyclosporin A and FKBP-FK506 complexes. *Cell* 66: 807–815, 1991.
239. **Loffing J, Loffing-Cueni D, Hegyi I, Kaplan MR, Hebert SC, Le Hir M, and Kaissling B.** Thiazide treatment of rats provokes apoptosis in distal tubule cells. *Kidney Int* 50: 1180–1190, 1996.
240. **Loffing J, Loffing-Cueni D, Valderrabano V, Klausli L, Hebert SC, Rossier BC, Hoenderop JG, Bindels RJ, and Kaissling B.** Distribution of transcellular calcium and sodium transport pathways along mouse distal nephron. *Am J Physiol Renal Physiol* 281: F1021–F1027, 2001.
241. **Lote CJ, Thewles A, Wood JA, and Zafar T.** The hypomagnesaemic action of FK506: urinary excretion of magnesium and calcium and the role of parathyroid hormone. *Clin Sci* 99: 285–292, 2000.
242. **Lukert BP and Raisz LG.** Glucocorticoid-induced osteoporosis: pathogenesis and management. *Ann Intern Med* 112: 352–364, 1990.
243. **Lytton J, Lee SL, Lee WS, van Baal J, Bindels RJ, Kilav R, Naveh-Manly T, and Silver J.** The kidney sodium-calcium exchanger. *Ann NY Acad Sci* 779: 58–72, 1996.
244. **Magaldi AJ, van Baak AA, and Rocha AS.** Calcium transport across rat inner medullary collecting duct perfused in vitro. *Am J Physiol Renal Fluid Electrolyte Physiol* 257: F738–F745, 1989.
245. **Magosci M, Yamaki M, Penniston JT, and Dousa TP.** Localization of mRNAs coding for isozymes of plasma membrane Ca^{2+} -ATPase pump in rat kidney. *Am J Physiol Renal Fluid Electrolyte Physiol* 263: F7–F14, 1992.
246. **Magyar CE, White KE, Rojas R, Apodaca G, and Friedman PA.** Plasma membrane Ca^{2+} -ATPase and NCX1 $\text{Na}^+/\text{Ca}^{2+}$ exchanger expression in distal convoluted tubule cells. *Am J Physiol Renal Physiol* 283: F29–F40, 2002.
247. **Mailliard WS, Haigler HT, and Schlaepfer DD.** Calcium-dependent binding of S100C to the N-terminal domain of annexin I. *J Biol Chem* 271: 719–725, 1996.
248. **Martin-Padura I, Lostaglio S, Schneemann M, Williams L, Romano M, Fruscella P, Panzeri C, Stoppacciaro A, Ruco L, Villa A, Simmons D, and Dejana E.** Junctional adhesion molecule, a novel member of the immunoglobulin superfamily that distributes at intercellular junctions and modulates monocyte transmigration. *J Cell Biol* 142: 117–127, 1998.
249. **Massheimer V, Boland R, and de Boland AR.** Rapid $1,25(\text{OH})_2$ -vitamin D_3 stimulation of calcium uptake by rat intestinal cells involves a dihydropyridine-sensitive cAMP-dependent pathway. *Cell Signal* 6: 299–304, 1994.
250. **Masumiya H, Wang R, Zhang J, Xiao B, and Chen SR.** Localization of the 12.6-kDa FK506-binding protein (FKBP12.6) binding site to the NH_2 -terminal domain of the cardiac Ca^{2+} release channel (ryanodine receptor). *J Biol Chem* 278: 3786–3792, 2003.
251. **McDiarmid SV, Colonna JO, Shaked A, Ament ME, and Busuttil RW.** A comparison of renal function in cyclosporine- and FK-506-treated patients after primary orthotopic liver transplantation. *Transplantation* 56: 847–853, 1993.
252. **Mena C, Devlin RD, Reddy SV, Gazitt Y, Choi SJ, and Roodman GD.** Annexin II increases osteoclast formation by stimulating the proliferation of osteoclast precursors in human marrow cultures. *J Clin Invest* 103: 1605–1613, 1999.
253. **Miller LA and Stapleton FB.** Urinary volume in children with urolithiasis. *J Urol* 141: 918–920, 1989.
- 253a. **Mizwicki MT, Bishop JE, Olivera CJ, Huhtakangas J, and Norman AW.** Evidence that annexin II is not a putative membrane receptor for $1\alpha,25(\text{OH})_2$ -vitamin D_3 . *J Cell Biochem* 91: 852–863, 2004.
254. **Monnens L, Bindels R, and Grunfeld JP.** Gitelman syndrome comes of age. *Nephrol Dial Transplant* 13: 1617–1619, 1998.
255. **Monroy A, Plata C, Hebert SC, and Gamba G.** Characterization of the thiazide-sensitive Na^+Cl^- cotransporter: a new model for ions and diuretics interaction. *Am J Physiol Renal Physiol* 279: F161–F169, 2000.
256. **Montell C, Birnbaumer L, and Flockerzi V.** The TRP channels, a remarkably functional family. *Cell* 108: 595–598, 2002.
257. **Montell C, Birnbaumer L, Flockerzi V, Bindels RJ, Bruford EA, Caterina MJ, Clapham DE, Harteneck C, Heller S, Julius D, Kojima I, Mori Y, Penner R, Prawitt D, Scharenberg AM, Schultz G, Shimizu N, and Zhu MX.** A unified nomenclature for the superfamily of TRP cation channels. *Mol Cell* 9: 229–231, 2002.
258. **Moreau R, Daoud G, Bernatchez R, Simoneau L, Masse A, and Lafond J.** Calcium uptake and calcium transporter expression by trophoblast cells from human term placenta. *Biochim Biophys Acta* 1564: 325–332, 2002.
259. **Moreau R, Daoud G, Masse A, Simoneau L, and Lafond J.** Expression and role of calcium-ATPase pump and sodium-calcium exchanger in differentiated trophoblasts from human term placenta. *Mol Reprod Dev* 65: 283–288, 2003.
260. **Moreau R, Hamel A, Daoud G, Simoneau L, and Lafond J.** Expression of calcium channels along the differentiation of cultured trophoblast cells from human term placenta. *Biol Reprod* 67: 1473–1479, 2002.
261. **Moreau R, Simoneau L, and Lafond J.** Calcium fluxes in human trophoblast (BeWo) cells: calcium channels, calcium-ATPase, and sodium-calcium exchanger expression. *Mol Reprod Dev* 64: 189–198, 2003.
262. **Morita K, Furuse M, Fujimoto K, and Tsukita S.** Claudin multigene family encoding four-transmembrane domain protein components of tight junction strands. *Proc Natl Acad Sci USA* 96: 511–516, 1999.
263. **Mosekilde L, Eriksen EF, and Charles P.** Effects of thyroid hormones on bone and mineral metabolism. *Endocrinol Metab Clin North Am* 19: 35–63, 1990.
264. **Motoyama HI and Friedman PA.** Calcium-sensing receptor regulation of PTH-dependent calcium absorption by mouse cortical ascending limbs. *Am J Physiol Renal Physiol* 283: F399–F406, 2002.
265. **Muller D, Hoenderop JG, Meij IC, van den Heuvel LP, Knoers NV, den Hollander AI, Eggert P, Garcia-Nieto V, Claverie-Martin F, and Bindels RJ.** Molecular cloning, tissue distribution, and chromosomal mapping of the human epithelial Ca^{2+} channel (ECAC1). *Genomics* 67: 48–53, 2000.
266. **Mullins LJ.** The generation of electric currents in cardiac fibers by Na/Ca exchange. *Am J Physiol Cell Physiol* 236: C103–C110, 1979.
267. **Mullins LJ.** Is stoichiometry constant in $\text{Na}-\text{Ca}$ exchange? *Ann NY Acad Sci* 639: 96–98, 1991.
268. **Murcia NS, Sweeney WE Jr, and Avner ED.** New insights into the molecular pathophysiology of polycystic kidney disease. *Kidney Int* 55: 1187–1197, 1999.
269. **Murcia NS, Woychik RP, and Avner ED.** The molecular biology of polycystic kidney disease. *Pediatr Nephrol* 12: 721–726, 1998.
270. **Nauli SM, Alenghat FJ, Luo Y, Williams E, Vassilev P, Li X, Elia AE, Lu W, Brown EM, Quinn SJ, Ingber DE, and Zhou J.** Polycystins 1 and 2 mediate mechanosensation in the primary cilium of kidney cells. *Nat Genet* 33: 129–137, 2003.
271. **Neer RM.** The evolutionary significance of vitamin D, skin pigment, and ultraviolet light. *Am J Phys Anthropol* 43: 409–416, 1975.
272. **Nemere I and Norman AW.** Parathyroid hormone stimulates calcium transport in perfused duodena from normal chicks: comparison with the rapid (transcaltactic) effect of $1,25$ -dihydroxyvitamin D_3 . *Endocrinology* 119: 1406–1408, 1986.
273. **Nemere I and Szego CM.** Early actions of parathyroid hormone and $1,25$ -dihydroxycholecalciferol on isolated epithelial cells from rat intestine. II. Analyses of additivity, contribution of calcium, and modulatory influence of indomethacin. *Endocrinology* 109: 2180–2187, 1981.
274. **Ng RC, Peraino RA, and Suki WN.** Divalent cation transport in isolated tubules. *Kidney Int* 22: 492–497, 1982.
275. **Nicoll DA, Quednau BD, Qui Z, Xia YR, Lusic AJ, and Philipson KD.** Cloning of a third mammalian $\text{Na}^+\text{Ca}^{2+}$ exchanger, NCX3. *J Biol Chem* 271: 24914–24921, 1996.
276. **Niemeyer BA, Bergs C, Wissenbach U, Flockerzi V, and Trost C.** Competitive regulation of CaT -like-mediated Ca^{2+} entry by protein kinase C and calmodulin. *Proc Natl Acad Sci USA* 98: 3600–3605, 2001.

277. **Nijenhuis T, Hoenderop JG, and Bindels RJ.** Downregulation of Ca^{2+} and Mg^{2+} transport proteins in the kidney explains tacrolimus (FK506)-induced hypercalciuria and hypomagnesemia. *J Am Soc Nephrol* 15: 549–557, 2004.
278. **Nijenhuis T, Hoenderop JG, Loffing J, van der Kemp AW, van Os CH, and Bindels RJ.** Thiazide-induced hypocalciuria is accompanied by a decreased expression of Ca^{2+} transport proteins in kidney. *Kidney Int* 64: 555–564, 2003.
279. **Nijenhuis T, Hoenderop JG, van der Kemp AW, and Bindels RJ.** Localization and regulation of the epithelial Ca^{2+} channel TRPV6 in the kidney. *J Am Soc Nephrol* 14: 2731–2740, 2003.
280. **Nilius B.** From TRPs to SOCs, CCEs, and CRACs: consensus and controversies. *Cell Calcium* 33: 293–298, 2003.
281. **Nilius B, Prenen J, Hoenderop JG, Vennekens R, Hoefs S, Weidema AF, Droogmans G, and Bindels RJ.** Fast and slow inactivation kinetics of the Ca^{2+} channels ECaC1 and ECaC2 (TRPV5 and TRPV6). Role of the intracellular loop located between transmembrane segments 2 and 3. *J Biol Chem* 277: 30852–30858, 2002.
282. **Nilius B, Prenen J, Vennekens R, Hoenderop JG, Bindels RJ, and Droogmans G.** Modulation of the epithelial calcium channel, ECaC, by intracellular Ca^{2+} . *Cell Calcium* 29: 417–428, 2001.
283. **Nilius B, Prenen J, Vennekens R, Hoenderop JG, Bindels RJ, and Droogmans G.** Pharmacological modulation of monovalent cation currents through the epithelial Ca^{2+} channel ECaC1. *Br J Pharmacol* 134: 453–462, 2001.
285. **Nilius B, Vennekens R, Prenen J, Hoenderop JG, Bindels RJ, and Droogmans G.** Whole-cell and single channel monovalent cation currents through the novel rabbit epithelial Ca^{2+} channel ECaC. *J Physiol* 527: 239–248, 2000.
286. **Nilius B, Vennekens R, Prenen J, Hoenderop JG, Droogmans G, and Bindels RJ.** The single pore residue Asp542 determines Ca^{2+} permeation and Mg^{2+} block of the epithelial Ca^{2+} channel. *J Biol Chem* 276: 1020–1025, 2001.
287. **Nilius B, Vriens J, Prenen J, Droogmans G, and Voets T.** TRPV4 calcium entry channel: a paradigm for gating diversity. *Am J Physiol Cell Physiol* 286: C195–C205, 2004.
288. **Nilius B, Weidema F, Prenen J, Hoenderop JJ, Vennekens R, Hoefs S, Droogmans G, and Bindels RM.** The carboxyl terminus of the epithelial Ca^{2+} channel ECaC1 is involved in Ca^{2+} -dependent inactivation. *Pflügers Arch* 445: 584–588, 2003.
289. **Nordin BE, Horsman A, Marshall DH, Simpson M, and Waterhouse GM.** Calcium requirement and calcium therapy. *Clin Orthop* 140: 216–239, 1979.
290. **Nordin BE, Need AG, Morris HA, Horowitz M, and Robertson WG.** Evidence for a renal calcium leak in postmenopausal women. *J Clin Endocrinol Metab* 72: 401–407, 1991.
292. **Nourry C, Grant SG, and Borg JP.** PDZ domain proteins: plug and play! *Sci STKE* 2003: RE7, 2003.
293. **Numazaki M, Tominaga T, Takeuchi K, Murayama N, Toyooka H, and Tominaga M.** Structural determinant of TRPV1 desensitization interacts with calmodulin. *Proc Natl Acad Sci USA* 100: 8002–8006, 2003.
294. **Ohtake K, Maeno T, Ueda H, Ogiwara M, Natsume H, and Morimoto Y.** Poly-L-arginine enhances paracellular permeability via serine/rhreonine phosphorylation of ZO-1 and tyrosine dephosphorylation of occludin in rabbit nasal epithelium. *Pharm Res* 20: 1838–1845, 2003.
295. **O'Keefe SJ, Tamura J, Kincaid RL, Tocci MJ, and O'Neill EA.** FK-506- and CsA-sensitive activation of the interleukin-2 promoter by calcineurin. *Nature* 357: 692–694, 1992.
296. **Okuse K, Malik-Hall M, Baker MD, Poon WY, Kong H, Chao MV, and Wood JN.** Annexin II light chain regulates sensory neuron-specific sodium channel expression. *Nature* 417: 653–656, 2002.
297. **Ookata K, Tojo A, Onozato ML, Kashiwagi M, Honda S, and Hirose S.** Distribution of stanniocalcin 1 in rat kidney and its regulation by vitamin D_3 . *Exp Nephrol* 9: 428–435, 2001.
298. **Panda DK, Miao D, Tremblay ML, Sirois J, Farookhi R, Hendy GN, and Goltzman D.** Targeted ablation of the 25-hydroxyvitamin D 1 α -hydroxylase enzyme: evidence for skeletal, reproductive, and immune dysfunction. *Proc Natl Acad Sci USA* 98: 7498–7503, 2001.
299. **Pappenheimer JR.** Physiological regulation of transepithelial impedance in the intestinal mucosa of rats and hamsters. *J Membr Biol* 100: 137–148, 1987.
300. **Parekh AB and Penner R.** Store depletion and calcium influx. *Physiol Rev* 77: 901–930, 1997.
301. **Peng JB, Brown EM, and Hediger MA.** Structural conservation of the genes encoding CaT1, CaT2, and related cation channels. *Genomics* 76: 99–109, 2001.
302. **Peng JB, Brown EM, and Hediger MA.** Epithelial Ca^{2+} entry channels: transcellular Ca^{2+} transport and beyond. *J Physiol* 551: 729–740, 2003.
303. **Peng JB, Chen XZ, Berger UV, Vassilev PM, Brown EM, and Hediger MA.** A rat kidney-specific calcium transporter in the distal nephron. *J Biol Chem* 275: 28186–28194, 2000.
304. **Peng JB, Chen XZ, Berger UV, Vassilev PM, Tsukaguchi H, Brown EM, and Hediger MA.** Molecular cloning and characterization of a channel-like transporter mediating intestinal calcium absorption. *J Biol Chem* 274: 22739–22746, 1999.
305. **Peng JB, Chen XZ, Berger UV, Weremowicz S, Morton CC, Vassilev PM, Brown EM, and Hediger MA.** Human calcium transport protein CaT1. *Biochem Biophys Res Commun* 278: 326–332, 2000.
306. **Peng JB, Zhuang L, Berger UV, Adam RM, Williams BJ, Brown EM, Hediger MA, and Freeman MR.** CaT1 expression correlates with tumor grade in prostate cancer. *Biochem Biophys Res Commun* 282: 729–734, 2001.
307. **Persechini A, Moncrief ND, and Kretsinger RH.** The EF-hand family of calcium-modulated proteins. *Trends Neurosci* 12: 462–467, 1989.
308. **Philipson KD and Nicoll DA.** Sodium-calcium exchange: a molecular perspective. *Annu Rev Physiol* 62: 111–133, 2000.
309. **Picotto G, Massheimer V, and Boland R.** Parathyroid hormone stimulates calcium influx and the cAMP messenger system in rat enterocytes. *Am J Physiol Cell Physiol* 273: C1349–C1353, 1997.
310. **Pitkin RM.** Calcium metabolism in pregnancy and the perinatal period: a review. *Am J Obstet Gynecol* 151: 99–109, 1985.
311. **Planells-Cases R, Aracil A, Merino JM, Gallar J, Perez-Paya E, Belmonte C, Gonzalez-Ros JM, and Ferrer-Montiel AV.** Arginine-rich peptides are blockers of VR-1 channels with analgesic activity. *FEBS Lett* 481: 131–136, 2000.
312. **Poujeol P, Bidet M, and Tauc M.** Calcium transport in rabbit distal cells. *Kidney Int* 48: 1102–1110, 1995.
313. **Prakriya M and Lewis RS.** CRAC channels: activation, permeation, and the search for a molecular identity. *Cell Calcium* 33: 311–321, 2003.
314. **Prakriya M and Lewis RS.** Separation and characterization of currents through store-operated CRAC channels and Mg^{2+} -inhibited cation (MIC) channels. *J Gen Physiol* 119: 487–508, 2002.
315. **Prince RL, Smith M, Dick IM, Price RI, Webb PG, Henderson NK, and Harris MM.** Prevention of postmenopausal osteoporosis. A comparative study of exercise, calcium supplementation, and hormone-replacement therapy. *N Engl J Med* 325: 1189–1195, 1991.
316. **Prod'homme B, Pietrobon D, and Hess P.** Interactions of protons with single open L-type calcium channels. Location of protonation site and dependence of proton-induced current fluctuations on concentration and species of permeant ion. *J Gen Physiol* 94: 23–42, 1989.
317. **Puliyanda DP, Ward DT, Baum MA, Hammond TG, and Harris HW Jr.** Calcipain-mediated AQP2 proteolysis in inner medullary collecting duct. *Biochem Biophys Res Commun* 303: 52–58, 2003.
318. **Quamme GA and Dirks JH.** Intraluminal and contraluminal magnesium on magnesium and calcium transfer in the rat nephron. *Am J Physiol Renal Fluid Electrolyte Physiol* 238: F187–F198, 1980.
319. **Quan A and Baum M.** Endogenous angiotensin II modulates rat proximal tubule transport with acute changes in extracellular volume. *Am J Physiol Renal Physiol* 275: F74–F78, 1998.
320. **Raber G, Willems PH, Lang F, Nitschke R, van Os CH, and Bindels RJ.** Co-ordinated control of apical calcium influx and basolateral calcium efflux in rabbit cortical collecting system. *Cell Calcium* 22: 157–166, 1997.

321. **Ray WA, Griffin MR, Downey W, and Melton LJ III.** Long-term use of thiazide diuretics and risk of hip fracture. *Lancet* 1: 687–690, 1989.
322. **Reichel H, Koeffler HP, and Norman AW.** The role of the vitamin D endocrine system in health and disease. *N Engl J Med* 320: 980–991, 1989.
323. **Reid IR.** Glucocorticoid osteoporosis—mechanisms and management. *Eur J Endocrinol* 137: 209–217, 1997.
324. **Reid IR and Ibbertson HK.** Evidence for decreased tubular reabsorption of calcium in glucocorticoid-treated asthmatics. *Horm Res* 27: 200–204, 1987.
325. **Reilly RF and Shugrue CA.** cDNA cloning of a renal Na⁺-Ca²⁺ exchanger. *Am J Physiol Renal Fluid Electrolyte Physiol* 262: F1105–F1109, 1992.
326. **Rety S, Sopkova J, Renouard M, Osterloh D, Gerke V, Tabaries S, Russo-Marie F, and Lewit-Bentley A.** The crystal structure of a complex of p11 with the annexin II N-terminal peptide. *Nat Struct Biol* 6: 89–95, 1999.
327. **Reuter H, Henderson SA, Han T, Ross RS, Goldhaber JI, and Philipson KD.** The Na⁺-Ca²⁺ exchanger is essential for the action of cardiac glycosides. *Circ Res* 90: 305–308, 2002.
328. **Rho SH and Park CS.** Extracellular proton alters the divalent cation binding affinity in a cyclic nucleotide-gated channel pore. *FEBS Lett* 440: 199–202, 1998.
329. **Riccardi D, Hall AE, Chattopadhyay N, Xu JZ, Brown EM, and Hebert SC.** Localization of the extracellular Ca²⁺/polyvalent cation-sensing protein in rat kidney. *Am J Physiol Renal Physiol* 274: F611–F622, 1998.
330. **Ritchie G, Kerstan D, Dai LJ, Kang HS, Canaff L, Hendy GN, and Quamme GA.** 1,25(OH)₂D₃ stimulates Mg²⁺ uptake into MDCT cells: modulation by extracellular Ca²⁺ and Mg²⁺. *Am J Physiol Renal Physiol* 280: F868–F878, 2001.
331. **Rocha AS, Magaldi JB, and Kokko JP.** Calcium and phosphate transport in isolated segments of rabbit Henle's loop. *J Clin Invest* 59: 975–983, 1977.
332. **Rodino MA and Shane E.** Osteoporosis after organ transplantation. *Am J Med* 104: 459–469, 1998.
333. **Rose E and Boles RS Jr.** Hypercalcemia in thyrotoxicosis. *Med Clin North Am* 1: 1715–1724, 1953.
334. **Safe S.** Transcriptional activation of genes by 17 beta-estradiol through estrogen receptor-Sp1 interactions. *Vitam Horm* 62: 231–252, 2001.
335. **Sands JM, Naruse M, Baum M, Jo I, Hebert SC, Brown EM, and Harris HW.** Apical extracellular calcium/polyvalent cation-sensing receptor regulates vasopressin-elicited water permeability in rat kidney inner medullary collecting duct. *J Clin Invest* 99: 1399–1405, 1997.
336. **Schindl R, Kahr H, Graz I, Groschner K, and Romanin C.** Store depletion-activated CaT1 currents in rat basophilic leukemia mast cells are inhibited by 2-aminoethoxydiphenyl borate. Evidence for a regulatory component that controls activation of both CaT1 and CRAC (Ca²⁺ release-activated Ca²⁺ channel) channels. *J Biol Chem* 277: 26950–26958, 2002.
337. **Schoenmakers TJ and Flik G.** Sodium-extruding and calcium-extruding sodium/calcium exchangers display similar calcium affinities. *J Exp Biol* 168: 151–159, 1992.
338. **Schreiber SL.** Chemistry and biology of the immunophilins and their immunosuppressive ligands. *Science* 251: 283–287, 1991.
339. **Schroder B, Vossing S, and Breves G.** In vitro studies on active calcium absorption from ovine rumen. *J Comp Physiol* 169: 487–494, 1999.
340. **Schulze DH, Polumuri SK, Gille T, and Ruknudin A.** Functional regulation of alternatively spliced Na⁺/Ca²⁺ exchanger (NCX1) isoforms. *Ann NY Acad Sci* 976: 187–196, 2002.
341. **Scott K, Sun Y, Beckingham K, and Zuker CS.** Calmodulin regulation of *Drosophila* light-activated channels and receptor function mediates termination of the light response in vivo. *Cell* 91: 375–383, 1997.
342. **Shao A, Wood RJ, and Fleet JC.** Increased vitamin D receptor level enhances 1,25-dihydroxyvitamin D₃-mediated gene expression and calcium transport in Caco-2 cells. *J Bone Miner Res* 16: 615–624, 2001.
343. **Shareghi GR and Agus ZS.** Magnesium transport in the cortical thick ascending limb of Henle's loop of the rabbit. *J Clin Invest* 69: 759–769, 1982.
344. **Shareghi GR and Stoner LC.** Calcium transport across segments of the rabbit distal nephron in vitro. *Am J Physiol Renal Fluid Electrolyte Physiol* 235: F367–F375, 1978.
345. **Shennan DB and Peaker M.** Transport of milk constituents by the mammary gland. *Physiol Rev* 80: 925–951, 2000.
346. **Shimizu T, Nakamura M, Yoshitomi K, and Imai M.** Interaction of trichlormethiazide or amiloride with PTH in stimulating Ca²⁺ absorption in rabbit CNT. *Am J Physiol Renal Fluid Electrolyte Physiol* 261: F36–F43, 1991.
347. **Shimizu T, Yoshitomi K, Nakamura M, and Imai M.** Effect of parathyroid hormone on the connecting tubule from the rabbit kidney: biphasic response of transmural voltage. *Pflügers Arch* 416: 254–261, 1990.
348. **Shimizu T, Yoshitomi K, Nakamura M, and Imai M.** Effects of PTH, calcitonin, and cAMP on calcium transport in rabbit distal nephron segments. *Am J Physiol Renal Fluid Electrolyte Physiol* 259: F408–F414, 1990.
349. **Shimizu T, Yoshitomi K, Nakamura M, and Imai M.** Site and mechanism of action of trichlormethiazide in rabbit distal nephron segments perfused in vitro. *J Clin Invest* 82: 721–730, 1988.
350. **Shimmins J, Smith DA, Aitken M, Linsley GS, Orr JS, and Gillespie FC.** The measurement of calcium absorption using an oral and intravenous tracer. 2. Clinical studies. *Calcif Tissue Res* 6: 301–315, 1971.
351. **Shimura F and Wasserman RH.** Membrane-associated vitamin D-induced calcium-binding protein (CaBP): quantification by a radioimmunoassay and evidence for a specific CaBP in purified intestinal brush borders. *Endocrinology* 115: 1964–1972, 1984.
352. **Siekierka JJ, Hung SH, Poe M, Lin CS, and Sigal NH.** A cytosolic binding protein for the immunosuppressant FK506 has peptidyl-prolyl isomerase activity but is distinct from cyclophilin. *Nature* 341: 755–757, 1989.
353. **Simon DB, Lu Y, Choate KA, Velazquez H, Al-Sabban E, Praga M, Casari G, Bettinelli A, Colussi G, Rodriguez-Soriano J, McCredie D, Milford D, Sanjad S, and Lifton RP.** Paracellin-1, a renal tight junction protein required for paracellular Mg²⁺ resorption. *Science* 285: 103–106, 1999.
354. **Simon DB, Nelson-Williams C, Bia MJ, Ellison D, Karet FE, Molina AM, Vaara I, Iwata F, Cushner HM, Koolen M, Gainza FJ, Gittleman HJ, and Lifton RP.** Gitelman's variant of Bartter's syndrome, inherited hypokalaemic alkalosis, is caused by mutations in the thiazide-sensitive Na-Cl cotransporter. *Nat Genet* 12: 24–30, 1996.
355. **Singer D, Biel M, Lotan I, Flockerzi V, Hofmann F, and Dascal N.** The roles of the subunits in the function of the calcium channel. *Science* 253: 1553–1557, 1991.
356. **Singh BB, Liu X, Tang J, Zhu MX, and Ambudkar IS.** Calmodulin regulates Ca²⁺-dependent feedback inhibition of store-operated Ca²⁺ influx by interaction with a site in the C terminus of TrpC1. *Mol Cell* 9: 739–750, 2002.
357. **Slepchenko BM and Bronner F.** Modeling of transcellular Ca transport in rat duodenum points to coexistence of two mechanisms of apical entry. *Am J Physiol Cell Physiol* 281: C270–C281, 2001.
358. **Soldatov NM.** Ca²⁺ channel moving tail: link between Ca²⁺-induced inactivation and Ca²⁺ signal transduction. *Trends Pharmacol Sci* 24: 167–171, 2003.
359. **Song Y, Peng X, Porta A, Takanaga H, Peng JB, Hediger MA, Fleet JC, and Christakos S.** Calcium transporter 1 and epithelial calcium channel messenger ribonucleic acid are differentially regulated by 1,25 dihydroxyvitamin D₃ in the intestine and kidney of mice. *Endocrinology* 144: 3885–3894, 2003.
360. **Songyang Z, Fanning AS, Fu C, Xu J, Marfatia SM, Chishti AH, Crompton A, Chan AC, Anderson JM, and Cantley LC.** Recognition of unique carboxyl-terminal motifs by distinct PDZ domains. *Science* 275: 73–77, 1997.
361. **Sooy K, Kohut J, and Christakos S.** The role of calbindin and 1,25dihydroxyvitamin D₃ in the kidney. *Curr Opin Nephrol Hypertens* 9: 341–347, 2000.

362. **Sooy K, Schermerhorn T, Noda M, Surana M, Rhoten WB, Meyer M, Fleischer N, Sharp GW, and Christakos S.** Calbindin- D_{28k} controls $[Ca^{2+}]_i$ and insulin release. Evidence obtained from calbindin- D_{28k} knockout mice and beta cell lines. *J Biol Chem* 274: 34343–34349, 1999.
363. **Spencer R, Charman M, Wilson PW, and Lawson EM.** The relationship between vitamin D-stimulated calcium transport and intestinal calcium-binding protein in the chicken. *Biochem J* 170: 93–101, 1978.
364. **Star RA, Nonoguchi H, Balaban R, and Knepper MA.** Calcium and cyclic adenosine monophosphate as second messengers for vasopressin in the rat inner medullary collecting duct. *J Clin Invest* 81: 1879–1888, 1988.
365. **Stauffer TP, Hilfiker H, Carafoli E, and Strehler EE.** Quantitative analysis of alternative splicing options of human plasma membrane calcium pump genes. *J Biol Chem* 268: 25993–26003, 1993.
366. **Steiner S, Aicher L, Raymackers J, Meheus L, Esquer-Blasco R, Anderson NL, and Cordier A.** Cyclosporine A decreases the protein level of the calcium-binding protein calbindin-D 28kDa in rat kidney. *Biochem Pharmacol* 51: 253–258, 1996.
367. **Stempfle HU, Werner C, Siebert U, Assum T, Wehr U, Rambeck WA, Meiser B, Theisen K, and Gartner R.** The role of tacrolimus (FK506)-based immunosuppression on bone mineral density and bone turnover after cardiac transplantation: a prospective, longitudinal, randomized, double-blind trial with calcitriol. *Transplantation* 73: 547–552, 2002.
368. **Story GM, Peier AM, Reeve AJ, Eid SR, Mosbacher J, Hricik TR, Earley TJ, Hergarden AC, Andersson DA, Hwang SW, McIntyre P, Jegla T, Bevan S, and Patapoutian A.** ANKTM1, a TRP-like channel expressed in nociceptive neurons, is activated by cold temperatures. *Cell* 112: 819–829, 2003.
369. **Strehler EE and Zacharias DA.** Role of alternative splicing in generating isoform diversity among plasma membrane calcium pumps. *Physiol Rev* 81: 21–50, 2001.
370. **Strubing C, Krapivinsky G, Krapivinsky L, and Clapham DE.** TRPC1 and TRPC5 form a novel cation channel in mammalian brain. *Neuron* 29: 645–655, 2001.
371. **Suki WN.** Calcium transport in the nephron. *Am J Physiol Renal Fluid Electrolyte Physiol* 237: F1–F6, 1979.
372. **Suki WN and Rouse D.** Hormonal regulation of calcium transport in thick ascending limb renal tubules. *Am J Physiol Renal Fluid Electrolyte Physiol* 241: F171–F174, 1981.
373. **Suki WN, Rouse D, Ng RC, and Kokko JP.** Calcium transport in the thick ascending limb of Henle. Heterogeneity of function in the medullary and cortical segments. *J Clin Invest* 66: 1004–1009, 1980.
374. **Sutton RA and Dirks JH.** The renal excretion of calcium: a review of micropuncture data. *Can J Physiol Pharmacol* 53: 979–988, 1975.
375. **Suzuki M, Ohki G, Ishibashi K, and Imai M.** A single amino acid mutation results in a rapid inactivation of epithelial calcium channels. *Biochem Biophys Res Commun* 291: 278–285, 2002.
376. **Talavera K, Janssens A, Klugbauer N, Droogmans G, and Nilius B.** Extracellular Ca^{2+} modulates the effects of protons on gating and conduction properties of the T-type Ca^{2+} channel α_1G (CaV3.1). *J Gen Physiol* 121: 511–528, 2003.
377. **Tan S and Lau K.** Patch-clamp evidence for calcium channels in apical membranes of rabbit kidney connecting tubules. *J Clin Invest* 92: 2731–2736, 1993.
378. **Tang VW and Goodenough DA.** Paracellular ion channel at the tight junction. *Biophys J* 84: 1660–1673, 2003.
379. **Thomasset M, Desplan C, Warembourg M, and Perret C.** Vitamin-D dependent 9 kDa calcium-binding protein gene: cDNA cloning, mRNA distribution and regulation. *Biochimie* 68: 935–940, 1986.
380. **Tokumitsu H, Mizutani A, Minami H, Kobayashi R, and Hidaka H.** A calyculin-associated protein is a newly identified member of the Ca^{2+} /phospholipid-binding proteins, annexin family. *J Biol Chem* 267: 8919–8924, 1992.
381. **Tsien RW, Hess P, McCleskey EW, and Rosenberg RL.** Calcium channels: mechanisms of selectivity, permeation, and block. *Annu Rev Biophys Chem* 16: 265–290, 1987.
382. **Tsiokas L, Arnould T, Zhu C, Kim E, Walz G, and Sukhatme VP.** Specific association of the gene product of PKD2 with the TRPC1 channel. *Proc Natl Acad Sci USA* 96: 3934–3939, 1999.
383. **Tsukamoto Y, Saka S, and Saitoh M.** Parathyroid hormone stimulates ATP-dependent calcium pump activity by a different mode in proximal and distal tubules of the rat. *Biochim Biophys Acta* 1103: 163–171, 1992.
384. **Tsukita S and Furuse M.** Pores in the wall: claudins constitute tight junction strands containing aqueous pores. *J Cell Biol* 149: 13–16, 2000.
385. **Ullrich KJ, Schmidt-Nielsen B, O'Dell R, Pehling G, Gottschalk CW, Lassiter WE, and Mylle M.** Micropuncture study of composition of proximal and distal tubular fluid in rat kidney. *Am J Physiol* 204: 527–531, 1963.
386. **Van Abel M, Hoenderop JG, Dardenne O, St Arnaud R, van Os CH, Van Leeuwen HJ, and Bindels RJ.** 1,25-Dihydroxyvitamin D_3 -independent stimulatory effect of estrogen on the expression of ECaC1 in the kidney. *J Am Soc Nephrol* 13: 2102–2109, 2002.
387. **Van Abel M, Hoenderop JG, van der Kemp AW, van Leeuwen JP, and Bindels RJ.** Regulation of the epithelial Ca^{2+} channels in small intestine as studied by quantitative mRNA detection. *Am J Physiol Gastrointest Liver Physiol* 285: G78–G85, 2003.
388. **Van Abel M, Hoenderop JG, van Leeuwen HJ, and Bindels R.** Down-regulation of calcium transporters in kidney and duodenum by the calcimimetic compound NPS R-467 (Abstract). *J Am Soc Nephrol* 14: 459A, 2003.
389. **Van Baal J, Hoenderop JG, Groenendijk M, van Os CH, Bindels RJ, and Willems PH.** Hormone-stimulated Ca^{2+} transport in rabbit kidney: multiple sites of inhibition by exogenous ATP. *Am J Physiol Renal Physiol* 277: F899–F906, 1999.
390. **Van Baal J, Raber G, de Slegte J, Pieters R, Bindels RJ, and Willems PH.** Vasopressin-stimulated Ca^{2+} reabsorption in rabbit cortical collecting system: effects on cAMP and cytosolic Ca^{2+} . *Pflügers Arch* 433: 109–115, 1996.
391. **Van Baal J, Yu A, Hartog A, Fransen JA, Willems PH, Lytton J, and Bindels RJ.** Localization and regulation by vitamin D of calcium transport proteins in rabbit cortical collecting system. *Am J Physiol Renal Fluid Electrolyte Physiol* 271: F985–F993, 1996.
392. **Van Cromphaut SJ, Dewerchin M, Hoenderop JG, Stockmans I, Van Herck E, Kato S, Bindels RJ, Collen D, Carmeliet P, Bouillon R, and Carmeliet G.** Duodenal calcium absorption in vitamin D receptor-knockout mice: functional and molecular aspects. *Proc Natl Acad Sci USA* 98: 13324–13329, 2001.
393. **Van Cromphaut SJ, Rummens K, Stockmans I, Van Herck E, Dijcks FA, Ederveen AG, Carmeliet P, Verhaeghe J, Bouillon R, and Carmeliet G.** Intestinal calcium transporter genes are upregulated by estrogens and the reproductive cycle through vitamin D receptor-independent mechanisms. *J Bone Miner Res* 18: 1725–1736, 2003.
394. **Van de Graaf SF, Hoenderop JG, Gkika D, Lamers D, Prenen J, Rescher U, Gerke V, Staub O, Nilius B, and Bindels RJ.** Functional expression of the epithelial Ca^{2+} channels (TRPV5 and TRPV6) requires association of the S100A10-annexin 2 complex. *EMBO J* 22: 1478–1487, 2003.
395. **Vanden Abeele F, Roudbaraki M, Shuba Y, Skryma R, and Prevarskaya N.** Store-operated Ca^{2+} current in prostate cancer epithelial cells. Role of endogenous Ca^{2+} transporter type 1. *J Biol Chem* 278: 15381–15389, 2003.
396. **Van Eylen F, Svoboda M, and Herchuelz A.** Identification, expression pattern and potential activity of Na/Ca exchanger isoforms in rat pancreatic B-cells. *Cell Calcium* 21: 185–193, 1997.
397. **Van Kuijk MA, van Aabel RA, Busch AE, Lang F, Russel FG, Bindels RJ, van Os CH, and Deen PM.** Molecular cloning and expression of a cyclic AMP-activated chloride conductance regulator: a novel ATP-binding cassette transporter. *Proc Natl Acad Sci USA* 93: 5401–5406, 1996.

398. **Van Os CH.** Transcellular calcium transport in intestinal and renal epithelial cells. *Biochim Biophys Acta* 906: 195–222, 1987.
399. **Van Rossum DB, Patterson RL, Ma HT, and Gill DL.** Ca²⁺ entry mediated by store depletion, S-nitrosylation, and TRP3 channels. Comparison of coupling and function. *J Biol Chem* 275: 28562–28568, 2000.
400. **Varadi G, Lory P, Schultz D, Varadi M, and Schwartz A.** Acceleration of activation and inactivation by the beta subunit of the skeletal muscle calcium channel. *Nature* 352: 159–162, 1991.
401. **Varghese R, Gagliardi AD, Bialek PE, Yee SP, Wagner GF, and Dimattia GE.** Overexpression of human stanniocalcin affects growth and reproduction in transgenic mice. *Endocrinology* 143: 868–876, 2002.
402. **Vassilev PM, Peng JB, Johnson J, Hediger MA, and Brown EM.** Inhibition of CaT1 channel activity by a noncompetitive IP₃ antagonist. *Biochem Biophys Res Commun* 280: 145–150, 2001.
403. **Vennekens R.** *Molecular and Biophysical Analysis of the Epithelial Calcium Channels ECAC1 and ECAC2.* Leuven, Belgium: Leuven Univ. Press, 2002.
404. **Vennekens R, Hoenderop JG, Prenen J, Stuver M, Willems PH, Droogmans G, Nilius B, and Bindels RJ.** Permeation and gating properties of the novel epithelial Ca²⁺ channel. *J Biol Chem* 275: 3963–3969, 2000.
405. **Vennekens R, Prenen J, Hoenderop JG, Bindels RJ, Droogmans G, and Nilius B.** Modulation of the epithelial Ca²⁺ channel ECAC by extracellular pH. *Pflügers Arch* 442: 237–242, 2001.
406. **Vennekens R, Prenen J, Hoenderop JG, Bindels RJ, Droogmans G, and Nilius B.** Pore properties and ionic block of the rabbit epithelial calcium channel expressed in HEK 293 cells. *J Physiol* 530: 183–191, 2001.
407. **Voets T, Janssens A, Droogmans G, and Nilius B.** Outer pore architecture of a Ca²⁺-selective TRP channel. *J Biol Chem.* In press.
408. **Voets T, Janssens A, Droogmans G, and Nilius B.** A single pore residue determines calcium selectivity, inward rectification and pore size of TRPV6 (CaT1/ECAC2) (Abstract). *Biophys J* 2724-Pos, 2003.
409. **Voets T, Janssens A, Prenen J, Droogmans D, and Nilius G.** Mg²⁺-dependent gating and strong inward rectification of the cation channel TRPV6. *J Gen Physiol* 121: 245–260, 2003.
410. **Voets T, Prenen J, Fleig A, Vennekens R, Watanabe H, Hoenderop JG, Bindels RJ, Droogmans G, Penner R, and Nilius B.** CaT1 and the calcium release-activated calcium channel manifest distinct pore properties. *J Biol Chem* 276: 47767–47770, 2001.
411. **Voets T, Prenen J, Vriens J, Watanabe H, Janssens A, Wissenbach U, Bödding M, Droogmans G, and Nilius B.** Molecular determinants of permeation through the cation channel TRPV4. *J Biol Chem* 277: 33704–33710, 2002.
412. **Voets T, Vennekens R, Prenen J, Droogmans G, and Nilius B.** Magnesium-dependent gating of the epithelial calcium channel ECAC2 (CAT1) (Abstract). *Biophys J* 211c, 2002.
414. **Wagner GF, Dimattia GE, Davie JR, Copp DH, and Friesen HG.** Molecular cloning and cDNA sequence analysis of coho salmon stanniocalcin. *Mol Cell Endocrinol* 90: 7–15, 1992.
415. **Wagner GF, Guiraudon CC, Milliken C, and Copp DH.** Immunological and biological evidence for a stanniocalcin-like hormone in human kidney. *Proc Natl Acad Sci USA* 92: 1871–1875, 1995.
416. **Walter SJ and Shirley DG.** The effect of chronic hydrochlorothiazide administration on renal function in the rat. *Clin Sci* 70: 379–387, 1986.
417. **Walters JR, Howard A, Charpin MV, Gniecko KC, Brodin P, Thulin E, and Forsen S.** Stimulation of intestinal basolateral membrane calcium-pump activity by recombinant synthetic calbindin-D_{9k} and specific mutants. *Biochem Biophys Res Commun* 170: 603–608, 1990.
418. **Wang CL.** A note on Ca²⁺ binding to calmodulin. *Biochem Biophys Res Commun* 130: 426–430, 1985.
419. **Wang Y, Zhang J, Yi XJ, and Yu FS.** Activation of ERK1/2 MAP kinase pathway induces tight junction disruption in human corneal epithelial cells. *Exp Eye Res* 78: 125–136, 2004.
420. **Wang YZ, Li H, Bruns ME, Uskokovic M, Truitt GA, Horst R, Reinhardt T, and Christakos S.** Effect of 1,25,28-trihydroxyvitamin D₂ and 1,24,25-trihydroxyvitamin D₃ on intestinal calbindin-D_{9k} mRNA and protein: is there a correlation with intestinal calcium transport? *J Bone Miner Res* 8: 1483–1490, 1993.
421. **Ward DT and Riccardi D.** Renal physiology of the extracellular calcium-sensing receptor. *Pflügers Arch* 445: 169–176, 2002.
422. **Wasnich RD, Benfante RJ, Yano K, Heilbrun L, and Vogel JM.** Thiazide effect on the mineral content of bone. *N Engl J Med* 309: 344–347, 1983.
423. **Weber K, Erben RG, Rump A, and Adamski J.** Gene structure and regulation of the murine epithelial calcium channels ECAC1 and 2. *Biochem Biophys Res Commun* 289: 1287–1294, 2001.
424. **Weinman EJ and Eknoyan G.** Chronic effects of chlorothiazide on reabsorption by the proximal tubule of the rat. *Clin Sci Mol Med* 49: 109–113, 1975.
425. **Weinstein AM and Windhager EE.** The paracellular shunt of proximal tubule. *J Membr Biol* 184: 241–245, 2001.
426. **Wendelaar Bonga SE.** The stress response in fish. *Physiol Rev* 77: 591–625, 1997.
427. **White KE, Gesek FA, Reilly RF, and Friedman PA.** NCX1 Na/Ca exchanger inhibition by antisense oligonucleotides in mouse distal convoluted tubule cells. *Kidney Int* 54: 897–906, 1998.
428. **Wilcox ER, Burton QL, Naz S, Riazuddin S, Smith TN, Ploplis B, Belyantseva I, Ben-Yosef T, Liburd NA, Morell RJ, Kachar B, Wu DK, Griffith AJ, and Friedman TB.** Mutations in the gene encoding tight junction claudin-14 cause autosomal recessive deafness DFNB29. *Cell* 104: 165–172, 2001.
429. **Wilson FH, Disse-Nicodeme S, Choate KA, Ishikawa K, Nelson-Williams C, Desitter I, Gunel M, Milford DV, Lipkin GW, Achard JM, Feely MP, Dussol B, Berland Y, Unwin RJ, Mayan H, Simon DB, Farfel Z, Jeunemaitre X, and Lifton RP.** Human hypertension caused by mutations in WNK kinases. *Science* 293: 1107–1112, 2001.
430. **Wissenbach U, Niemeyer BA, Fixemer T, Schneidewind A, Trost C, Cavalie A, Reus K, Meese E, Bonkhoff H, and Flockner V.** Expression of CaT-like, a novel calcium-selective channel, correlates with the malignancy of prostate cancer. *J Biol Chem* 276: 19461–19468, 2001.
431. **Witcher DR, De Waard M, Sakamoto J, Franzini-Armstrong C, Pragnell M, Kahl SD, and Campbell KP.** Subunit identification and reconstitution of the N-type Ca²⁺ channel complex purified from brain. *Science* 261: 486–489, 1993.
432. **Wittner M, Di Stefano A, Mandon B, Roinel N, and de Rouffignac C.** Stimulation of NaCl reabsorption by antidiuretic hormone in the cortical thick ascending limb of Henle's loop of the mouse. *Pflügers Arch* 419: 212–214, 1991.
433. **Wittner M, Mandon B, Roinel N, de Rouffignac C, and Di Stefano A.** Hormonal stimulation of Ca²⁺ and Mg²⁺ transport in the cortical thick ascending limb of Henle's loop of the mouse: evidence for a change in the paracellular pathway permeability. *Pflügers Arch* 423: 387–396, 1993.
434. **Wong V and Goodenough DA.** Paracellular channels! *Science* 285: 62, 1999.
435. **Wood RJ, Tchack L, and Taparua S.** 1,25-Dihydroxyvitamin D₃ increases the expression of the CaT1 epithelial calcium channel in the Caco-2 human intestinal cell line. *BMC Physiol* 1: 11, 2001.
436. **Yamagishi N, Yukawa YA, Ishiguro N, Soeta S, Lee IH, Oboshi K, and Yamada H.** Expression of calbindin-D_{9k} messenger ribonucleic acid in the gastrointestinal tract of dairy cattle. *J Vet Med A Physiol Pathol Clin Med* 49: 461–465, 2002.
437. **Yang T, Hassan S, Huang YG, Smart AM, Briggs JP, and Schnermann JB.** Expression of PTHrP, PTH/PTHrP receptor, and Ca²⁺-sensing receptor mRNAs along the rat nephron. *Am J Physiol Renal Physiol* 272: F751–F758, 1997.
438. **Yeh BI, Sun TJ, Lee JZ, Chen HH, and Huang CL.** Mechanism and molecular determinant for regulation of rabbit transient receptor potential type 5 (TRPV5) channel by extracellular pH. *J Biol Chem* 278: 51044–51052, 2003.
439. **Yildirim E, Dietrich A, and Birnbaumer L.** The mouse C-type transient receptor potential 2 (TRPC2) channel: alternative splicing

- and calmodulin binding to its N terminus. *Proc Natl Acad Sci USA* 100: 2220–2225, 2003.
440. **Yoshizawa T, Handa Y, Uematsu Y, Takeda S, Sekine K, Yoshihara Y, Kawakami T, Arioka K, Sato H, Uchiyama Y, Masushige S, Fukamizu A, Matsumoto T, and Kato S.** Mice lacking the vitamin D receptor exhibit impaired bone formation, uterine hypoplasia and growth retardation after weaning. *Nat Genet* 16: 391–396, 1997.
441. **Young MM, Jasani C, Smith DA, and Nordin BE.** Some effects of ethinyl oestradiol on calcium and phosphorus metabolism in osteoporosis. *Clin Sci* 34: 411–417, 1968.
442. **Young MM and Nordin BE.** Calcium metabolism and the menopause. *Proc R Soc Med* 60: 1137–1138, 1967.
443. **Yu AS, Boim M, Hebert SC, Castellano A, Perez-Reyes E, and Lytton J.** Molecular characterization of renal calcium channel beta-subunit transcripts. *Am J Physiol Renal Fluid Electrolyte Physiol* 268: F525–F531, 1995.
444. **Yue L, Peng JB, Hediger MA, and Clapham DE.** CaT1 manifests the pore properties of the calcium-release-activated calcium channel. *Nature* 410: 705–709, 2001.
445. **Zelinski JM, Sykes DE, and Weiser MM.** The effect of vitamin D on rat intestinal plasma membrane CA-pump mRNA. *Biochem Biophys Res Commun* 179: 749–755, 1991.
446. **Zhou Y, Morais-Cabral JH, Kaufman A, and MacKinnon R.** Chemistry of ion coordination and hydration revealed by a K⁺ channel-Fab complex at 2.0 Å resolution. *Nature* 414: 43–48, 2001.
447. **Zhuang L, Peng JB, Tou L, Takanaga H, Adam RM, Hediger MA, and Freeman MR.** Calcium-selective ion channel, CaT1, is apically localized in gastrointestinal tract epithelia and is aberrantly expressed in human malignancies. *Lab Invest* 82: 1755–1764, 2002.